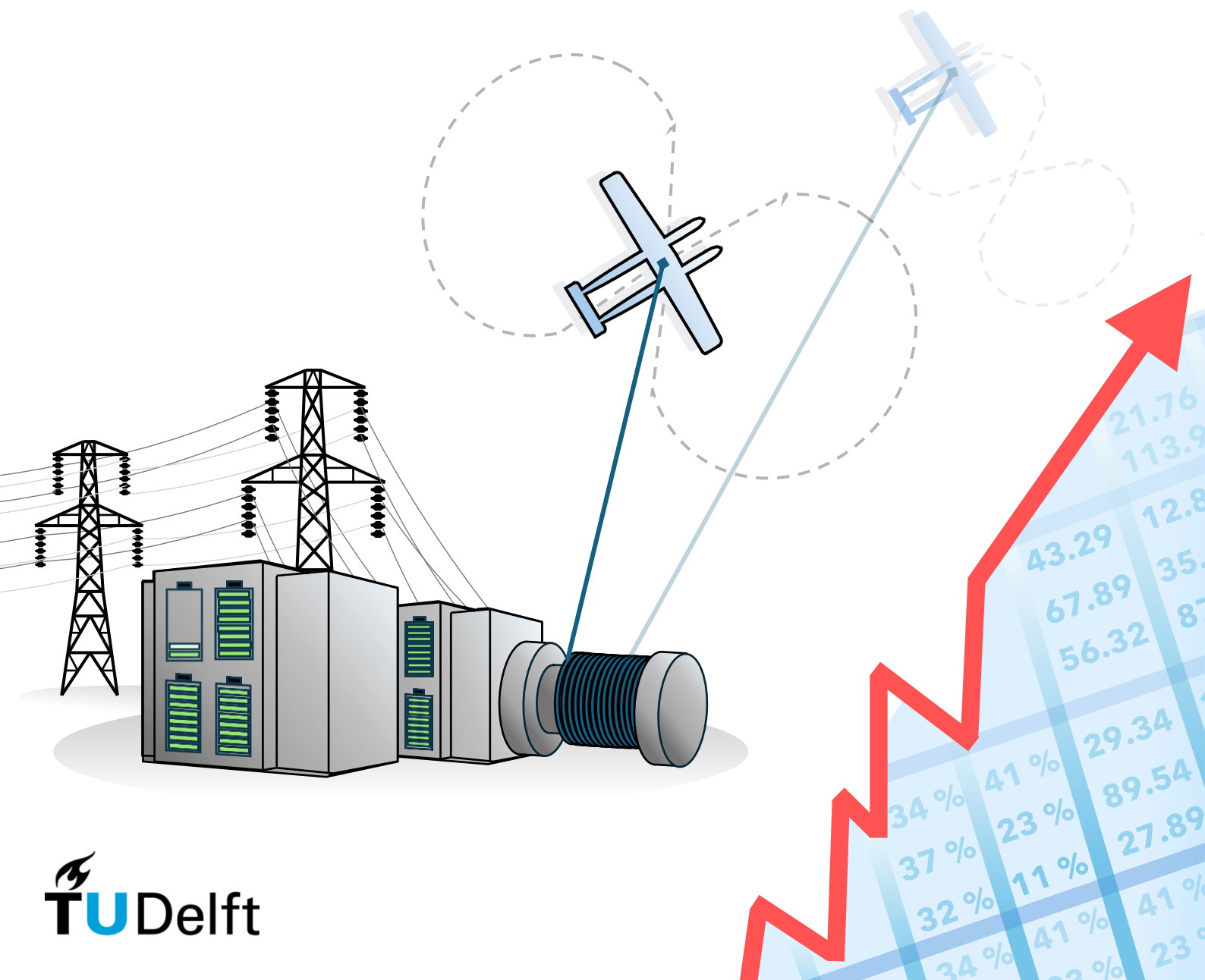


# Value maximization of grid-connected Hybrid Power Systems using ground-gen Airborne Wind Energy

A techno-economic analysis of energy arbitrage utilizing power smoothing storage capacity

Bart Zweers



Copyright ©2024 by Bart Zweers  
All rights reserved



# Value maximization of grid-connected Hybrid Power Systems using ground-gen Airborne Wind Energy

A techno-economic analysis of energy arbitrage  
utilizing power smoothing storage capacity

by

**Bart Zweers**

in partial fulfillment of the requirements for the degree of

**Master of Science**

in Sustainable Energy Technology

at the Delft University of Technology,

to be defended publicly on Wednesday, October 30, 2024 at 10:00 AM

Student number: 4372565

Thesis duration: 11 December, 2023 to 30 October, 2024

## **Thesis committee**

(Chair)	Dr.-Ing. Roland Schmehl	TU Delft
	Dr. Ir. Jianning Dong	TU Delft
	Ir. Rishikesh Joshi	TU Delft

An electronic version of this thesis is available at <http://repository.tudelft.nl/>.

# Preface

This report marks the end of my master's degree in Sustainable Energy Technology from the TU Delft. Throughout the entire master's program, I have enjoyed developing skills to analyze and integrate all kinds of technologies and systems. It is because of this I was excited to be able to work on this thesis topic since it involves understanding and integrating different kinds of technologies. Due to the various topics of research surrounding airborne wind energy at the moment, it was possible to find a research topic that aligned with current research and my area of interest. I am glad to have been able to finish my university career doing a project that involves everything I have learned and enjoyed during my time at the TU Delft.

I would first and foremost like to thank my thesis supervisor Dr.-Ing Roland Schmehl for his insights and guidance throughout the entire process. Since I was introduced to the concept of airborne wind energy at the start of this thesis I had a lot of catching up to do and I have Roland to thank for getting the hang of it and finding the best approach to my research. Adding to this I would like to thank my daily supervisor Rishikesh Joshi for his kindness and patience in helping me understand the field of research and create my little part in it. At many points when I didn't know how to move forward, Rishi helped me along patiently and explained everything I didn't understand calmly. I would like to thank my friend Dylan Eijkelhof for introducing me to the airborne wind research group and brainstorming possible thesis topics that would suit me. I would also like to thank the members of IEA task 48 WP1 as well as Dr. Jenna Iori for giving me valuable input to help steer my research in the right direction at critical points.

I would like to thank all my friends for asking after my thesis and how I was doing, which helped me gain much-needed perspective throughout the process. Special thanks to my sister Nienke for having both the skills in organizationally supporting my process and understanding me to the point of knowing exactly where I needed to be pushed. Finally and most importantly, I would like to thank my mother, Tanja, for allowing me to pursue my academic goals at my own pace without any judgment and with unconditional support.

*Bart Zweers  
Delft, October 2024*

# Abstract

Airborne wind energy (AWE) is a wind energy technology in the development phase consisting of tethered kites that reach high altitudes consisting of relatively stable wind speeds. While no company has yet reached the point of commercial viability, a variety of AWE technology concepts and designs have been under development and are currently at low- to intermediate technology readiness levels. When AWE systems are grid-connected a power smoothing element is needed to smooth the oscillating power output of the system for the grid. This oscillation is the result of the tethered kites operating in a pumping cycle consisting of a phase where the tether is reeled out, producing electricity, and a phase where the tether is reeled in, consuming a small amount of electricity. This fluctuating electricity output requires smoothing to comply with the ramp limits of the grid, which define the system design of the storage element used for this application. In this thesis, a framework for modeling a grid-connected hybrid power system (HPS) consisting of AWE and batteries participating in the day-ahead market (DAM) has been developed in the MATLAB environment. The framework incorporates an existing AWE performance and cost model with power smoothing performance, battery degradation, and DAM storage arbitrage. Multiple use case scenarios are evaluated to test the economic performance of multiple configurations of the HPS. These scenarios are; an AWE system with an ultracapacitor (UC); an AWE system with batteries; a battery system operating in DAM arbitrage and an AWE system with batteries operating in DAM arbitrage. The configurations were evaluated using multiple performance metrics, primarily the internal rate of return (IRR) as a metric for economic performance.

Power smoothing requires high power output and due to the nature of battery technology, a battery system sized for that power output results in a certain over-sizing factor in terms of energy capacity. Simulations of the HPS performance with a battery smoothing system were used to identify the quantity of excess storage capacity present. A simulation of the HPS participating in storage arbitrage was then used to determine the economic viability of using the battery system for both power smoothing and arbitrage. The arbitrage behavior of the storage system was determined by a heuristic selling logic model developed to simulate the combined use of a storage system for power smoothing and arbitrage. The arbitrage logic is based on price volatility and power smoothing constraints. The arbitrage behavior was set to trade energy at high/low price points of the DAM taking into account the trade-off between profit and excessive use of the battery resulting in increased battery degradation. Integration of the AWE-produced energy and the discharged battery energy sold on the DAM, the profitability of all use cases defined by the scenarios was assessed and compared.

Simulation of the UC and battery power smoothing configurations showed the performance and the costs associated with each storage technology type. The battery power smoothing system resulted in significantly lower system cost overall and consequently an increase in profitability (IRR of 12.37%) compared to the more expensive UC power smoothing configuration (IRR of 10.20%). The battery system operated in DAM storage arbitrage showed a negative profit, concluding that at the battery price point and DAM simulated, the arbitrage revenue is significantly lower over the lifetime than the initial and operational costs. The HPS configuration with batteries used for power smoothing combined with arbitrage showed a marginal increase in economic performance with an IRR of 12.43%. This showed a potential value increase of the system when using excess capacity arbitrage but not at a significant rate. Lower battery prices and more optimal arbitrage operation could increase the added value further.

Keywords: Airborne wind energy (AWE), hybrid power systems (HPS), power smoothing, day-ahead market (DAM), system design, battery arbitrage

# Contents

<b>Preface</b>	<b>iv</b>
<b>Abstract</b>	<b>v</b>
<b>1 Introduction</b>	<b>1</b>
1.1 Background	1
1.2 Motivation and aim	5
<b>2 Literature Review</b>	<b>6</b>
2.1 Airborne Wind Energy	6
2.1.1 Pumping cycle	6
2.1.2 Power smoothing storage	7
2.1.3 Market value of Airborne Wind Energy	9
2.2 Hybrid Power Systems	12
2.2.1 Hybrid Power Profitability	12
2.2.2 Power stability	15
2.3 Electricity markets	17
2.3.1 Electricity market types	17
2.3.2 Storage arbitrage	18
2.4 Problem analysis	20
2.4.1 Research gap	20
2.4.2 Research Questions	20
2.4.3 Methodology	21
<b>3 Model Development</b>	<b>22</b>
3.1 Model overview	22
3.2 Scenario parameters	24
3.3 Airborne Wind Energy Performance	26
3.3.1 Power curve	26
3.3.2 Intermediate storage	29
3.3.3 Cost of Energy	31
3.4 Storage Energy Performance	34
3.4.1 Battery smoothing performance	34
3.4.2 Cost of Storage	37
3.5 Bidding dispatcher	39
3.5.1 Storage arbitrage bidding	39
3.5.2 Combined storage smoothing and arbitrage bidding	42
3.5.3 Arbitrage operation optimization	46
3.6 Hybrid Power System value assessment	48
<b>4 Results and Evaluation</b>	<b>51</b>
4.1 Scenario configurations	51
4.2 Scenario 1: AWE + UC	52
4.3 Scenario 2: AWE + battery	56
4.4 Scenario 3: Battery Arbitrage	60
4.5 Scenario 4: AWE + Battery arbitrage	63

4.6 Discussion of results . . . . .	68
4.6.1 Comparison value assessment . . . . .	68
4.6.2 Sensitivity analysis . . . . .	72
<b>5 Conclusion</b>	<b>76</b>
5.1 Key findings . . . . .	76
5.2 Reflections and recommendations . . . . .	77
<b>Bibliography</b>	<b>78</b>

# Nomenclature

## Abbreviations

AEP	Annual Energy Produced
AWE	Airborne Wind Energy
DAM	Day Ahead Market
DoD	Depth of Discharge of storage system
DSO	Distribution System Operator
FCR	Frequency Containment Reserve
FIT	Feed-in-tariff
FW	Fixed-wing system
FR	Frequency Restoration Reserve
GG	Ground-generation system
HPP	Hybrid Power Plant
HPS	Hybrid Power System
ID	Intra Day market
IRR	Internal Rate of Return
IR	Inertial Response
kWh	Kilowatt-hour
kW	Kilowatt
LCoE	Levelized Cost of Electricity
Li-ion	Lithium-ion batteries
LPoE	Levelized Profit of Electricity
LP	Linear Programming optimization method
LRoE	Levelized Revenue of Electricity
MILP	Mixed Integer Linear Programming optimization method
MIQCP	Mixed Integer Quadratic Constrained optimization method
MW	Mega Watt
NPV	Net Present Value
PV	Photovoltaic
QSM	Quasi-steady model
RES	Renewable Energy Source
SoC	State of Charge of storage system
TRL	Technology Readiness Level
TSO	Transmission System Operator
UC	Ultracapacitor
VoSA	Value of Storage Arbitrage

## Greek symbols

$\alpha$	Wind shear exponent
$\eta$	Round-trip efficiency
$\mu$	Mean value
$\sigma$	Volatility or standard deviation
$\Sigma$	Summation sign

### **Roman symbols**

AR	Aspect Ratio
p	Price
S	Wing surface area
T	Economic lifetime of the project
t	time instant
w	Window of time instances
C	C rate of storage system
$C_f$	Capacity factor
E	Energy
f	Frequency
$F_t$	Tether force
$l_t$	Tether length
N	Lifetime of component
P	Power
R	Revenue
$v_w$	Wind Speed

### **Subscripts**

avg	Average
AWE	Airborne Wind Energy
batt	Battery
cha	Charged
cycles	Full load cycles
cycle	Pumping cycle
DAM	Day ahead market
dis	Discharged
e	Electrical
gen	Generator
i	Reel-in
max	Maximum
o	Reel-out
peak	Peak
rated	System rated output

repl	Replacement
req	Required
res	Reserved
sm	Smoothing
sub	Subsidy
u	u-direction
v	v-direction
years	Calendar years

# List of Tables

2.1	Comparison of attributes of electrical storage technologies . . . . .	9
3.1	Overview input parameters per scenario . . . . .	24
3.2	Properties as input variables for AWE power estimations . . . . .	27
3.3	Overview cost of AWE system . . . . .	32
3.4	Scenario input parameters for Storage performance . . . . .	34
3.5	Storage technology sizing for power smoothing . . . . .	35
3.6	Overview cost of storage system . . . . .	37
4.1	Overview component configuration per scenario . . . . .	51
4.2	Parameter inputs scenario 1: AWE + UC . . . . .	53
4.3	Results scenario 1: AWE + UC . . . . .	53
4.4	Parameter inputs scenario 2: AWE + Battery . . . . .	57
4.5	Results scenario 2: AWE + Battery . . . . .	57
4.6	Parameter inputs scenario 3: Battery arbitrage . . . . .	60
4.7	Results scenario 3: Battery arbitrage . . . . .	61
4.8	Parameter inputs scenario 4: AWE + Battery arbitrage . . . . .	64
4.9	Results scenario 4: AWE + Battery arbitrage . . . . .	65
4.10	Qualative comparison of scenario configuration performance . . . . .	68
4.11	Sensitivity IRR to battery price . . . . .	73

# List of Figures

1.1	Comparison of two ground-generation AWE types and horizontal axis wind turbines indicating operating altitudes . . . . .	2
1.2	Overview reeling phase and power output relative to cycle average. . . . .	2
1.3	Overview components and configuration of grid-connected hybrid power plant . . . . .	3
1.4	Example of DAM price for the NL bidding zone on 20-10-2024 [1]. . . . .	4
1.5	Example of AWE-HPS combining pumping cycle AWE with battery storage. . . . .	4
2.1	Intermediate storage charging and discharging energy areas [2] . . . . .	7
2.2	Electric power smoothing solution configuration [2] . . . . .	8
2.3	Average LCoE of AWE and onshore wind turbine technologies [3] . . . . .	10
2.4	Estimated output per day of wind and solar power in the months of the years indicated [4]. . . . .	12
2.5	Possible grid-connected HPS configurations: (a) Wind + PV + Storage, (b) Wind + Storage, (c) Wind + PV, (d) PV + Storage. . . . .	13
2.6	The Haringvliet hybrid power plant, operated by Vattenfall [5] . . . . .	14
2.7	Conservative and advanced cost projections of utility-scale battery system cost [6] . . . . .	15
2.8	DAM merit order market clearing price determination . . . . .	18
3.1	Overview of the HPP value assessment framework. . . . .	23
3.2	Day Ahead Market price hourly over 2019 . . . . .	25
3.3	Wind speed at 100 m altitude hourly over 2019 . . . . .	26
3.4	Power curve of 100 kW AWE system . . . . .	27
3.5	Power output of 100 kW AWE system in specified wind context . . . . .	28
3.6	Reeling electrical power at rated wind speed 100 kW AWE system . . . . .	29
3.7	Reeling energy at rated wind speed 100 kW AWE system . . . . .	30
3.8	The four components of the AWE system; 1. Kite; 2. Tether; 3. Ground station; 4. Intermediate storage . . . . .	31
3.9	Smoothing Energy and Power performance through ultracapacitor . . . . .	36
3.10	Smoothing Energy and Power performance through battery . . . . .	37
3.11	Storage arbitrage operation of a 10 hr window. . . . .	41
3.12	Storage charging behavior operation . . . . .	42
3.13	Storage charging behavior multiple windows . . . . .	43
3.14	Combined smoothing and arbitrage charging behavior relative to DAM price . . . . .	44
3.15	Combined smoothing and arbitrage charging behavior with battery capacity . . . . .	45
3.16	Combined smoothing and arbitrage charging behavior capacity limit example . . . . .	46
3.17	Arbitrage operation window size effect on energy cycled through storage and IRR . . . . .	47
4.1	Scenario 1 AWE ultra-capacitor overview . . . . .	52
4.2	Smoothing Energy and Power performance through battery . . . . .	54
4.3	Scenario 2 AWE Battery overview . . . . .	56
4.4	Smoothing Energy and Power performance through battery . . . . .	59
4.5	Scenario 3 Battery arbitrage overview . . . . .	60

---

4.6	Arbitrage Energy and Power performance through battery . . . . .	62
4.7	Scenario 4 AWE Battery arbitrage overview . . . . .	63
4.8	Smoothing Energy and Power performance through battery . . . . .	66
4.9	Share of replacement frequency by operation type . . . . .	67
4.10	LCoE values and energy discharged to grid of the four scenarios . . . . .	69
4.11	NPV values and CapEx of the four scenarios . . . . .	70
4.12	IRR values of scenario 1, 2, and 4 and the discount rate assumed in this thesis	70
4.13	Payback year of each project, from top to bottom: scenario 4, 3, 2 and 1 . . . .	71
4.14	Storage component replacement frequency breakdown by factors of life- time years and lifetime cycles per scenario . . . . .	72
4.15	Sensitivity IRR to battery price scenario 2 and 4 . . . . .	74
4.16	Sensitivity IRR to battery round-trip efficiency scenario 4 . . . . .	74
4.17	Sensitivity IRR to battery size efficiency scenario 4 . . . . .	75

# 1 | Introduction

## 1.1. Background

There is a global effort to mitigate greenhouse gas (GHG) emissions and reduce global warming. Energy use is responsible for most of the global greenhouse gas emissions, therefore a transition of the global energy system is of the utmost importance. Mitigating GHG emissions can be achieved by transitioning to higher shares of renewable energy (RE) and phasing down fossil fuel-based energy [7]. The problem with phasing down fossil fuel generation and replacing it with renewable generation is that this generation is susceptible to intermittency and therefore requires creative solutions to replace the phased-down fossil fuel-based generation. One of these solutions is combining different RE sources in a Hybrid Power Plant (HPP), a mix of generating technologies that can potentially transform the nature of variable renewable technologies by combining individual strengths and weaknesses [8]. These combinations of one or more renewable sources and a possible storage system are one way to diversify the renewable energy portfolio that helps avoid the intermittency created by the power sources. Distribution of the renewable capacity among different technologies will smooth the aggregated renewable output [9]. The effectiveness of the distribution depends on how complementary the technologies are. Including various renewable power production in the portfolio provides a more stable combined output. Airborne Wind Energy (AWE) could provide this energy diversification due to its versatility and adaptability. AWE is a wind energy concept that uses tethered kites to capture more stable wind resources at variable and higher altitudes.

AWE is an emerging wind energy technology [10] still in the early development phase. AWE systems operate at higher altitudes than conventional wind turbines (100 – 500 meters) [10]. Due to this higher operating altitude, the tethered kites experience more constant and stronger wind speeds than turbines at lower altitudes. In addition to the capability of flying at higher speeds the AWE systems can also vary the height of operation to the optimal point, resulting in less variable energy production compared to conventional wind energy technologies [11]. The dominant form of onshore and offshore wind energy is the horizontal axis, three-bladed turbine. Many turbine types have been commercially viable for a long time and are installed in great capacity globally [12]. A comparison of the two main AWE concepts and a conventional wind turbine can be seen in Figure 1.1.

Several types of AWE systems are in development today, the main difference between them being the kite and generation types [13]. The two most researched kite types are fixed-wing and soft-wing kites, which can be seen in Figure 1.1. The other main distinction is the generation type, whether energy is generated at the ground or the kite. Both these concepts rely on crosswind flight operation and were first described by Loyd [14]. Fly-generation systems have a generator located at the kite that directly converts aerodynamic energy to electrical energy that is transmitted down through the kite. For ground generation systems, a tethered kite flies crosswind patterns while unwinding a winch at the ground. A generator connected to the winch produces energy while the tether is winding out, this is called the reel-out phase. When the tether reaches its limit, the kite glides down and the tether reels in. During this reel-in phase, the generator consumes energy. These two phases are the pumping cycle [15].

The reeling phases of the pumping cycle with their corresponding power output can be seen in Figure 1.2. The tethered kite operates at varying altitudes, alternating between reeling out the kite, producing mechanical power, and reeling in the kite, requiring mechanical power. The kite is flown in crosswind maneuvers in the reel-out phase to maxi-

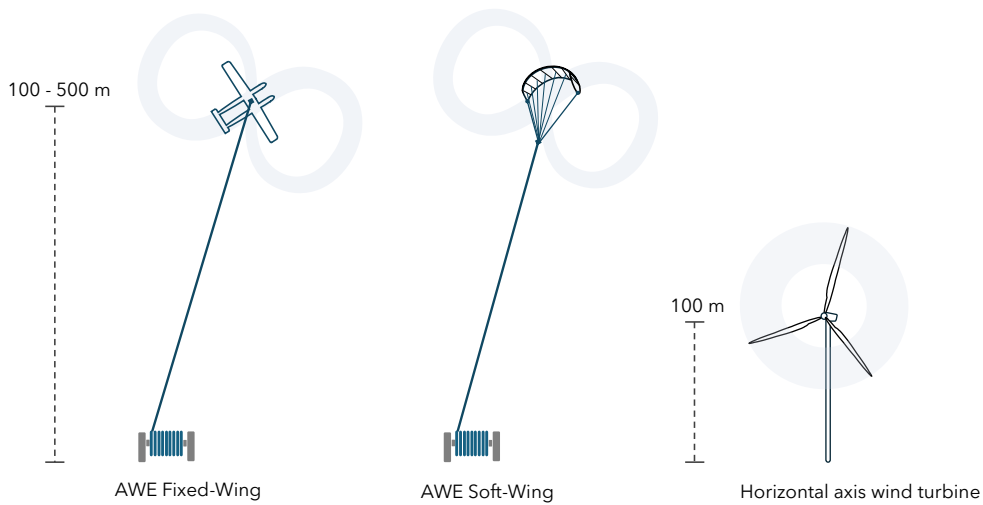


Figure 1.1: Comparison of two ground-generation AWE types and horizontal axis wind turbines indicating operating altitudes

mize the power to the generator. During reel-in no maneuvers are performed, instead, the kite is flown to a minimal tether length to require the least amount of energy. As such the reel-in phase consumes only a small fraction of the energy generated during the reel-out phase [15]. The variable energy within the pumping cycle results in oscillating power, to supply energy to the grid that oscillation requires smoothing. Power smoothing is the application of a storage component for providing a constant power output to the grid regardless of fluctuations that occur during cycle operation.

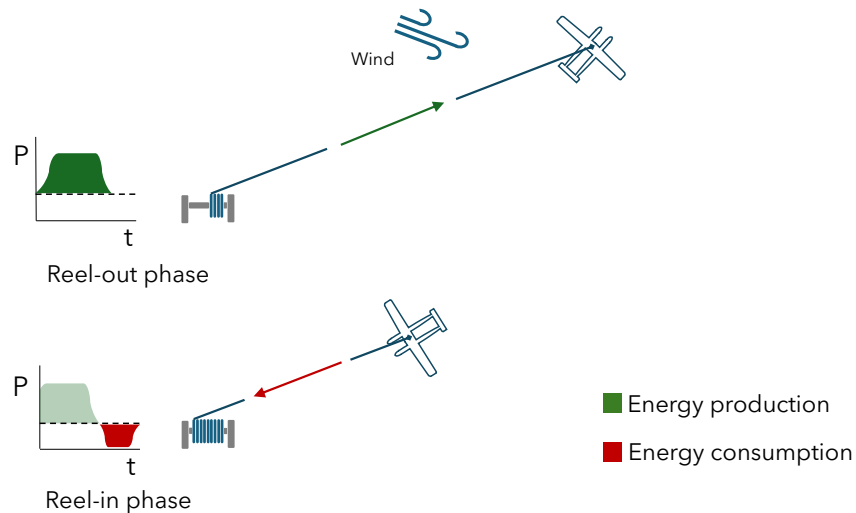


Figure 1.2: Overview reeling phase and power output relative to cycle average.

When considering renewable technologies for energy production the advantages of AWE over conventional wind turbines could prove beneficial in energy generation portfolios.

The high and adjustable operating range provides access to a wide range of wind resources, the small foundation and portable nature of the system lead to flexible implementation and the system is suitable for a wide range of applications. This capture of wider wind resources can be valuable in a HPS as these aim to balance the strengths and weaknesses of generation sources to provide constant energy production. That same constant production improves profitability in electricity markets as this depends on providing energy that is predictable and controllable [16].

As shares of renewable energy sources (RES) on the electricity grid increase, the flexibility of the grid decreases. This is due to fossil-fuel-based power plants such as gas and coal power having the ability to scale their output or dispatch of power. Since RES are not able to do this and on top of that as susceptible to variable resources, reliable electricity supply is harder. Energy storage, such as lithium-ion batteries, is a source of flexibility that can be implemented on the electricity grid. Beyond storage by itself, there is an increased benefit when combining storage with RES, as this can increase the reliability of the energy supply without further stress to the transmission system [17]. The combination of RES power and storage technologies is a hybrid power system (HPS), defined as a combination of one or multiple RES components, such as wind or solar PV energy, and often a storage technology. An overview of an example hybrid power system configuration can be seen in Figure 1.3. Many different configurations exist, as a HPS can be any combination and be configured off-grid or grid-connected.

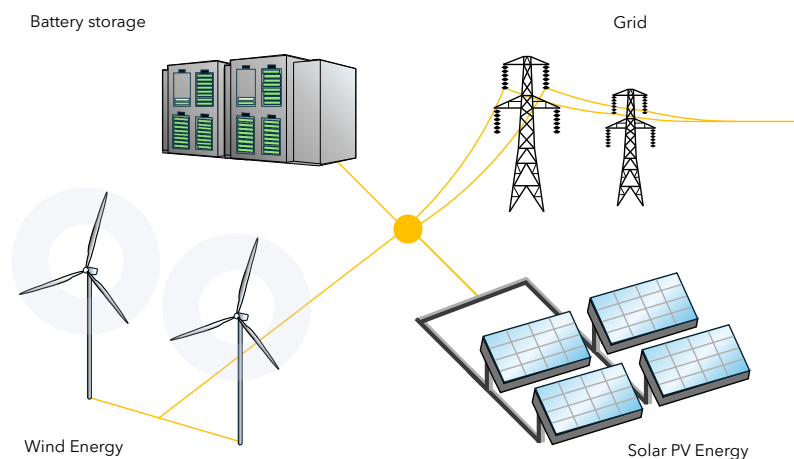


Figure 1.3: Overview components and configuration of grid-connected hybrid power plant

When energy production plants are connected to the grid and participate in electricity markets they are exposed to fluctuating prices. The profit of the plant depends on how well the market value of energy can be captured. An example of one electricity market, the day ahead market (DAM) prices are seen in Figure 1.4. These DAM prices clearly show the dynamics at play when selling energy in this market. The price fluctuation is significant throughout the day, resulting in hours at which energy is produced varying in terms of the market value that is captured for this energy. Due to this many renewable energy technologies are combined with storage systems to improve stability of output and adjust the moment when energy is supplied to the grid. The types of storage applications for this combination are explained further in Chapter 2. The use of storage to shift the moment of dispatch away from the moment of generation is considered energy arbitrage. This arbitrage using storage components of HPPs has been proven to improve revenue-generating capabilities [18]. The extra revenue this generates depends on electricity market dynamics further explained in Chapter 2.



Figure 1.4: Example of DAM price for the NL bidding zone on 20-10-2024 [1].

The basics of arbitrage revenue are the storing of energy at low electricity prices and selling at high prices. The revenue is largely based on the volatility of the price, where higher price fluctuations allow for higher revenues. An intuitive example of how this works is storing energy generated by solar PV at noon during the day and selling it at night. During the point of high PV generation, the prices will be lower due to an excess of generation and at night the prices will be higher due to higher energy demand for lighting and appliances.

This research aims to model a grid-connected AWE-HPS participating in the electricity market and evaluate the results. The model is made using MATLAB and is used to evaluate the economic performance of the AWE-HPS for different configurations under a certain wind and market price environment. Performance metrics describing the cost, profit, and return on investment are calculated to compare the different configurations and assess the market value of each system. An example overview of a grid-connected ground-gen fixed-wing AWE-HPS is shown in Figure 1.5.

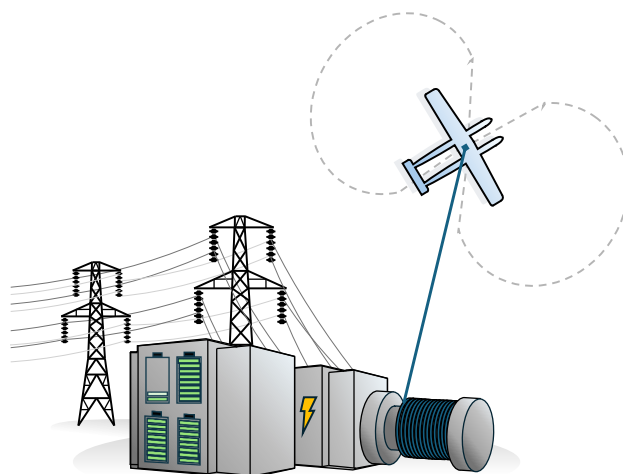


Figure 1.5: Example of AWE-HPS combining pumping cycle AWE with battery storage.

## 1.2. Motivation and aim

Looking at the developments discussed in this chapter, the area of interest for this research is the market value maximization of grid-connected ground-gen AWE systems combined with a storage component. The AWE system's ability to capture consistent wind resources and the opportunities of storage arbitrage point to a need to investigate the profitability of such a system. In this research, the ground-generation fixed-wing AWE system is used combined with the market and wind environment of a particular region in the Netherlands. The concepts and developments researched are valid across multiple contexts however and as such the lessons learned in this research are applicable universally.

This research aims to assess the economic performance of a ground-gen fixed-wing AWE system in grid connection and identify opportunities to increase the value of the system in this grid-connected context.

Problem analysis and formulation of a research question will stem from a literature review. After this, the research approach is carried out. The required background for this research is based both in understanding the AWE and storage technologies as well as the workings of electricity markets and battery arbitrage. The literature review focuses on these aspects.

The report will be presented in the following structure:

- Chapter 2 is the literature review, describing both the background knowledge that is the context of this research and an analysis of the problem by defining the gaps in current research.
- Chapter 3 is about the model developed to answer the research questions.
- Chapter 4 is about the scenarios applied to the developed model to answer the research questions and what analysis using these scenarios shows. The results of the simulated scenarios are then discussed.
- Chapter 6 is about the answer of the research question gained through the application of the developed model, ending in recommended further research.

## 2 | Literature Review

This literature review was conducted to gain knowledge on multiple dimensions of research that underline this thesis topic. Exploration of the background knowledge needed to be able to conduct research on the goals set is summarized in Section 2.1 to 2.3. This exploration will include the state of the art of research relevant to the research goal of this thesis. Section 2.4 includes an evaluation of the areas not covered by present research, the formulation of the research question, and finally the approach set for this thesis to answer the research question.

### 2.1. Airborne Wind Energy

The most commonly studied AWE concepts are ground-gen pumping kite power. Most research is focused on off-grid systems that exclude the power fluctuation effect on the supplied power. Research on power smoothing solutions for AWE systems has been conducted for fixed-wing AWE systems, therefore this thesis considers fixed-wing ground-gen pumping cycle AWE systems.

#### 2.1.1. Pumping cycle

Wind energy has been around for a long time, with large utility-scale horizontal wind turbine plants existing all over the globe. These turbines capture wind energy at heights around 100 meters and represent large shares of the renewable portfolios of many energy systems. This wind energy technology has evolved with many innovations aimed at maximizing the energy yield at their hub heights by controlling the power output through system design and control innovations [19]. Airborne Wind Energy is a new emerging technology that aims to capture more stable winds at higher altitudes. AWE systems can adjust the operation height for the varying wind speeds allowing the kite to operate at the optimum altitude and maximize the potential energy yield [10]. Besides the ability to capture wind energy at variable and higher altitudes the AWE systems also potentially require less material and footprint than wind turbines. The construction of both the kite and the foundation need less material, due to fewer moments and forces being exerted on the system [20].

The main concept of AWE is the ground-generated pumping cycle system. In this AWE system, a tethered kite operates at varying altitudes, alternating between reeling out the kite, producing mechanical power, and reeling in the kite, requiring mechanical power. The reeling phases with their corresponding power output can be seen in Figure 1.2, located in Section 1.1. The variable energy output within the pumping cycle results in oscillating power, to supply energy to the grid that oscillation requires smoothing. Power smoothing is the application of a storage component for providing a constant power output to the grid regardless of fluctuations that occur during cycle operation. This AWE cycle operation can be described using the power profile, which consists of the cycle average, the peaks, and the reel-out and reel-in phases. These power profile aspects define the required power smoothing and depend on the wind speeds. The function of the power smoothing component is to provide constant power to the grid at every wind speed by maintaining the net cycle average to the grid. The power smoothing component is connected between the AWE system and the grid connection [2]. A representation of the pumping cycle energy relative to the net average output can be seen in Figure 2.1. The pumping cycle reeling energy levels depend on the wind speed, as does the cycle average.

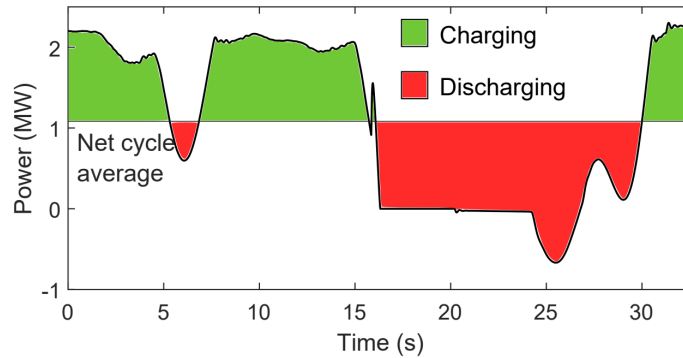


Figure 2.1: Intermediate storage charging and discharging energy areas [2]

Research into the value of AWE-produced energy requires simulation of power output using an AWE power profile. On top of that research into additional value that can be extracted from a power-smoothing storage component requires simulation of the power smoothing profile. These simulated properties can be determined using a model that computes fixed-wing AWE system output. The model used in this thesis is developed by Joshi et al [21], which provides estimations of the net power output of a fixed-wing AWE system. Based on a multitude of inputs that can be set for any number of system properties, the power output of the system is determined. This model simulates a kite as a point mass operated in circular flight maneuvers while reeling out the tether. This operation is divided into segments where for each segment the cycle power is maximized by optimising the operational parameters. These parameters are defined by the kite, tether, and drivetrain properties. This cycle power is used to determine the power output for a wind environment and the reeling power used to obtain this power output. The power output provides an AWE system power curve that can be used to calculate the energy yield for a wind environment. The reeling power at each wind speed can be used to determine the required power and energy for smoothing the oscillating AWE output for connection to the grid.

The AWE performance determined by the performance model developed by Joshi et al [21] can be combined with an AWE cost model developed by Joshi and Trevisi [22] to determine the cost associated with the energy yield. This cost model uses parametric costs that estimate capital expenditures (CapEx) and operational expenditures (OpEx) associated with each component of the defined airborne wind energy system. The cost model take into account a power smoothing component for grid-connection, in this research that component was excluded. By excluding this cost component the model developed in this thesis could determine power smoothing sizing and cost to be able to compare the cost and sizing of different storage technologies.

### 2.1.2. Power smoothing storage

The previous section described the AWE pumping cycle and the corresponding power profile. An intermediate storage component is needed to supply a stable power output to the grid. To use electrical storage technologies for this function, the mechanical power transmitted from the tether to the winch needs to be converted using a generator. The electrical power can then be smoothed before being supplied to the grid. This configuration of electrical power smoothing of an AWE system can be seen in Figure 2.2. In a techno-economic analysis of different storage technologies that can be used for power smoothing, Joshi et al [2] conclude that electrical ultracapacitors are the best technology to be used for smoothing.

The electrical power smoothing utilizing ultracapacitors is efficient due to the high power output at low installed capacities. However, due to the high cost of these systems, it was deemed interesting to investigate the possibility of using a battery system for electrical

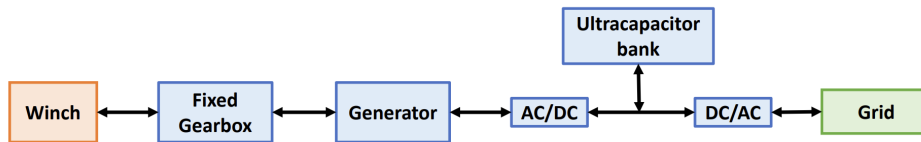


Figure 2.2: Electric power smoothing solution configuration [2]

power smoothing. To understand the storage technology requirements and performance, certain storage aspects need to be understood. These include the C-rate, response time, cycle lifetime, self-discharge, and round-trip efficiency. All these aspects will be described and the corresponding specifications for ultracapacitors and batteries provided. The attributes of both these technologies are described in Table 2.1.

Capacitors can store and release energy through chemical processes, these capacitors are often referred to as supercapacitors or ultracapacitors (UCs). The principle of UCs is the electric double layer, where charge separation exists at the interface between a solid electrode and the electrolyte. UCs are used because they have high power density (500 – 5000 W/kg), long cycle time ( $> 10^5$ ), high efficiency (85 – 97%), fast response speed ( $< 5$  ms), and a long lifetime (about 40 years), and short charging time. However, the drawbacks of UCs are a high self-discharge rate, high capital cost, and low energy capacities [23].

Batteries are long-term energy storage devices, the most widely used and researched of these are Li-ion batteries. Rechargeable batteries operate by an anode that provides electrons and a cathode that absorbs electrons. A separator insulates between the anode and cathode. An electrolyte is responsible for transporting electrons between the cathode and the anode. The advantages of batteries are high energy density (80 – 200 Wh/kg), high power density (500 – 2000 W/kg), long cycle life ( $10^3 - 10^4$  cycles) and low self-discharge. But the corresponding cyclic depth-of-discharge (DoD) can result in low system lifetime [23].

The main difference between UCs and batteries is the cost per installed capacity and the ratio between the installed capacity (kWh) and the rated power output (kW). The capital cost of UCs are in the range of 60 000 €/kWh [24], while batteries could potentially be produced at 130 - 220 €/kWh in the near future. The ratio is called the C-rate of a storage technology, the inverted is also often referred to as the duration of the storage technology. The duration of storage is the length of time a storage system can generate at full output before needing to recharge [25]. Within these defined specifications the duration of a battery at an equal capacity and power would be one hour. This one-hour duration is derived from a full 1 kWh capacity being discharged in one hour at 1 kW output. The C-rate of this same battery would be one, as the ratio of energy capacity over power output is one. Battery systems can be built at varying C-rates but often exist in the range of 0.1 – 2 C. Ultracapacitors have significantly higher C-rates at near 200.

The round-trip efficiency of a storage technology is the energy supplied by the storage device during discharge divided by the energy provided during the charging [6]. This defines the value that can be gained from storing energy since a lower round-trip efficiency lowers the energy that is usable after storage. Alongside the efficiency of cycling through the storage, another metric is the self-discharge rate. This is defined as the percentage of capacity that is lost in the system over a day. For rechargeable batteries, the round-trip efficiency is often in the range of 90 – 97% and the self-discharge rate is at 0.1 – 0.3 %. This makes batteries suitable for long-term storage. UCs have efficiencies of  $> 97\%$ , but self-discharge rates of 5 – 40% per day, making UCs less suitable for long-term storage.

Response time (RT) or ramp rate is the time that a storage system takes to go from rest to

rated output power level. Faster ramp rates correspond with lower response times and a lower response can lead to more value, depending on the application. Response time is mainly determined by inverter selection and storage system design. If low response times are critical to the desired operation, a system design and inverter can be chosen that can respond at the desired rate [24]. Depending on the system design both battery system and UC systems can achieve response times  $<5$  ms [23].

The lifetime of a storage system is defined by both possible full load cycles and possible calendar years. Calendar life is defined as the years a storage system can be operational without degradation due to cycling being taken into account. Cycle life is defined as the full capacity charge-discharge cycles the system can run in its useful lifetime, defined by the lifetime until the useful capacity is 80% of the original capacity. For a storage system under a certain cycling operation, the lifetime is defined by either the cycle- or calendar lifetime depending on which limit is reached first. A significant amount of full-load cycling will lead to an actual lifetime that is significantly shorter than the calendar life [6]. UCs have very high calendar and cycle lifetime at 16 years and  $10^6$  cycles [24]. In the case of batteries, the calendar lifetime is 10 years, while the cycle lifetime is in the range of  $10^3 - 10^4$  cycles [23].

Attribute	Description	UC	Batteries
Cost	Capital cost per unit capacity	60 k€/kWh	130 - 220 €/kWh
C-rate	Ratio power over energy $P/E$	200	1
$N_{\text{cycles}}$	Lifetime in full load cycles	$> 10^5$	$10^3 - 10^4$
$N_{\text{years}}$	Lifetime in calendar years	16	10
RT	Potential response time	$<5$ ms	$<5$ ms
$\eta$	Round-trip efficiency	$> 97\%$	90 - 97%

Table 2.1: Comparison of attributes of electrical storage technologies

The use of UC technology in its application of power smoothing AWE produced energy has been researched and proven in previous research [2]. The use of batteries for this same application could provide the potential for additional value to the system due to the attributes described in Table 2.1. The feasibility of the use of batteries depends on the grid requirements for power smoothing, these are described further in Section 2.2.2. The additional value of the battery system depends on the market dynamics that allow value addition through storage capacity, these dynamics are described further in Section 2.3.2.

### 2.1.3. Market value of Airborne Wind Energy

The pumping cycle operation has been proven to work and generate energy, however no commercial models yet exist to prove the commercial viability. In a study on the state of the art for niche wind energy technologies at lower technology readiness levels (TRL), an assessment was made for AWE. As of 2023, they found AWE to be at TRLs ranging from three to five, generally considered the discovery and development phase [12]. TRL three is considered as the level where the concept has been proven, TRL five being the level at which the technology is validated in the relevant environment [26]. The next phase after this would be the deployment phase, where commercial models of the technology are implemented.

Given the current state of AWE technology, research is currently focused on modeling AWE

systems and building prototypes. In terms of researching the technology diffusion of AWE, a study that modeled scenarios for the development and market growth of AWE showed a substantial decrease in AWE cost in the future [3]. This study concludes that the levelized cost of energy (LCoE) of AWE will end up at a lower cost point than onshore wind energy, as can be seen in Figure 2.3. These projections are based on several assumptions, however, such as the growth evolving similar to the historical growth of established wind technologies. The cost model described in Section 2.1.1 computes the LCoE of a 100 kW fixed-wing AWE system at current cost levels to be 158 €/MWh, significantly higher than the LCoE levels shown in Figure 2.3. The LCoE does not factor in the value of the generated electricity quantified by the electricity price and is therefore not the only metric to research when determining the value of AWE-produced energy.

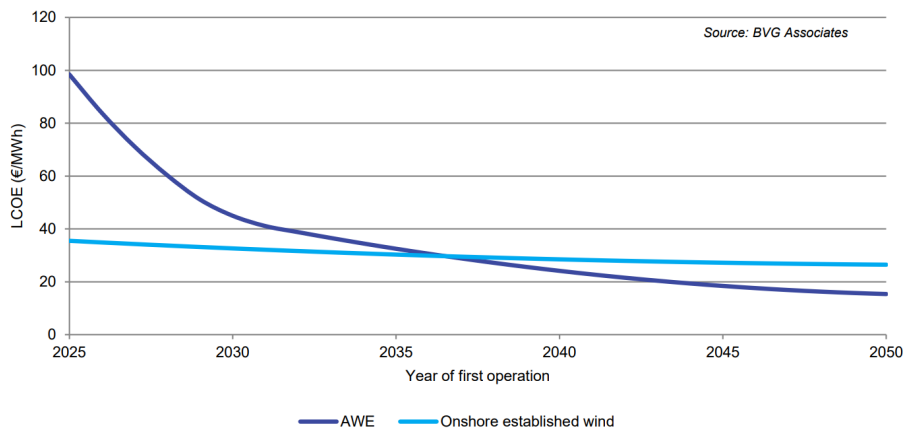


Figure 2.3: Average LCoE of AWE and onshore wind turbine technologies [3]

Studies exist on the added value of commercial AWE to the electricity system. Malz et al [27] created a framework for including the effect of varying market electricity prices in assessing AWES performance. Using the framework, the marginal value of an incremental increase in AWE share of the electricity system is calculated. This marginal value represents the change in electricity system costs when more AWE is included in this system. This study concluded the increased AWE share will not increase the overall wind energy share, showing the value of AWE is highest when replacing wind turbines. The concluding added value of AWE that was found is based on an AWE LCoE of 35 - 45 €/MWh. The analysis done in this study shows there is economic value to AWE commercial models as a part of the electricity system. The LCoE connected to this value, however, is significantly lower than the current cost models.

Considering one of the advantages of AWE is the portability and scale-ability of the system, one study focused on the optimal sizing of a HPP using AWE for off-grid applications. Reuchlin et al [28], developed a model that determines the optimal sizing of AWE, solar PV, batteries, and diesel generators by optimizing for the lowest overall LCoE. This study concluded an added value of AWE due to the lower battery requirement needed to supply a load. The framework does not include scenarios of grid-connection and as such does not show the added value of AWE for a system exposed to price fluctuation.

Another use case based on the portability and low overall mass of AWE systems is harvesting wind energy on Mars, researched by Schmehl et al [29]. This research analyses the performance of a combination of AWE, solar PV, and short-term battery storage to power a subsurface Mars habitat. The Mars AWE-HPP was proposed by Ouroumova et al [30], in an aerospace engineering design synthesis exercise at the TU Delft. The proposed HPP was further studied for feasibility by Rodriguez [31], who implemented a QSM model to more accurately determine the potential. In this AWE-HPP, intermediate storage was in-

cluded for power smoothing but not used for additional storage capacities. The system was scheduled for an operation that optimally uses AWE and solar PV energy to supply the habitat demand. Different system design configurations showed the effect of using multiple smaller AWE systems in phase-shifted operation, reducing the required intermediate storage for buffering AWE output.

The potential value of AWE compared to wind turbines was researched by Vos et al [32]. They found that onshore AWE outperforms conventional onshore wind due to higher wind resource availability and the AWE generation profile. The AWE generation profile was found to sometimes complement conventional onshore turbines, showing the potential of combining these wind energy technologies. The main limiting factor for deployment of AWE on a large scale was found to be the achievable power density per ground surface area. Considering the AWE system costs and learning curve of 3% used in the analysis, it is possible that AWE deployment could become competitive in the energy sector in the 2030s.

Joshi [33] researched the system design and revenue generation of Airborne wind energy in his 2020 thesis. Using ERA5 wind data and ENTSOE DAM price data (both at a resolution of 1 hour) the effect of wind conditions on DAM prices was analysed for three locations. The effect of different performance metrics (LCoE, NPV, LRoE) on the system design of an optimal AWES is significant, showing the case for value-driven design when participating in the DAM.

The commercial viability of AWE systems is hard to determine due to the phase the technology is currently in. Most energy yields reported for AWE are simulated potential yields. Due to this fact, the actual system design and costs of commercial models are as of yet uncertain. The research on commercial viability relies on either using current prototype model costs with the application of a learning curve on the associated costs or using projected future costs on a component level. The application of a learning curve has been done by Reuchlin et al [34]. In this research, the costs of a specific Kitepower model were taken and a learning curve similar to the historic learning curve of horizontal wind turbines was applied.

Joshi and Trevisi [22], developed parametric cost models aimed at estimating capital (CapEx) and operational (OpEx) expenditures associated with each AWE system component. These cost models were created using contributions from AWE companies, tether and ground station manufacturers, suppliers, and university research groups to provide input. These contributor inputs were combined with publicly available reports and articles to ascertain cost references. These costs represent current system costs and commercial performance is subject to AWE technology policies such as Feed-in-Tariffs (FIT) in terms of potential revenue.

## 2.2. Hybrid Power Systems

Hybrid power systems exist in different configurations and sizes and offer several advantages to separate energy systems. The advantages of output stability and its effect on economic performance and considerations are addressed in many studies. Many of the existing installed HPPs include storage systems for optimal dispatch, these storage components serve multiple purposes in a HPP.

### 2.2.1. Hybrid Power Profitability

Traditionally, in a power system dominated by fossil fuel-based energy production, the power output is directly related to the fuel used. Shifts in required energy can easily be facilitated by increasing the fuel consumed. In a power system with high shares of renewable energy, the power is related to natural resources such as sunlight and wind speed and as such can not be influenced to produce more energy to meet demand. The effect of RES share in the global energy system in terms of intermittency can be seen in Figure 2.4. This figure shows the research by Mulder et al [4], where the effect of intermittent energy sources was analyzed and the need for storage quantified. The daily and seasonal mismatch between energy generation and demand were simulated.

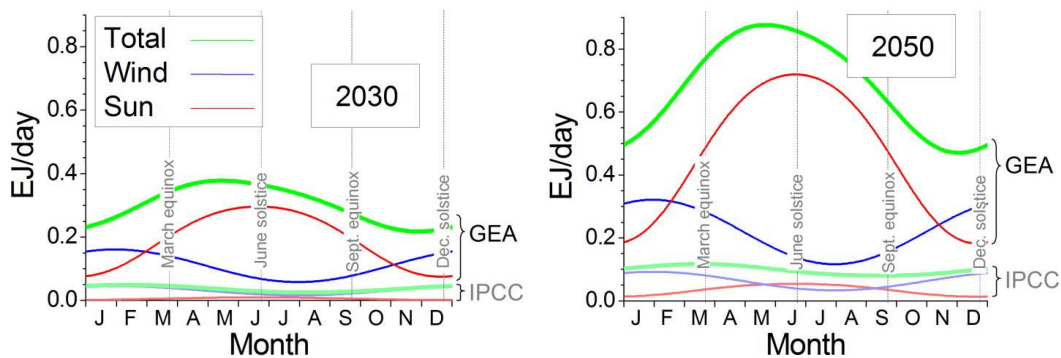


Figure 2.4: Estimated output per day of wind and solar power in the months of the years indicated [4].

Intermittency has resulted in a lot of studies and applications for storage systems that can provide the inertial response (IR) that renewable power cannot provide inherently. This is why many RES power plants are combined with storage capacity to provide a more stable plant output to the grid. A HPP is a combination of one or more renewable energy sources and usually, but not always, a storage system. Value synergy between the sources and storage can then be attained, in terms of shared and stable, and predictable output on a plant level.

HPP research generally focuses on the profit of the plant to assess the added value of combining or co-locating the different sources. The value of co-location depends on the anti-correlation between renewable sources which determines the capacity factor of the whole plant. There is value in the stable dispatchability of a power plant. The different HPS types can be seen in Figure 2.5, these combinations represent the additional values synergy they can provide. Wind and solar PV can complement the energy yield of each other, while

storage components can store that energy yield for later moments, shifting the dispatch over time. For the storage component of a HPP the value lies in the added value of shifting energy temporally. The value of shifting energy over time can be internal or external, by either storing energy to discharge at moments of higher prices or to improve the stability of the plant [16].

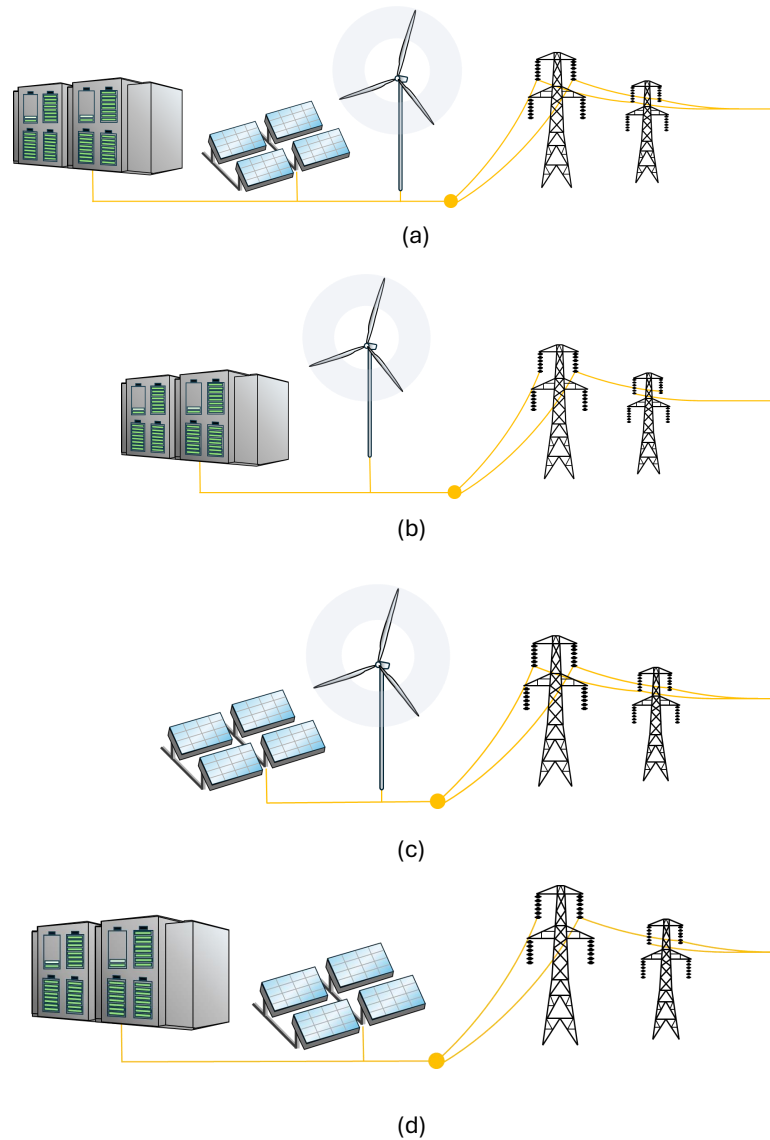


Figure 2.5: Possible grid-connected HPS configurations: (a) Wind + PV + Storage, (b) Wind + Storage, (c) Wind + PV, (d) PV + Storage.

To research the impact on grid connection and infrastructure use of hybrid power plants, Vattenfall has built a HPP in the Netherlands, at Haringvliet. A picture of the Haringvliet HPP can be seen in Figure 2.6. Operational since 2021 it consists of 22 MW of wind energy, 38 MW of solar PV energy, and 12 MWh of battery storage. Its operation is evaluated for the production time, to review the increased flexibility due to co-location [35]. Thus far they have found a reduction in the costs of the combined operation compared to separate plants, due to utilization of shared grid connection and control. Additional revenue is possible since the HPP is less dependent on subsidies to participate in markets [5].



Figure 2.6: The Haringvliet hybrid power plant, operated by Vattenfall [5]

Modeling the economic performance of a HPP depends on multiple factors, such as which markets the plant operates in and how profit is modeled. Zhu et al [36] researched HPP profitability and found that perfect forecast assumptions impact the modeled profit significantly. Perfect forecast assumption is explained further in Section 2.3. A lot of value in HPP configurations with storage lies in the storage system's ability to compensate for errors made in the predicted output of the renewable produced output. Zhu et al found that wind forecast errors affected the HPP profit a lot more than the market price forecast. This shows an opportunity for HPP storage components to gain profit from imbalance resolutions in high wind power penetrated bidding zones.

Dykes et al [16] have researched the opportunities for renewable hybrid power plants and their participation in several market types. They find that combining different variable energy sources and storage technologies increases both the overall revenue in trading produced electricity and the ability to participate in capacity markets due to the stability provided. The effect of renewable energy moving to subsidy-free operation affects HPP participation in different markets were analyzed. Several market archetype scenarios that are shown describe that sizing of the HPP system varies significantly based on the market context applied.

The growth of renewable energy production and the increased focus on hybrid power plants have resulted in several studies that focus on HPP market interaction and profitability. These studies involve either the combination of wind and batteries or wind, solar, and batteries. While the motivation and goals are often aligned, the methods tend to differ. Since there are several methods to assess both economic profitability and technical potential, these studies show the possibilities in assessing market interactions of HPPs using AWE.

Van Holthoon [37] in his 2021 thesis describes the market types a HPP can participate in. The research concluded no significant added value of combining storage and wind at the current battery technology costs and further described the revenue to occur independently of its combination with wind power. Participation in Day-ahead and free bidding/contracted frequency restoration were modeled to maximize Net Present Value. Mehta et al [38] also researched the value synergy of wind energy and batteries, with special focus given to the influence of market participation on the added value of batteries in the system. Their analysis showed batteries added value in the frequency restoration market but battery costs were too high for added value in spot market participation. However, the main objective was to compare against wind-only cases and depends on the use of a wind forecast error function.

From studies on battery systems in HPP configurations, it becomes clear that the costs of both the battery packs and the overall system are an important factor in the added value. NREL projects the costs of battery storage regularly. The latest projections from 2021 show battery system costs of 130 €/kWh for a low costs assessment and 225 €/kWh for a high-cost scenario [39]. Costs were converted from 2020 US dollars to 2020 euros through the exchange rate. These projections are for 2030, a year that was previously used in research on the deployment of commercial AWE systems [34].

Iori et al [40] when researching design drivers for storage systems in HPPs concluded that the storage components come at a significant cost. The optimal sizing of the storage in an HPP was found to depend significantly on the storage cost assumptions used. The storage costs assumption used in this research is based on an NREL report on storage modeling inputs. In this report from NREL [6], the future cost reduction of battery systems was projected. These projections show battery costs of 38% relative to 2019 values for an optimistic scenario and 75% in a conservative scenario. They conclude that cost reductions will be higher for long-duration batteries (low C rate) than for short-duration batteries (high C rate). The cost projections can be seen in Figure 2.7.

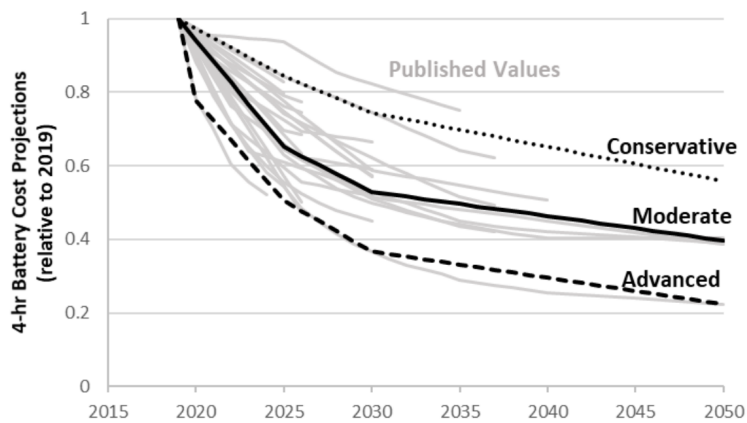


Figure 2.7: Conservative and advanced cost projections of utility-scale battery system cost [6]

### 2.2.2. Power stability

Power smoothing of Renewable Energy has been researched since these technologies have penetrated the electricity market. Storage systems have become crucial to high temporal imbalances between electricity supply and demand. Energy storage systems (ESS) are used for various purposes in the electricity system such as frequency regulation and renewable energy smoothing. Application of batteries in these different usages have different requirements for integration with power systems [41]. The stability of the grid can also be provided through the transmission of energy from other locations, mitigating the intermittency. This increase in transmission capacity is a great remedy to the intermittency of renewable power but should be combined with other solutions, due to the stress on the grid this transmission represents, resulting in congestion of the electricity network [9].

There are two types of renewable energy smoothing that the storage component of a HPP can provide. Smoothing of the HPP output is required since the frequency of the grid should be maintained within prescribed limits. The first is the smoothing of the power output due to the randomness of renewable sources, where the storage component compensates when the output of the RES drops. An example of this is a sudden drop in wind speed resulting in a low wind turbine output. The second type is a high-frequency smoothing of a

power output resulting from operations such as the pumping cycle AWE. This pumping cycle smoothing was described previously in section 2.1.

Both types of smoothing are defined by the prescribed limits of the grid. These limits are defined in a ramp rate relative to the active power. In the case of most European countries, the power ramps should remain within 10-20% of the active power within the timescale of a minute [2]. In weaker regions, i.e. where the frequency is harder to maintain, Transmission System Operators (TSOs) often achieve stability by active power curtailment. The ramp limits are adopted to not have to resort to these measures. Ramp limits are often assumed at the 10% rated capacity/minute [42]. However, more recent studies in grid frequency ramp rates and energy storage systems have concluded this value is too strict for the best development in power systems [43].

For smaller power plants that can be connected to the distribution network, these ramp limits depend on the regulations set by the relevant DSO. In the case of DSOs in the Netherlands, these regulations include considerations of the technical specifications of the energy-producing unit. Agreements can be made between energy-producing plants and DSOs that widen the ramp limit band to allow certain power fluctuations that occur to ensure optimal exploitation of the energy production [44].

Studies have been conducted on the applicability of batteries for power smoothing of different sources when connected to the grid. System control strategies are developed to provide battery systems with a measure of smoothing response. These control strategies synthesize the rotating mass and damping effect of large, high-mass generators [45]. Using these strategies battery systems can be used for higher frequencies of power fluctuation. In the case of smaller power plants connected to the distribution network, battery systems are considered suitable for power smoothing. This is because many distribution networks that connect renewable energy sources utilize a battery system at substations to further smooth grid power [43].

In the application of batteries for smoothing power fluctuations in renewable energy output there is a trade-off between battery effort and the degree to which the power is smoothed [46]. Given the response times of certain batteries of less than 5 milliseconds and the ramp limits of the respective networks to which HPPs are connected, power smoothing of high and low frequency can be performed by battery systems. It may even be that given the low depth of discharge of power smoothing AWE energy, the resulting microcycles have a positive effect on the battery lifetime. Soto et al [47], studied the impact of microcycles on li-ion batteries and concluded that the microcycles have a negligent effect on battery performance degradation. It was even found that in some cases these microcycles can have a positive effect on the performance lifetime.

## 2.3. Electricity markets

To identify possible maximization of market value for AWE systems a basic understanding of the dynamics of electricity market trading is required. The goal of this section is to describe the different electricity markets. In this section, the detailed working of the markets that allow for additional market value is discussed.

### 2.3.1. Electricity market types

Since the diffusion of renewable energy technologies in global energy production there has been a large growth of the share these technologies have in the market. The cost of producing electricity by ways of wind and solar plants have decreased significantly and continues to do so. Due to this increased competitiveness in the market, there will be a shift in the strategies that maximize the revenue of renewable plants [16]. The electricity market is comprised of multiple types that work differently. The main difference is whether the traded commodity is either produced electricity (at a particular moment) or available capacity (over a certain time frame). Electricity producers exchange their produced power on different market types, transmission of the power is handled by the transmission system operator (TSO) and distribution of power to consumers is handled by the distribution system operator (DSO). The following market types exist:

- **Forward and Future market** This market type involves parties that either supply or demand energy and can agree upon trading a certain amount of produced energy on a timeframe of years up to a day before the actual consumption of the electricity. This type of trading provides certainty and reduces risk exposure to availability and pricing.
- **Day-ahead market** As the name implies, the day-ahead market (DAM) contains bids offered one day before the delivery time of the electricity. Suppliers offer their expected produced electricity per hour over the next day for the price they will sell for. Consumers submit their electricity needs per hour over the next day and the price they are willing to pay. The hourly electricity price is the price at which all demand is met by the supply. Every participant pays/receives this price regardless of the offered/submitted willingness [37].
- **Intra-day market** This market handles bids offered within the 24-hour timeframe of a day. The main function of this market is to react to any imbalance between agreed offers and demands. This market includes trades up to minutes before delivery and varying electricity delivery duration.
- **Balancing market** Due to the nature of other markets being a reliance on the prediction of future production and consumption of electricity, imbalance within the system can occur. To avoid a failure of the electricity grid, the TSO is responsible for maintaining the frequency of the grid. To achieve this they maintain contracts with entities that offer balancing capacity. The TSO passes on the costs of fixing the imbalance to the party responsible for the imbalance [37]. Traditionally renewable energy has not participated in this market type due to the intermittency reducing the ability to offer stable capacity [16].

Within the context of this thesis, the focus is on the DAM. Participation in this market type requires bids for all hours of the next day to be submitted at noon [48]. The minimum bid volume is 0.1 MWh for most countries in the EU [49]. Power plants that produce energy bids within the range of the DAM in Europe can be connected to the Transmission network of high-voltage lines or the distribution network of middle-voltage lines. In the case of the Netherlands, wind power plants of multi-MW rated powers are usually connected to the transmission network, and wind power plants below 1 MW are connected to the distribution network [50]. For DAM participation both network types can be considered.

Supply and demand are matched in the DAM by dispatching generators that offer power in the order ranging from lowest to highest price. The highest price offered by a generator that is dispatched is the market clearing price for that hour. The ordering of dispatch based on price is known as the merit order. Renewable plants typically offer power for low prices and therefore the share of renewable plants in a bidding one effects the clearing price. As can be seen in Figure 2.8, the clearing price within the represented hour of the DAM results in capacity offered at prices higher than the clearing price not being dispatched.

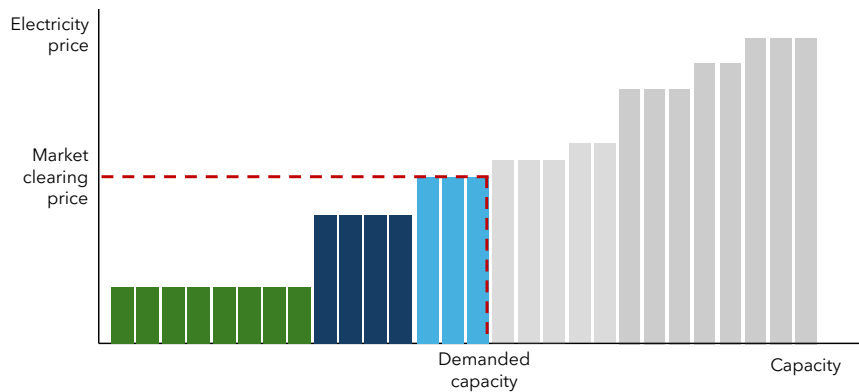


Figure 2.8: DAM merit order market clearing price determination

### 2.3.2. Storage arbitrage

In addition to the internal storage of RE-generated energy, a HPP can generate revenue by participating in energy arbitrage. Storage energy arbitrage involves the purchase of energy from the market for charging the battery. At a moment when the price is higher due to high demand, the battery can discharge to resell the energy at a gain. This capture of these price differences over time is researched most often in the DAM [51]. Modeling battery arbitrage is done under a set of assumptions, in the case of small capacities the assumption is often that the system is a price taker. This means the energy traded does not affect the price of said energy. The objective of these models is to maximize the revenue of the system by ensuring the difference in income and cost between the bids is optimal. These bids are modeled using an uncertainty factor between the predicted prices and the actual prices [52]. A large number of studies focused on energy arbitrage assume perfect foresight, meaning the aforementioned uncertainty is modeled as zero. This results in the model operating on assumed knowledge of future prices [51].

Beyond the assumptions of the model there is a wide range of modeling methods employed to simulate the optimal dispatch of a battery system used in arbitrage. These include heuristics, linear programming (LP), mixed-integer linear programming (MILP), mixed-integer non-linear programming (MINLP), and mixed-integer quadratically constrained programming (MIQCP). These models determine optimal bids for each hour of the DAM within the constraints of the storage system (energy and power limits, SoC limits). Heuristic models use insights into market dynamics to determine an operational strategy that would result in positive economic performance. One example of this is a model that operated the battery system at certain hours of the day for two cycles during the day [53]. Another case of a heuristic model is Mercier et al [54], where a heuristic model was used for operating the BESS to research the effect of dynamic SoC limits on the performance when

maximizing NPV. Heuristic models are often developed when optimization models are difficult to operate due to complex constraints.

The revenue from battery arbitrage depends on many factors, mainly the round-trip efficiency and battery cost. The round-trip efficiency influences the difference in energy bought and energy sold, limiting the net gain. A study researching the different storage arbitrage methods found a large variance in performance [55]. This study reviewed multiple bidding zones over multiple years to assess the volatility of the value of arbitrage. An important metric for comparing battery arbitrage performance is the value of storage arbitrage (VoSA). This metric is the yearly revenue from arbitrage relative to the installed capacity, the calculation of this metric can be seen in equation 2.1.

$$\text{VoSA} = \frac{R_t}{E \cdot C} \quad (2.1)$$

where:

$R_t$  = yearly revenue of arbitrage [k€]

$E$  = storage total capacity

$C$  = storage C rate or  $P/E$

By calculating this metric for different bidding zones and years, Mercier et al [55] found that storage arbitrage has a low marginal value beyond storage durations of 4 to 6 hours. For perfect foresight pricetaker simulated arbitrage, they found VoSA values of varying degrees but in the range of 1 - 135 k€/MW/year. In bidding zones and years deemed normal DAM volatility the values range around 20 - 40 k€/MW/year.

## 2.4. Problem analysis

Based on the literature review, this section contains the problem analysis. The previous sections of this chapter described the state of the art of research focused on the subjects underlying this thesis topic. Section 2.4.1 describes the research elements that are found to be missing. Following this Section 2.4.2 and Section 2.4.3 present the research question and methodology that result from the literature review respectively.

### 2.4.1. Research gap

The current research into the added value of AWE in a HPP is based on the optimization of the LCoE and only considers the off-grid application of the HPP. Grid connection would lead to different economic performance of the HPP due to exposure to fluctuating market prices. On the subject of AWE system market value capture, there is research focused on the system design of the AWE in grid-connected applications. This shows promising results for AWE systems within price fluctuating revenue context. The added value of AWE within the context of a grid-connected HPP has not been researched and could show a different configuration of HPP than the current configuration derived from off-grid LCoE-based HPP research. There is a need to investigate what AWE HPP configuration performs best when exposed to price fluctuation. This area has not been explored in the literature.

The pumping cycle ground-gen AWE system, when connected to the grid, requires an intermediate storage solution to smooth the power oscillation. Current configurations make use of ultracapacitor components for this application. From the literature study it is known that battery technology development and distribution network dynamics are evolving and power smoothing is increasingly viable using batteries. It is therefore beneficial to study the opportunities that arise from using batteries for this power smoothing component in the context of a grid-connected AWE battery HPP.

The literature study shows that in HPP configurations that contain battery systems, this storage is used in multiple functions. These battery systems improve the overall stability and dispatchability of the entire plant. Several AWE HPP systems exist, using battery systems to temporally shift the use of the AWE-generated energy. When the power smoothing component is changed from an ultracapacitor to an oversized battery, the oversizing results in an excess battery capacity that can be used much like a typical HPP battery component. There has thus far not been research into such a combined use of the storage component of a HPP. Determination of the value that can be obtained from using the power smoothing excess battery capacity would be beneficial for insight into AWE system design in grid connection.

### 2.4.2. Research Questions

Following the gap in research as defined in the previous section, the following research question is defined:

In a scenario of grid connection, how can the value of hybrid power systems using airborne wind energy be maximized?

To answer this question, several sub-questions are defined as follows:

1. To what extent can grid-connected profitability be increased when replacing the ultracapacitor intermediate storage with a battery system in the configuration of an Airborne Wind Energy system?
2. To what level can the excess capacity present in the battery power smoothing storage be used to increase profitability?

### 2.4.3. Methodology

To answer the research questions, a model will be developed for the operation of a grid-connected AWE system with a storage component for use in both power smoothing and battery arbitrage. The model will use wind and market resource data, as well as AWE performance metrics. This model will be able to determine the economic performance of an AWE-Batteries HPP in different configurations. Using the model, four scenarios consisting of different configurations of the system will simulate the value of the energy sold in each scenario.

The following steps will be taken to answer the research questions:

- Develop a model that simulates an AWE system using either a battery or ultracapacitor component for power smoothing purposes to compute the excess battery capacity and compare performance and cost.
- Develop a model for simulating a battery system participating in the electricity market that can incorporate the combination of power smoothing operation and market participation.
- Simulate the energy production, storage, and bidding of four different scenarios; an AWE system using an ultracapacitor for smoothing, an AWE system using batteries for smoothing, a battery system used in electricity market arbitrage, an AWE system using a battery system for smoothing and using the excess capacity in market arbitrage.

# 3 | Model Development

This chapter describes the model developed to answer the research questions. Section 3.1 shows a high-level overview of the developed model, Section 3.2 describes the input parameters used for the configurations, Section 3.3 explains the AWE component of the model, Section 3.4.1 explains the battery performance model, Section 3.5 explains the bidding operational strategy and Section 3.6 describes the outputs of the model and how these are used for value assessment. The model alongside all corresponding input files will be made available on the GitHub repository: <https://github.com/awegroup/AWE-HPS-DAM>.

## 3.1. Model overview

The model is developed in the MATLAB environment and has several distinct components. The model has two main input types - AWE and storage specifications and the scenario inputs for the four scenarios defined as described in Chapter 4.

The flowchart of the framework in Figure 3.1, shows the interface between the input data and the desired output data. The left side represents the system inputs while the right side represents the performance modelling. The Scenario parameters represent the configuration components and the required inputs to simulate the performance. This consists of wind and market price data, as well as system components used. These components are described in detail in Section 3.2.

The AWE performance is acquired by inputting the AWE specifications of the scenario into an AWE performance model developed by Joshi et al [21]. This model provides the power curve, and respective power smoothing power and energy levels per wind speed. The power curve is fitted and then used in combination with the wind speed data to calculate the AWE energy yield. The power smoothing levels are used to calculate the intermediate storage system sizing for both UC and Battery components. This is described in more detail in Section 3.3.

The storage performance determines the storage power and energy capacities based on the requirements of AWE power smoothing. The storage technology selected in scenario parameters determines the storage performance and capacities.

The bidding dispatcher determines the operation of the AWE-HPS in terms of bidding to the DAM market. Considering the dynamic nature of the constraints on the battery available capacity and power due to combined power smoothing and DAM bidding applications, a heuristic model for arbitrage operation is developed for this research. The model aims at operating arbitrage at local price peaks while maintaining power smoothing operation, the arbitrage operation is described in more detail in Section 3.5.1.

Using the performance previously described, the economic performance of the HPS system is evaluated based on cost, profit and return on investment. The assessment is based on the following performance metrics; the levelized cost of energy (LCoE), the levelized revenue of energy (LROE), the net present value (NPV), the internal rate of return (IRR) and the value of storage arbitrage (VoSA). This assessment is described in more detail in Section 3.6.

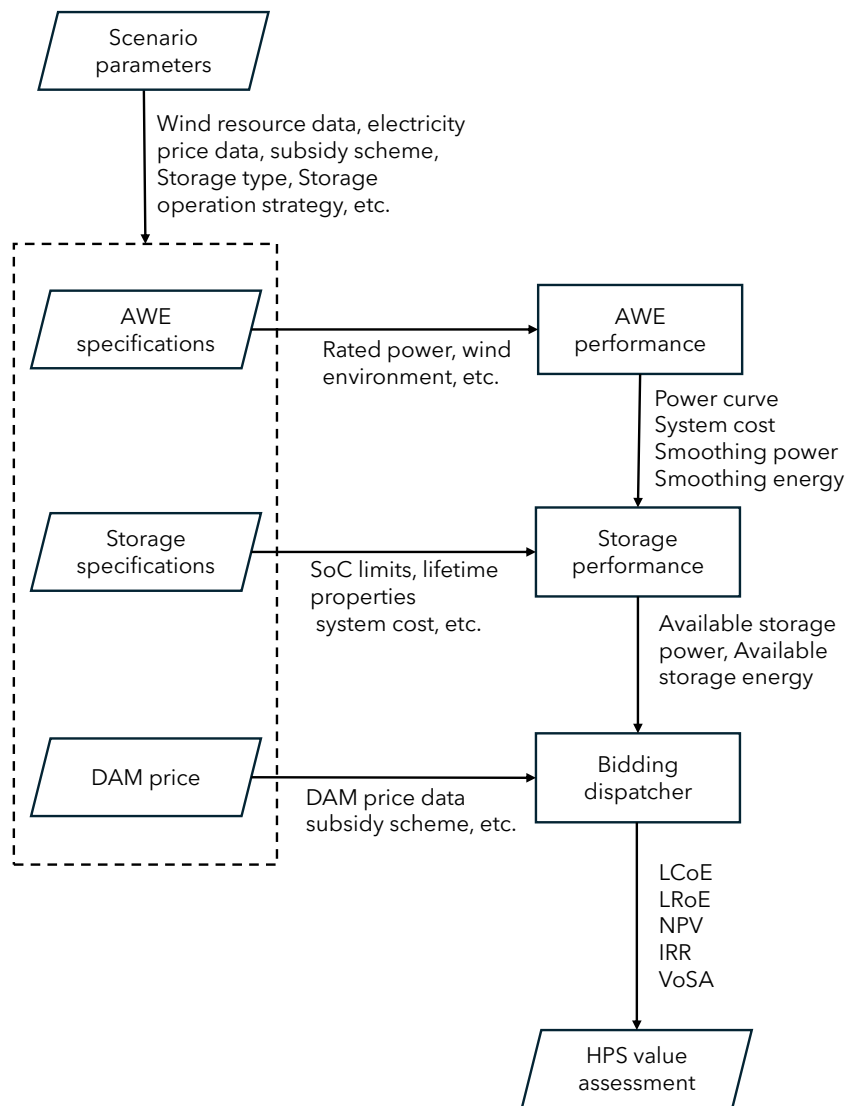


Figure 3.1: Overview of the HPP value assessment framework.

## 3.2. Scenario parameters

The range of scenario parameters is discussed in this section. An overview of the four scenarios of this thesis is presented alongside the corresponding inputs. Following this, a description is given of how the wind and market data are obtained and analyzed. Locations are selected based on the availability of data and suitability for HPP operation.

The simulated performance of the model operation is determined for each timestep of the simulation throughout a full year. The discrete timestep of the model is one hour, based on the DAM bids operating over one hour and the availability of wind environment data. Wind data will consist of wind speed data from ERA5. Market data consists of DAM pricing from ENTSO-E. To determine the levelized costs the lifetime of the project is assumed to be 25 years, where the operation is based on 25 consecutive iterations of the same year in terms of inputs used.

As described in Section 2.4.3, the model was developed to simulate and compare four different scenarios. These scenarios all consist of different configurations of power systems simulated within the same wind and market environment. The different parameter inputs of the four scenarios are shown in Table 3.1.

	Scenario 1: AWE + UC	Scenario 2: AWE + Battery	Scenario 3: Battery arbitrage	Scenario 4: AWE + Battery arbitrage
AWE system	100 kW	100 kW	-	100 kW
Storage system	UC	Battery	Battery	Battery
Storage application	Smoothing	Smoothing	Arbitrage	Smoothing and Arbitrage

Table 3.1: Overview input parameters per scenario

Locations suitable for the HPP framework are based on the wind speed and DAM price data. Initial location analysis based on current HPPs being operational at several locations already. The location selected is Haringvliet, since this location has a HPP already in operation [56]. This HPP, called Haringvliet Hybrid Powerplant is operated by Vattenfall and is a utility-scale plant used for gathering data to research the value synergy of wind power and battery storage. As illustrated in the model overview in Figure 3.1, all scenarios require wind speed and market data as inputs for the model. These time-series data were taken for the year 2019 since for this year both resources had complete data sets and are representative of a normal operating year. Others years since 2019 have in some instances been less than representative due to political or other external influences on the market. The DAM pricing from ENTSO-E was taken from the database and is consistent throughout the whole bidding zone of the Netherlands [57]. The wind speed data taken from the ERA5 database was taken for the coordinates of Haringvliet. Both these datasets can be seen in Figure 3.2.

The ENTSO-E Transparency platform was used to obtain the DAM price time-series data. ENTSO-E stands for European network of transmission system operators for electricity. It is comprised of transmission system operators from countries across Europe. The ENTSO-E platform is responsible for publishing data related to electricity generation, transmission, and consumption of the European market. The DAM price obtained for the NL bidding zone in 2019 has moderate volatility, with a standard deviation of 0.11 €/MWh. The average price in this bidding zone in 2019 was 41.2 €/MWh. A trend can be seen on an an-

nual basis, showing higher pricing in the winter months relative to the summer months. The average price in winter is 43.9 €/MWh whereas the average summer price was 38.5 €/MWh.

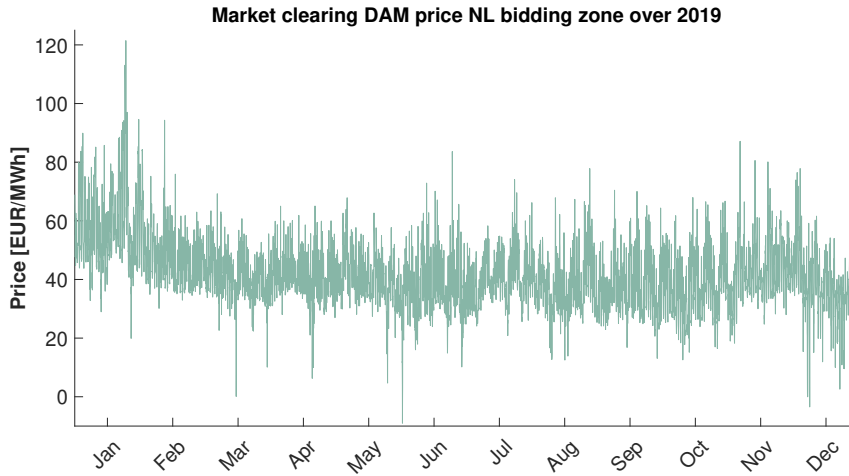


Figure 3.2: Day Ahead Market price hourly over 2019

The wind speed data is obtained from the ERA5 database [58]. The data represents the hourly wind speeds at 100 meters altitude over the year 2019 at the location of Haringvliet. The location is filled in by using coordinates, Haringvliet is at 4.49 longitude and 51.92 latitude. These coordinates were used to obtain the wind speeds which can be used to determine AWE performance. The ERA5 database consists of reanalysis data, meaning past observations and contemporary weather models are combined to simulate conditions for a specific location and time. The wind speed data is therefore a realistic representation of the wind speed at the selected location, regardless of measurements taken at the location and time specified. ERA5 obtained data consists of wind speeds in both u- and v-direction. This means these speeds have to be combined to calculate the hourly overall wind speed. The combined wind speed is calculated by taking the square root of the sum of u and v directional wind speeds squared. This calculation can be seen in Equation 3.1.

$$v_w = \sqrt{v_{w,u}^2 + v_{w,v}^2} \quad (3.1)$$

where:

- $v_w$  = Wind speed
- $v_{w,u}$  = Wind speed in u-direction
- $v_{w,v}$  = Wind speed in v-direction

As can be seen in Figure 3.3, the wind speed is highly variable with the same minor seasonal trend with higher average wind speeds in winter (8.2 m/s) and slightly lower wind speeds in summer (6.3 m/s). The overall average wind speed at 100 meters high was 7.2 m/s.

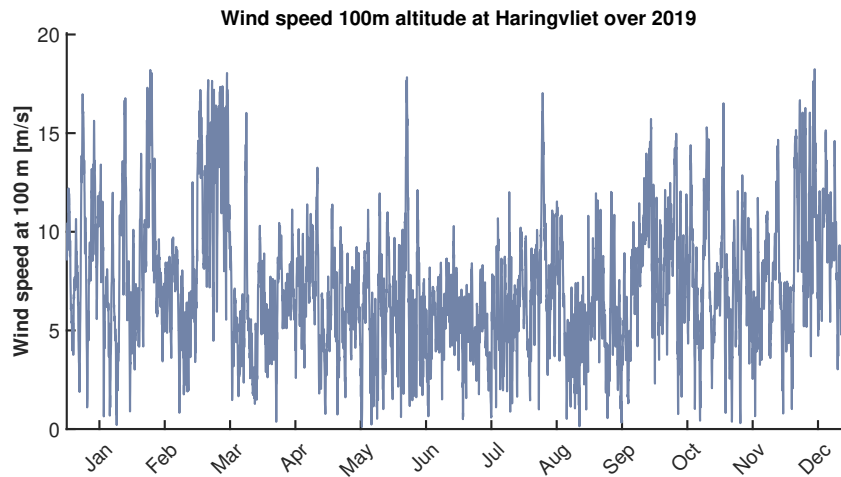


Figure 3.3: Wind speed at 100 m altitude hourly over 2019

### 3.3. Airborne Wind Energy Performance

This section describes and analyses the method of determining the performance of the airborne wind energy component of the HPP. The system energy production and LCoE will be evaluated.

#### 3.3.1. Power curve

Fixed-wing AWE as a technology is still in the research and development phase. Considering this, no operational data is available since there are no commercially installed systems. Therefore power estimations of the AWE have to be made in order to simulate the energy production of the AWE component. Due to the nature of the research questions, mainly the focus on the power smoothing aspect of the AWE system, an AWE model that computes multiple aspects of the performance is required. The power curve, being a set of output power per wind speed, is required to simulate the AWE power at each hourly wind speed at the specific location. In addition to that, certain data is needed on the system performance at those wind speeds concerning the reeling power, as these will influence the power smoothing requirements of a storage system. The AWE performance model developed by Joshi et al [21], was used to provide the necessary data.

The power output in the specified wind environment is generated using the AWE performance model developed by Joshi et al [21]. This model provides estimations of the net power output of a fixed-wing AWE system. Based on a multitude of inputs that can be set for any number of system properties, the properties used for this research can be found in the input file of the repository linked in this report. The most important of these properties are listed in Table 3.2. This model simulates a kite as a point mass operated in circular flight maneuvers while reeling out the tether. This operation is divided into segments where for each segment the cycle power is maximized by optimising the operational parameters. These parameters are defined by the kite, tether, and drivetrain properties. This cycle power is used to determine the power output for a wind environment and the reeling power used to obtain this power output.

Parameter	Description	Value
$P_{\text{rated}}$	Electrical rated power	100 kW
$P_{\text{gen, rated}}$	Electrical generator rated power	200 kW
S	Wing surface area	20 m <sup>2</sup>
AR	Aspect Ratio	10
$F_{\text{t, max}}$	Maximum tether force	40 kN
$l_{\text{t, max}}$	Maximum tether length	3500 m
$\alpha$	Wind shear exponent	0.12

Table 3.2: Properties as input variables for AWE power estimations

The power curve, representing the power output per wind speed, provided by the performance model given the properties set is shown in Figure 3.4. The model can be used to generate power curves for different configurations of fixed/wing ground/gen AWE systems, with the currently shown curve representing a 100 kW system defined by the inputs in Table 3.2. These power curves can then be used in combination with wind speed data to generate AWE component energy performance. As can be seen in Figure 3.4, the rated power of 100 kW is attained at wind speeds of 10 m/s, close to the average wind speed at the Haringvliet location.

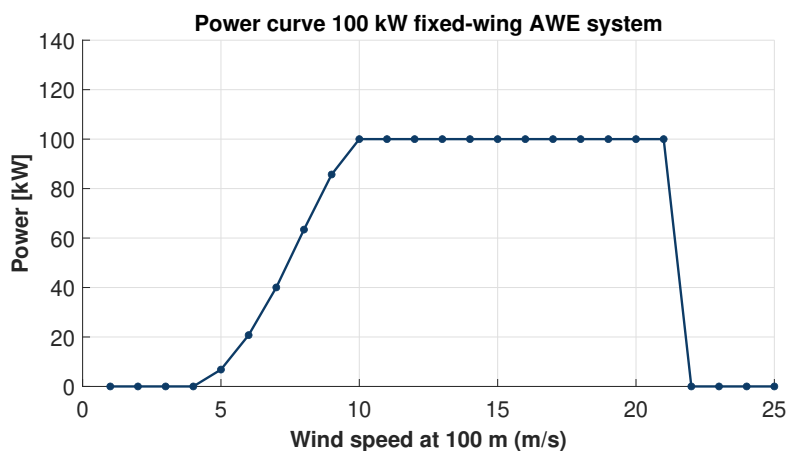


Figure 3.4: Power curve of 100 kW AWE system

The power curve represented in Figure 3.4 combined with the wind environment determined in Section 3.2 can be used to generate the hourly AWE production. The power production at each time point of the simulation is determined by assessing the wind speed at each point of the hourly wind speed series and storing the corresponding power output of that wind speed in a power time-series. Considering the resolution of the wind speed data is in five significant figures, whereas the power curve output provides values for each integer wind speed value, the power curve has been fitted to allow power output values between integer wind speeds. The hourly power production series is shown in Figure 3.5. Within the wind speed context of the chosen location, the AWE system has an Annual Energy Production (AEP) of 492 MWh and a capacity factor ( $C_f$ ) of 0.56. The capacity factor

is a metric of how optimally the AWE system is operated, the calculation of this metric is shown in Equation 3.3. Equation 3.4 illustrates that within the simulations of this research, the value of energy at any timepoint is equal to the power value. This is because the resolution of the simulations is defined at one hour, meaning producing any value of kW over one hour is equal to that value of energy in kWh.

$$\text{Capacity Factor} = \frac{\text{Annual Energy Production}}{\text{Maximum Annual Output}} \quad (3.2)$$

$$C_f = \frac{\sum_{t=1}^{t=8760} E_{e, \text{avg}}}{8760 \cdot E_{\text{rated}}} \quad (3.3)$$

$$E = P \cdot t = P \quad (3.4)$$

where:

$t$  = Time instant in hours

$C_f$  = Capacity factor

$P_{e, \text{avg}}$  = Electrical average power output at hour  $t$

$P_{\text{rated}}$  = Electrical rated power

As can be seen in Figure 3.5, the yearly overview clearly shows more frequent and higher power output in the winter months. The close and high output in March is the clearest example. The lower and more spread-out peaks in the summer months (June and July) clearly show the relatively lower output in summer. This corresponds to the analysis of the wind speed data in Section 3.2.

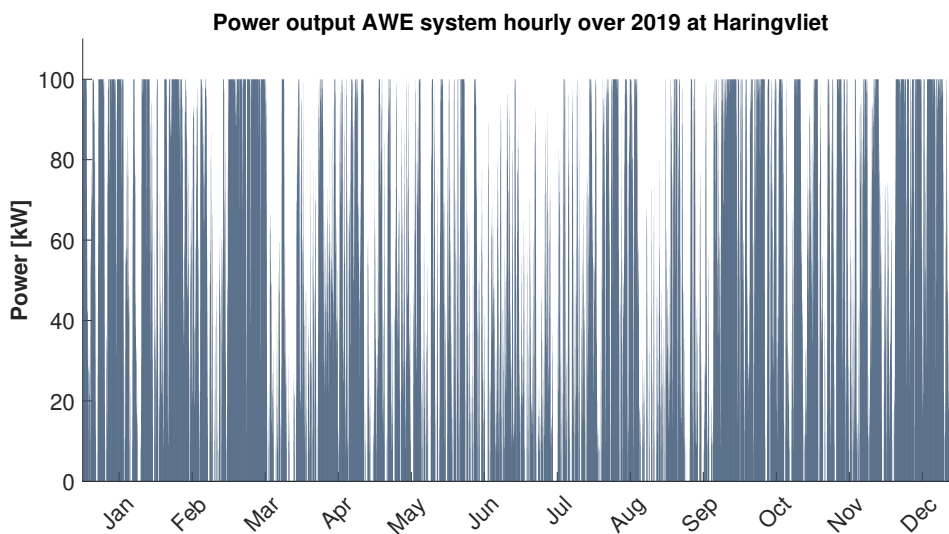


Figure 3.5: Power output of 100 kW AWE system in specified wind context

### 3.3.2. Intermediate storage

In addition to the power curve, the performance model also provides the cycle power and total energy required for smoothing per wind speed. These can be used to determine the power smoothing energy and power at each time point of the simulation. The maximum needed energy and power of the smoothing can also be used to determine the required specifications of the intermediate storage technology used. The power output needed for smoothing is determined by the maximum mismatch between the rated output and the power produced or consumed by the AWE system. This mismatch can be seen in Figure 3.6, where the reeling power peaks  $P_{m,o,peak}$  and  $P_{m,i,peak}$  can be seen alongside the average power output  $P_{m,avg}$ . This figure shows the reeling power at rated wind speed. The smoothing power

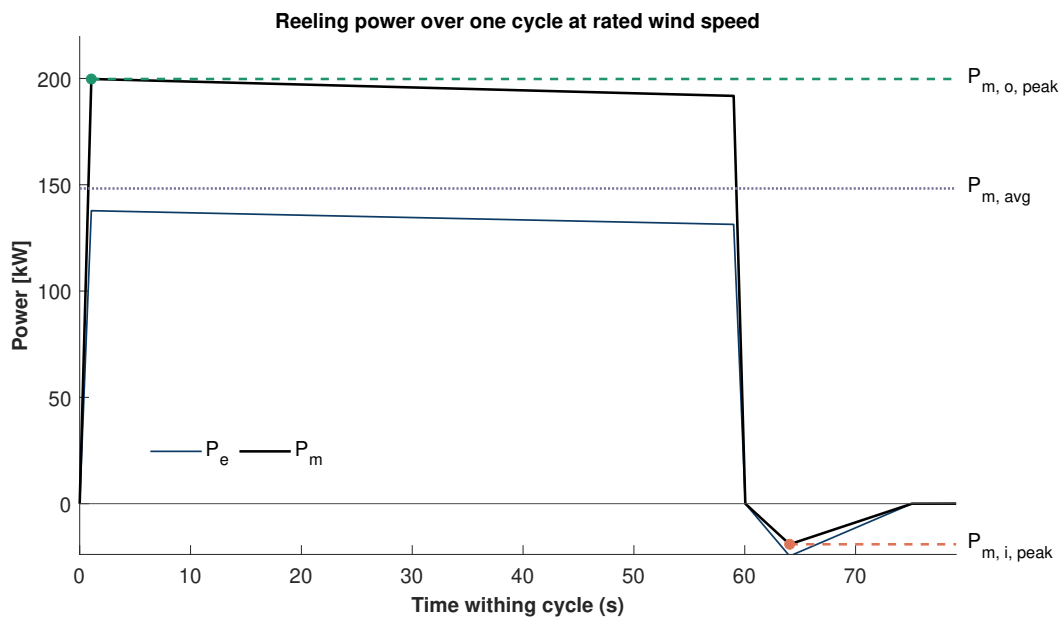


Figure 3.6: Reeling electrical power at rated wind speed 100 kW AWE system

The energy capacity needed for smoothing is determined by the difference in produced energy during reel-out and consumed energy during reel-in, relative to the average cycle energy. These energy levels can be seen in Figure 3.7, where the difference between average cycle energy ( $E_{m,avg}$ ) and produced reel-out energy ( $E_{m,o}$ ) can be seen represented by the green area. The consumed reel-in energy ( $E_{m,i}$ ) combined with the average cycle energy ( $E_{m,avg}$ ) can be seen as indicated by the orange area. Both these energy levels represent the excess or deficit relative to the average. Since the average cycle power is by definition the average of the power throughout the cycle, the green and orange energies are equal to each other. Both represent the smoothing energy needed at rated wind speed.

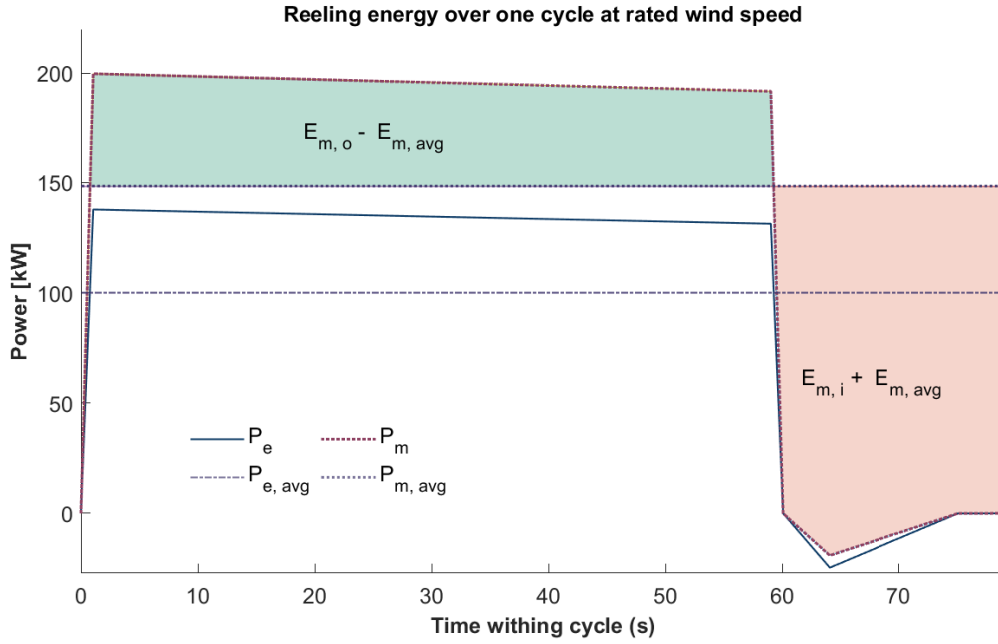


Figure 3.7: Reeling energy at rated wind speed 100 kW AWE system

For this system, the maximum intermediate energy that needs to be stored is 0.93 kWh and the maximum intermediate power output is 139 kW, both occur at cut-out wind speed. In the case of an ultracapacitor being used the installed capacity is based on the smoothing energy needed. The maximum energy needed to smooth the power of a cycle at cut-out wind speeds is taken from the AWE performance model. In the case of a battery system, the installed capacity is based on the maximum power needed. The battery C type determines what capacity of the battery is required to be able to supply at minimum the maximum power needed for smoothing. The calculations for the smoothing power i.e. the power of a battery system can be seen in Equation 3.5 and 3.7.

$$P_{sm, max} = \max \left[ P_{m, o, peak} - P_{m, avg}, | P_{m, i, peak} - P_{m, avg} | \right] \quad (3.5)$$

$$E_{sm, max} = E_{m, o} - \int_{t_{o, start}}^{t_{o, end}} P_{m, avg} dt = E_{m, i} + \int_{t_{i, start}}^{t_{i, end}} P_{m, avg} dt \quad (3.6)$$

$$E_{Batt, req} = \max \left[ \frac{P_{sm, max}}{C}, E_{sm, max} \right] \quad (3.7)$$

where:

$P_{sm, max}$	= Maximum smoothing power
$P_{m, avg}$	= Average cycle power
$P_{e, m, peak}$	= Peak reel-out mechanical power
$P_{i, m, peak}$	= Peak reel-in mechanical power
$E_{sm, max}$	= Maximum intermediate smoothing storage
$E_{m, o}$	= Produced energy during reel-out
$E_{m, i}$	= Consumed energy during reel-in
$E_{batt, req}$	= Required battery capacity
$t_{o, start}$	= Start of reel-out phase
$t_{o, end}$	= End of reel-out phase
$t_{i, start}$	= Start of reel-in phase
$t_{i, end}$	= End of reel-in phase
C	= Battery C-rating or $P/E$

### 3.3.3. Cost of Energy

The cost of producing energy using the AWE system can be calculated using an economic model that works in tandem with the QSM model used to compute the AWE performance. This cost model provides parametric costs that estimate CapEx and OpEx associated with each component of the defined airborne wind energy system [22]. The components of the AWE cost can be seen in Figure 3.8.

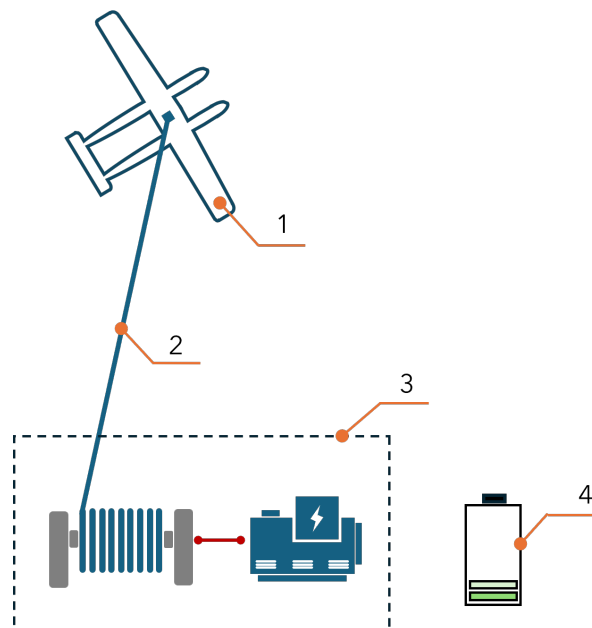


Figure 3.8: The four components of the AWE system; 1. Kite; 2. Tether; 3. Ground station; 4. Intermediate storage

The Capital (CapEx) and operational (OpEx) expenditures of the 100 kW AWE system are shown in Table 3.3, calculated using the economic model [22] set to the AWE specifications identical to those in Table 3.2. Power smoothing storage would generally be part of the ground station costs but considering the importance of this cost component has been

separately considered for this research. The cost of this fourth component, the intermediate storage, depends on the price per unit capacity and the frequency of replacement of the storage over the lifetime of the project. The use of an optimistic and conservative cost for battery systems and the replacement frequency that determines the OpEx will be discussed in detail in Section 3.4.1.

Component	CapEx	OpEx
(1) Kite	329 k€	0 k€
(2) Tether	7.4 k€	6.2 k€
(3) Ground station	88 k€	0 k€
(4) Ultracapacitor	55 k€	6.3 k€
(4) Battery optimistic	18.2 k€	1.82 k€
(4) Battery conservative	31.5 k€	3.15 k€

Table 3.3: Overview cost of AWE system

The total CapEx of the AWE system with ultracapacitor is 479 k€, and the total OpEx is 12.5 k€, also in the case of ultracapacitor use. Using these costs in addition to the AEP of the AWE system and a discount rate, the levelized cost of energy can be calculated as follows:

$$\text{Levelized Cost of Energy} = \frac{\text{Total lifetime costs}}{\text{Total lifetime energy production}} \quad (3.8)$$

$$\text{LCoE} = \frac{\text{CapEx} + \sum_{t=1}^T \frac{\text{OpEx}}{(1+r)^t}}{\sum_{t=1}^T \frac{E_t}{(1+r)^t}} \quad (3.9)$$

where:

- t = Time instant
- LCoE = Levelized cost of energy
- T = Economic lifetime of the project
- CapEx = Capital expenditures
- OpEx = Operational expenditures
- $E$  = Energy produced
- r = Discount rate

The LCoE of the AWE system with ultracapacitor is calculated using the CapEx and OpEx values as seen in Table 3.3, the AEP of the simulated year taken as the production at each year of the project lifetime and a discount rate of 10 %. The discount rate of 10 % was chosen since this rate is generally used for the economic assessment of wind energy projects. The LCoE of the AWE system is calculated as being 158 €/MWh, which is significantly high when compared to the average DAM price of the simulated context (41.2 €/MWh). As the costs modeled are not from a commercial AWE system but rather a conceptual model they do not represent the costs of a system when installed. To assess the costs of producing relative to the value of the produced energy this factor will have to be compensated.

This can be done by applying a learning curve compensation on the system costs, which can be done for learning curves observed for horizontal axis wind turbines. An alternative method is to apply a subsidy scheme to the DAM price data. To retain the cost model accuracy of the AWE cost used in this research, the subsidy scheme method is used. The application of a subsidy scheme is described in further detail in Chapter 4.

### 3.4. Storage Energy Performance

In this section, the component of the battery performance of the model is described. It explains the method to model the use of the battery component for smoothing and for arbitrage.

The previous section has described how the wind speed data time-series is used to obtain hourly time-series for the AWE power, smoothing power, and smoothing energy. Combining these series with the DAM price time-series means the storage performance can be obtained. The storage performance is modeled by calculating the state of charge (SoC), the percentage of capacity used, at each time point. It is modeled as a calculation of the SoC at the next time point where the rate at which it charges or discharges is defined by the operation, with round trip efficiency taken into account at discharging the battery. This operation of the storage system is defined by smoothing and/or DAM arbitrage and changes the available capacity and power as well as the time points where the battery operates. The performance metrics will be described first, then the calculation of the SoC will be described, followed by detailed descriptions of the effect of each operation type.

Parameter	Description	Value
Cost	Storage technology cost	€/kWh
$N_{\text{cycles}}$	Lifetime of unit	cycles
$N_{\text{years}}$	Lifetime of unit	years
$\text{SoC}_{\text{min}}$	State of charge lower limit	%
$\text{SoC}_{\text{max}}$	State of charge upper limit	%
$\eta$	round-trip efficiency	%

Table 3.4: Scenario input parameters for Storage performance

#### 3.4.1. Battery smoothing performance

The SoC of the battery as well as the rate at which it changes is limited by the specifications of the storage technology used. These specifications result in limits to the operation. In the case of the storage system only being used for power smoothing, the energy capacity of the battery used is defined by the smoothing energy per wind speed obtained in Section 3.3.2. The power of the storage used is defined by the power per wind speed. Considering the smoothing energy is intermediate and cyclical it is calculated as a capacity of the storage reserved for smoothing and taken as constant throughout a timestep. In addition to this reserved capacity, the depth of discharge (DoD) of the smoothing energy is calculated. This is needed since the energy used for smoothing is intermediate but it is an energy level charged and discharged several times throughout a timestep. Also due to the cyclical nature, the smoothing power per wind speed is a representation of the maximum power required of the storage component within a cycle. As such the smoothing power is calculated as the maximum power level needed for smoothing within a timestep but is not related to the energy level of the storage component.

$$E_{\text{res}, t} = E_{\text{sm}}(v_w, t) \quad (3.10)$$

$$P_{res, t} = P_{sm} (v_{w, t}) \quad (3.11)$$

$$E_{sm, t} = \frac{E_{res, t} \cdot 3600}{t_{cycle}} \quad (3.12)$$

where:

- t = Time instant hour
- t<sub>cycle</sub> = Cycle trajectory time
- E<sub>res, t</sub> = Reserved smoothing energy at hour t
- P<sub>res, t</sub> = Reserved smoothing power at hour t
- E<sub>sm</sub> (v<sub>w, t</sub>) = Smoothing energy at wind speed v<sub>w</sub>
- P<sub>sm</sub> (v<sub>w, t</sub>) = Smoothing power at wind speed v<sub>w</sub>
- E<sub>sm, t</sub> = Total energy cycled through storage capacity at hour t

The intermediate storage sizing is described in Section 3.3.2, and the resulting component sizing is shown in Table 3.5. An ultracapacitor smoothing storage is sized according to the maximum energy required. This energy level is the intermediate storage required at rated wind speeds, represented by E<sub>sm, max</sub> in Equation 3.6. A battery smoothing storage is sized according to the maximum power required. This maximum required power is represented by P<sub>sm, max</sub> in Equation 3.5.

Storage type	C rating	Power [kW]	Energy [kWh]
Ultracapacitor	200	186	0.93
Battery	1	140	140

Table 3.5: Storage technology sizing for power smoothing

To assess the effect of using either of these technologies for the smoothing component of the system the degradation of the storage system is modelled. Storage components are deemed to need replacement when they are at a point where the capacity is at 80 % of the original capacity. This moment is defined by the lifetime in terms of cycles. The cycles represent the amount of full-capacity cycles the storage can run before being degraded at 80 %. The battery degradation can therefore be calculated in terms of replacement frequency per year using Equation 3.13.

$$f_{repl} = \max \left[ \frac{1}{N_{years}}, \frac{\sum_{t=1}^{t=8760} E_{sm, t}}{E_{batt, max} \cdot N_{cycles}} \right] \quad (3.13)$$

where:

- $f_{\text{repl}}$  = Yearly replacement frequency  
 $E_{\text{sm}, t}$  = Total energy cycled through storage capacity at hour  $t$   
 $E_{\text{batt}, \text{max}}$  = Capacity of storage system  
 $N_{\text{cycles}}$  = Lifetime cycles  
 $N_{\text{years}}$  = Lifetime years

The replacement of the storage system directly factors into the OpEx of the entire HPP system and is affected by the storage technology used and the amount of energy that goes through the battery system. As can be seen in Equation 3.13, the system is either replaced after the lifetime of the technology is reached in years or after the amount of full load cycles has reached the lifetime cycles, whichever is reached first. This calculation does not account for the effect of microcycles on the degradation of a storage system, this effect was discussed in Section 2.2.2. The oversizing of the installed storage capacity to achieve the charge rates required for AWE smoothing in the case of batteries results in the smoothing discharge cycles for this smoothing being relatively small (<2% of total capacity), Section 2.2.2 described studies that show these type of cycles have a reducing effect on battery degradation.

Using the calculations described in this section the time-series of the smoothing energy and power is obtained. When looking at this battery operation with an ultracapacitor installed, it can be observed that given the specifications of the ultracapacitor, the smoothing uses most of the available capacity at rated wind speeds, seen in Figure 3.9a, and about 70 % of the available power capacity (200 C) at rated wind speed, seen in Figure 3.9.

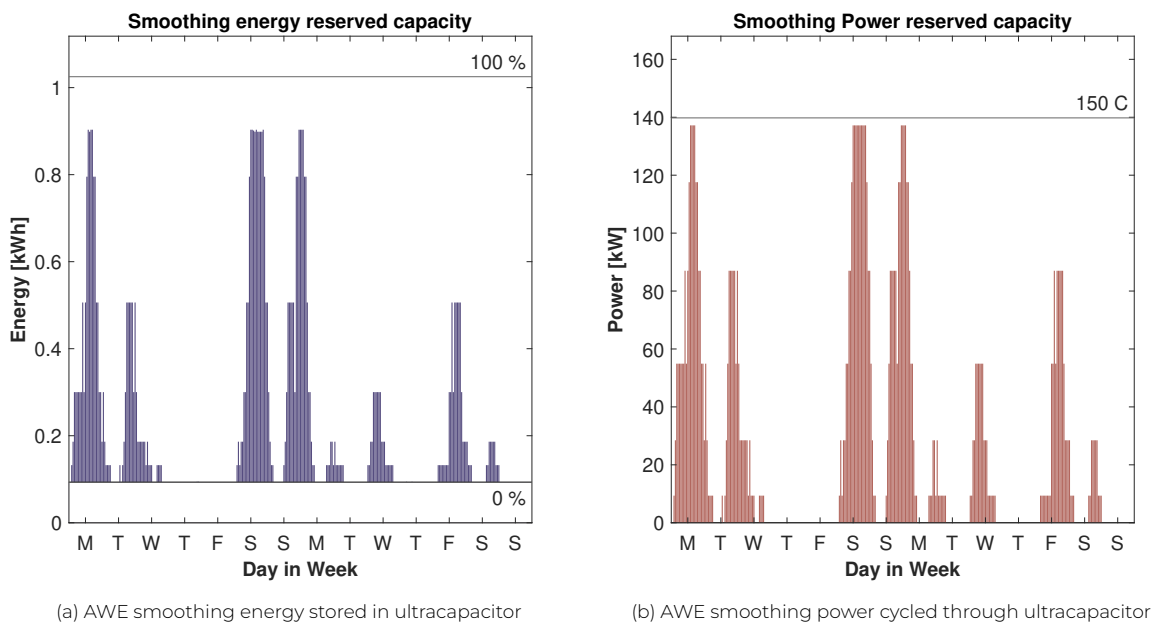


Figure 3.9: Smoothing Energy and Power performance through ultracapacitor

When looking at this battery operation with a battery system, it can be observed that given the specifications of the battery, the smoothing uses an almost insignificant fraction of the available capacity at rated wind speeds, seen in Figure 3.10a, and most of the available power capacity (1 C) at rated wind speed, seen in Figure 3.10b. This is the inverted situation of the ultracapacitor version seen in Figure 3.9. It also shows that outside of rated wind speeds there is significant excess energy and power capacity in the storage system.

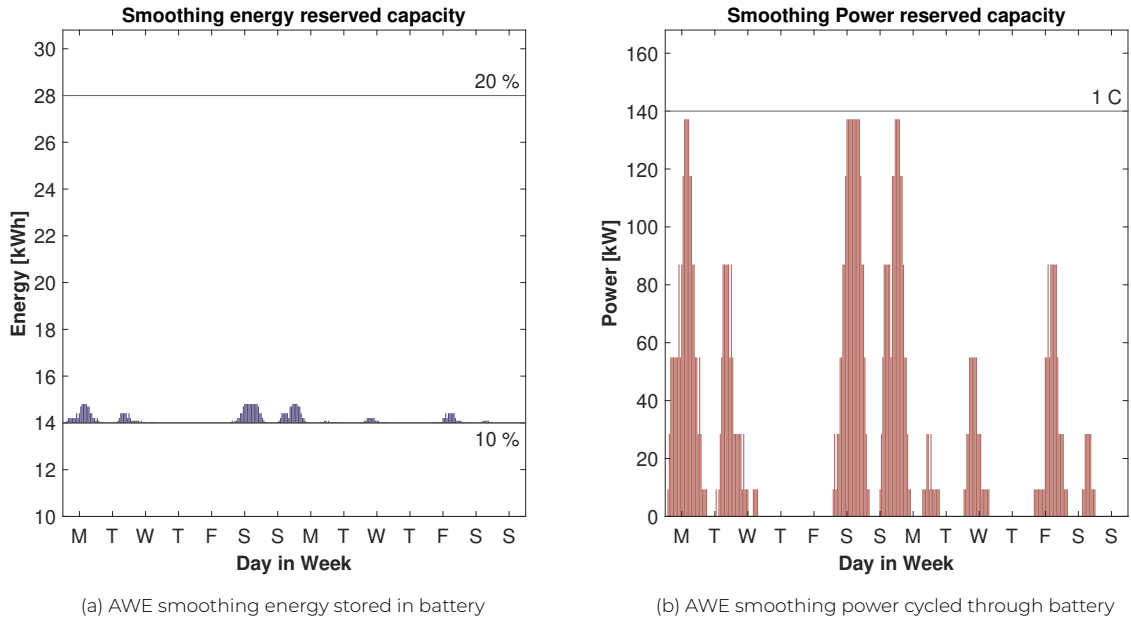


Figure 3.10: Smoothing Energy and Power performance through battery

### 3.4.2. Cost of Storage

The Capital (CapEx) and operational (OpEx) expenditures of the ultracapacitor and battery storage systems as used in the case of power smoothing are shown in Table 3.6. In this use case, the costs of the storage are part of the AWE system. The cost of storage can be measured in the levelized cost of storage (LCoS) and is defined as the cost of storage over the discounted discharged energy of the battery. This can be calculated in the case of using the battery for arbitrage as there is a certain amount of discharged energy traded.

Component	CapEx	OpEx
Ultracapacitor smoothing	55 k€	6.3 k€
Battery optimistic smoothing	18.2 k€	1.82 k€
Battery conservative smoothing	31.5 k€	3.15 k€
Battery optimistic arbitrage	18.2 k€	1 k€
Battery conservative arbitrage	31.5 k€	1.85 k€

Table 3.6: Overview cost of storage system

The total CapEx of the storage system used for stand-alone arbitrage is 479 k€, and the total OpEx is 12.5 k€. Using these costs in addition to the Energy discharged by the battery and a discount rate, the levelized cost of storage can be calculated as follows:

$$\text{Levelized Cost of Storage} = \frac{\text{Total lifetime costs}}{\text{Total lifetime energy discharged}} \quad (3.14)$$

$$\text{LCoS} = \frac{\text{CapEx} + \sum_{t=1}^T \frac{\text{OpEx}}{(1+r)^t}}{\sum_{t=1}^T \frac{E_{\text{dis},t}}{(1+r)^t}} \quad (3.15)$$

where:

- t = Time instant
- LCoS = Levelized cost of storage
- T = Economic lifetime of the project
- CapEx = Capital expenditures
- OpEx = Operational expenditures
- $E_{\text{dis}, t}$  = Energy discharged by storage system
- r = Discount rate

The LCoS of the battery arbitrage system is calculated using the CapEx and OpEx values as seen in table 3.6, the discharged energy of the simulated year taken as the production at each year of the project lifetime and a discount rate of 10 %. The LCoS of the Battery system is calculated as being 66 €/MWh in the optimistic case and 116 €/MWh in the realistic case. These values show the relative cost of storing the energy. However, within the context of this research, the main interest is in the OpEx of the battery system since the case of operating power smoothing and arbitrage combined relies on a context where the battery system is required for smoothing and any added value will add to the revenue of the investment. Therefore the main interest lies in the relation between OpEx and revenue, which will be further described in Section 3.6.

## 3.5. Bidding dispatcher

This research aimed to evaluate the added value that can be extracted from any excess capacity of a storage system. Section 3.4.1 explained how the battery performance modeling lead to the evaluation of excess capacity that is available in the system. This section will focus on the operational strategy of that capacity that could lead to added DAM value capture. Section 3.5.1 explains the operational strategy of a battery system operating in DAM arbitrage. Section 3.5.2 explains the operational strategy of an AWE system with a battery component used for both power smoothing and DAM arbitrage. Section 3.5.3 describes the tradeoffs and optimization of the storage arbitrage bidding.

### 3.5.1. Storage arbitrage bidding

In the case of the storage system only being used for energy arbitrage, the energy capacity of the battery used is defined by a strategy set for buying and selling energy on the DAM. This strategy is typically simulated using an optimization algorithm set to maximize the net gain of trading energy by determining the optimal dispatch of bids. In this research, the modeling of the battery arbitrage is set up to also be able to combine the operation of arbitrage with the operation of power smoothing. It was therefore not within the scope of this research to create an optimization algorithm for this combined operation. Instead, a heuristic approximation of an optimal arbitrage bidding operation is created and used to assess the added value of trading excess battery capacity on the DAM. In this section, the operation of a stand-alone battery system of comparable sizing to the excess capacity of a smoothing battery system is modelled. The arbitrage revenue will not be the optimal dispatch of trade but will show potential added value since it can show the relation between added revenue and additional cost. This method of simulation provides a lower-bound benchmark of storage value from arbitrage.

The participation in the DAM of the model is simulated under perfect-forecast and price-taker assumptions. Perfect forecast results in the system hourly DAM prices being taken as known in advance and with full certainty. The calculated timepoints and charge levels at which the battery charges is therefore assumed to have been bid at noon the day before. The price-taker effect, meaning the energy bids of the battery are assumed not to affect the prices themselves can be confidently made since this is a relatively small system. The charge/discharge behavior of the model is defined by the decision to charge the maximum available capacity at DAM price minima and discharge the maximum available capacity at DAM price maxima. The selection of the hours that are considered to be minima or maxima is based on the average and volatility bounds. These volatility bounds are defined by the volatility of the market data, identical to the mathematical standard deviation. Based on research into the value of storage arbitrage, these price points are searched for within a short window of the price time-series, considering there is a low marginal value of storing energy after 5-6 hrs [55]. The convention of positive power for charging is taken, with storage round-trip losses taken into account at discharge. The storage operation can be described by the following equations:

$$E_{t+1} - E_t = \begin{cases} P_{\max} & \text{if } p_{\text{DAM},t} < (1 - \sigma_{\text{DAM}}) \cdot \mu_{\text{DAM},w} \\ -P_{\max} & \text{if } p_{\text{DAM},t} \geq (1 + \sigma_{\text{DAM}}) \cdot \mu_{\text{DAM},w} \\ 0 & \text{otherwise} \end{cases} \quad t = 1, \dots, w \quad (3.16)$$

$$E_{\min} \leq E_t \leq E_{\max} \quad (3.17)$$

$$\sigma_{\text{DAM}} = \sqrt{\frac{1}{8760 - 1} \sum_{t=1}^{8760} (p_{\text{DAM},t} - \mu_{\text{DAM}})^2} \quad (3.18)$$

where:

- $t$  = hour within window
- $E_{t+1}$  = Energy at next timepoint
- $E_t$  = Energy at current timepoint
- $P_{\text{max}}$  = upper limit storage power
- $E_{\text{max}}$  = upper limit storage energy
- $E_{\text{min}}$  = lower limit storage energy
- $p_{\text{DAM},t}$  = DAM price at current hour
- $\mu_{\text{DAM}}$  = DAM price average yearly
- $\mu_{\text{DAM},w}$  = DAM price average within window
- $\sigma_{\text{DAM}}$  = volatility of DAM price yearly
- $w$  = number of timesteps within window

An example of the arbitrage operation defined by Equation 3.16 can be seen in Figure 3.11. This example shows a window of 10 hours where two DAM price points result in either charge or discharge behavior. In this figure, the black graph is the DAM price at each hour. It can be observed at hours 0, 1, and 2 that the DAM price is within the volatility limits determined by the average DAM price within the window and the volatility of the DAM price over the whole year. At the third hour, the DAM price rises above the volatility upper limit and is determined as an hour to discharge the battery. The fourth hour is once again within the volatility bounds and corresponds with the third term of Equation 3.16, meaning the SoC does not change. At the fifth hour, the price is lower than the volatility bounds and is determined as an hour to charge the battery. The sixth hour is once again lower than the volatility bounds but due to the battery still being at charged capacity it is not able to charge further. The remaining hours are within the volatility bounds and result in no SoC change.

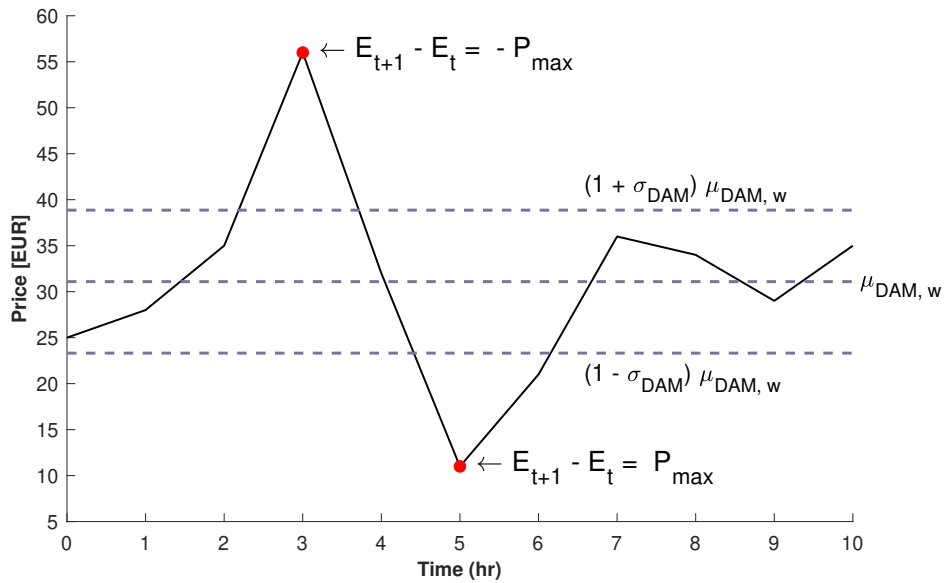


Figure 3.11: Storage arbitrage operation of a 10 hr window.

This operation does not result in the optimal dispatch of the battery capacity for arbitrage. Due to the volatility bounds, it does result in charging behavior that approximates dispatch at local peaks. The inclusion of the window for which the operation is calculated is to operate within the storage duration of around 5-6 hours, which was found to result in the highest arbitrage revenue. The inclusion of the volatility bounds was to not excessively use the battery capacity for hours at low price differences and thus low revenue. The resulting operation provides arbitrage behavior that is sub-optimal in the yearly revenue but comparable in its relation between battery use and revenue. Therefore the revenue is lower than what is possible in the context but the relation between battery use cycles and revenue.

The calculations defined by equation 3.16 and 3.17 are done for all consecutive windows. When For instance, if the window is 5 hours, then the calculation is done for all 1752 windows within that year. Resulting in a time-series of battery charge operation. The operation resulting from a window of 4 hours can be seen in figure 3.12. The line in the background represents the DAM price, it can be seen the battery charges at local low price points and discharges within a short window at a high price point. It can also be observed the discharge output is lower than those of the charging hours, as these are subject to the round-trip efficiency.

The battery charge and discharge behavior that occurs based on the operation defined in Equation 3.16 can be seen in Figure 3.12. The DAM price over 12 hours can be seen at the top with the battery charging behavior on the bottom. The arbitrage operation for these 12 hours was computed with the charge/discharge window set to four hours. It can be seen that the four-hour window indicated by the dotted lines results in one charge/discharge cycle. The battery discharges the available energy of the battery at a local high price point and discharges at a lower price point later in the window. The operational strategy results in the trading of energy within price fluctuation on a relatively short timescale.

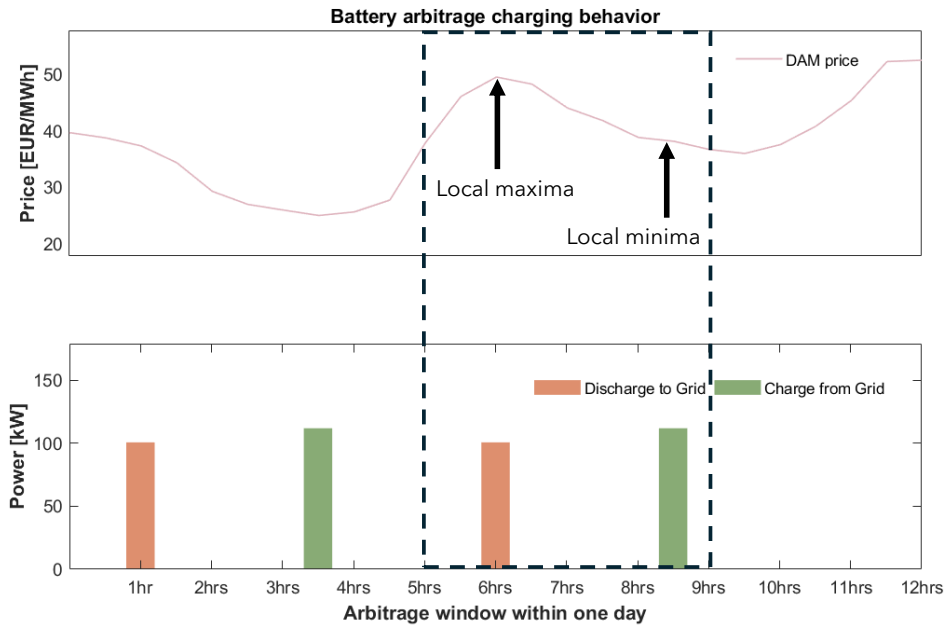


Figure 3.12: Storage charging behavior operation

With the same parameters of operation as used in Figure 3.12, the operation of 6 consecutive windows can be seen in Figure 3.13. As can be seen here, the operational strategy does not ideally capture all the peaks but only computes relative fluctuating time points for the charging and discharging. Considering the perfect price forecast assumption a more optimal charge/discharge behavior would be theoretically possible. However due to the operational strategy being required to also take into account simultaneous power smoothing and arbitrage the choice for a heuristic simulation instead of optimized was chosen. The operational strategy of the combined storage applications is further explained in Section 3.5.2.

The bidding strategy is based on the selection of local high and low price points to attain revenue that outweighs the cost associated with the battery degradation due to the use of the battery. This strategy and the relation between energy arbitrage revenue and battery replacement due to the arbitrage cycling will be assessed in Chapter 4. The

### 3.5.2. Combined storage smoothing and arbitrage bidding

An alternative operation of the battery is one where the battery is simultaneously used for both power smoothing and battery arbitrage. In this operation, the battery component can be used as in the case of stand-alone battery arbitrage when the AWE component is not producing power, while it is used in a limited capacity when the AWE is producing energy. When the AWE power is being smoothed there is excess energy available in the battery, but the power of the system is severely limited by the smoothing power. As such the operation of the battery in combined smoothing and arbitrage can be described by the following Equations 3.19 and 3.20.

$$E_{t+1} - E_t = \begin{cases} P_{\max} - P_{\text{sm}} & \text{if } p_{\text{DAM},t} < (1 - \sigma_{\text{DAM}}) \cdot \mu_{\text{DAM},w} \\ P_{\text{sm}} - P_{\max} & \text{if } p_{\text{DAM},t} \geq (1 + \sigma_{\text{DAM}}) \cdot \mu_{\text{DAM},w} \\ 0 & \text{otherwise} \end{cases} \quad t = 1, \dots, w \quad (3.19)$$

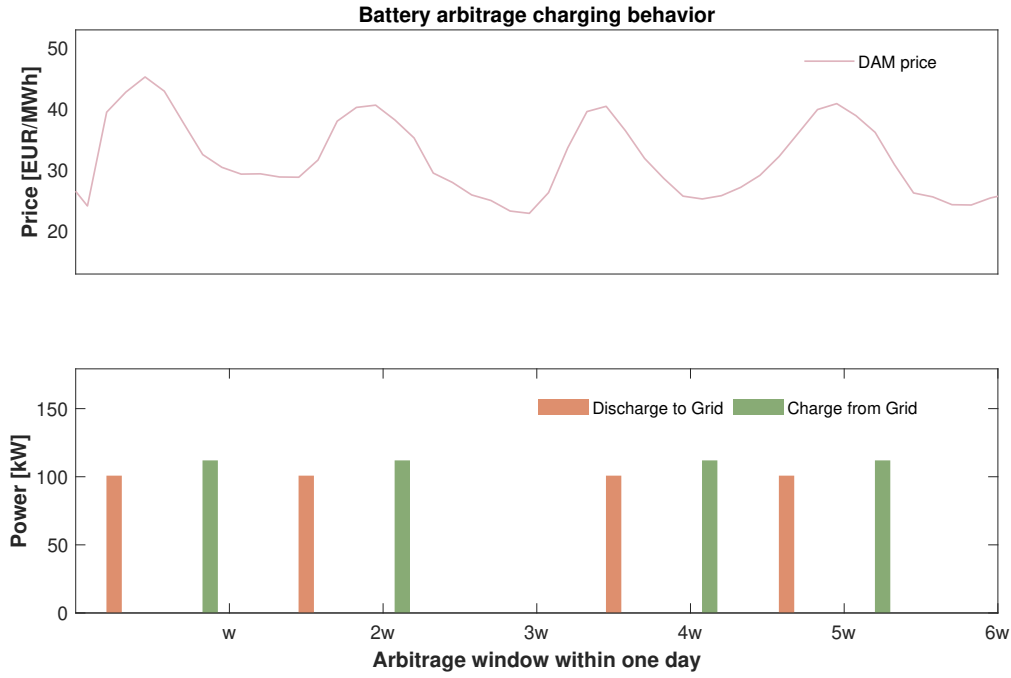


Figure 3.13: Storage charging behavior multiple windows

$$E_{\min} + E_{sm} \leq E_t \leq E_{\max} - E_{sm} \quad (3.20)$$

where:

- $t$  = timestep within window
- $E_{t+1}$  = Energy at next timepoint
- $E_t$  = Energy at current timepoint
- $P_{\max}$  = upper limit storage power
- $P_{sm}$  = upper limit storage power
- $E_{\max}$  = upper limit storage energy
- $E_{\min}$  = lower limit storage energy
- $E_{sm}$  = lower limit storage energy
- $p_{DAM,t}$  = DAM price at current time
- $\mu_{DAM,w}$  = DAM price average within window
- $\sigma$  = volatility of the DAM prices
- $w$  = number of timesteps within window

The calculations done using equation 3.19 and 3.20 are once again done for all consecutive storage windows. The operation resulting from a window of 4 hours can be seen in figure 3.14. The plotted line at the top represents the DAM price, the bar graph at the bottom represents the battery power sorted per application type. Throughout most of the hours later in this week, it can be observed the kite is producing near rated power. This can be observed through the smoothing power dominating the power to near capacity, represented by the horizontal line. At these hours the battery is almost exclusively operating for smoothing. At the hours at the start of this week, it can be seen the kite is operating at lower power outputs, leaving excess battery power capacity available for arbitrage use.

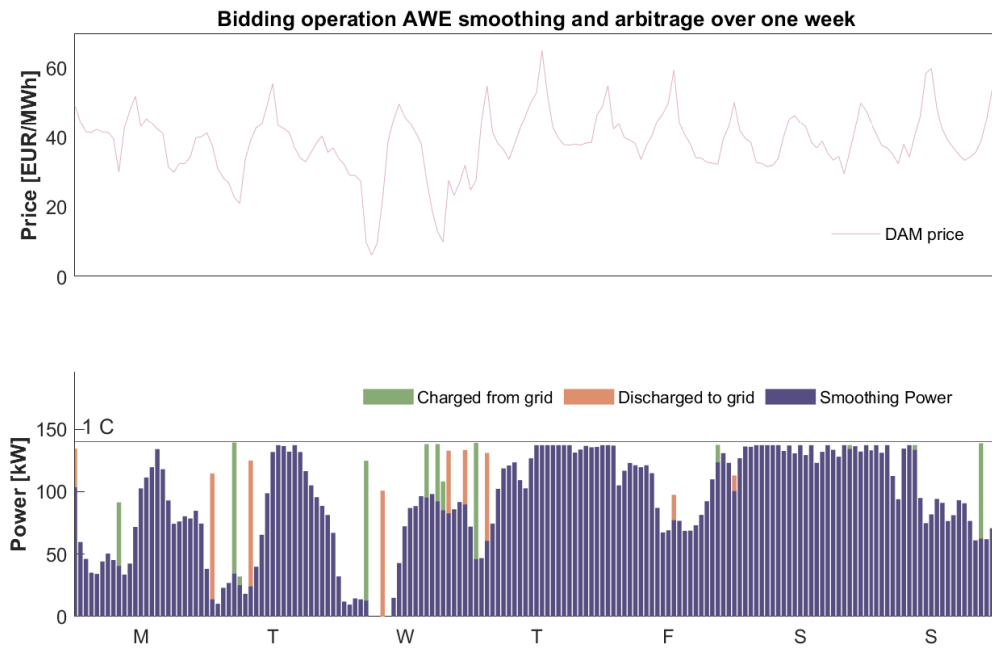


Figure 3.14: Combined smoothing and arbitrage charging behavior relative to DAM price

Figure 3.15 shows the same week of operation with the battery state of charge at the top. This SoC clearly shows the battery operating within the set limits, namely 10 and 90%. When the kite is operating below rated output at the start of the week the battery state of charge is charged/discharged completely to these limits. This is comparable behavior to that shown in Section 3.5.1. This is as expected since the operation of the battery when no power smoothing is needed will be identical to the storage arbitrage case. The SoC limits include the limit imposed by the smoothing energy that needs to be available at all times. This is however hard to see in this figure due to the smoothing energy being very small compared to the total capacity as explained in Section 3.4.1.

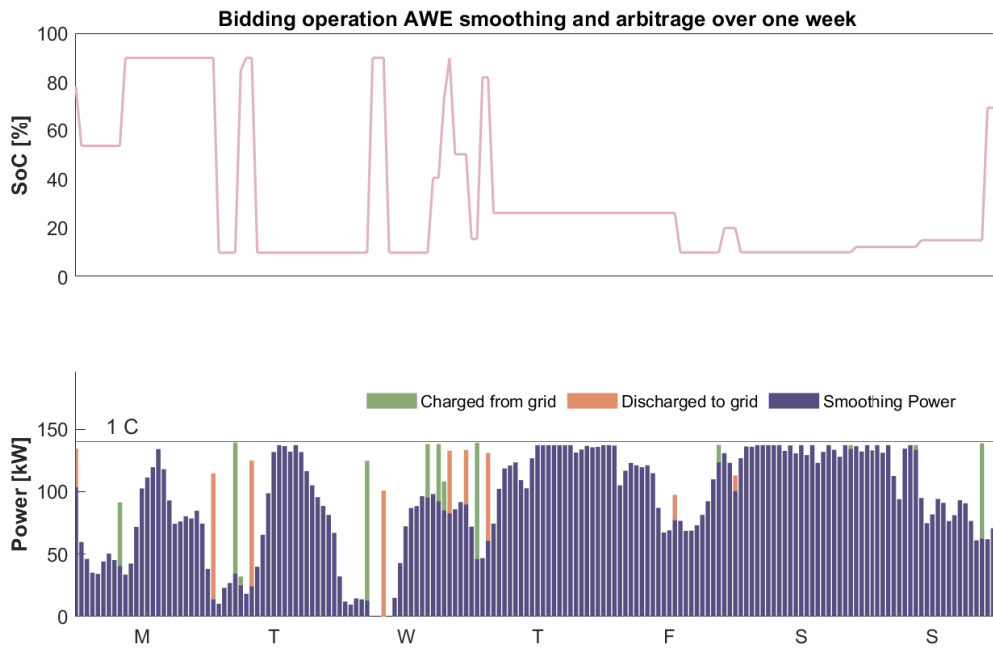


Figure 3.15: Combined smoothing and arbitrage charging behavior with battery capacity

A good example of the arbitrage operation with smoothing limits can be seen in Figure 3.16. In this figure the operation throughout the Friday represented in Figure 3.15 is further delved into. This shows the operational strategy determined the first discharge instance because of a profitable DAM price having been defined. Even though more battery power was available at this point, indicated by the distance between the smoothing power and the horizontal 1C line, due to the state of charge level being limited to needing the capacity for smoothing the full power capacity was not used for arbitrage. The inverted behavior can be seen at the charging point later in the week. At this point, the full capacity of the battery was available for charging but due to nearly all of the available power being used for smoothing the battery was only charged for a small amount.

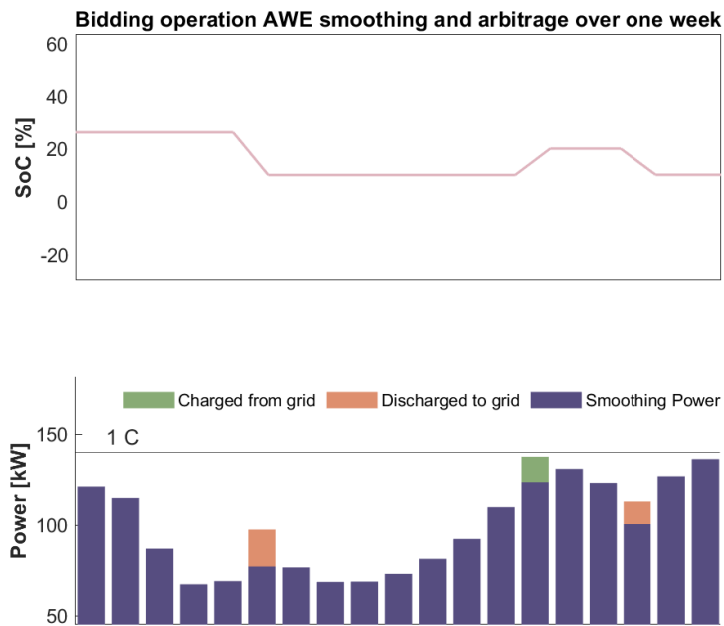


Figure 3.16: Combined smoothing and arbitrage charging behavior capacity limit example

### 3.5.3. Arbitrage operation optimization

As described in Section 3.12, the operational strategy of the storage arbitrage depends on certain parameters. These parameters are the time window and the volatility bounds. These parameters should be set to values that ensure that trading increases revenue more than the OpEx increases. Since battery degradation is taken into account in the simulation of this research, there is a balance point in terms of battery use. If the amount of energy cycled through the battery is high, the battery will need to be replaced sooner. The window and volatility bounds can be set to either increase or decrease the arbitrage load hours. A window that contains more hours will result in more frequent operation of the battery in arbitrage. Higher volatility bounds will exclude more price points and therefore decrease the frequency of arbitrage operations.

To optimize the arbitrage operation the tradeoff is the quantity of energy cycled through the battery and the value of that energy at the moment of discharge. The optimal parameter values can be found by alternating the values and comparing the IRR value of the system in the given wind and market environment. The IRR is a good metric for assessment of the tradeoff since the difference in IRR for certain parameter values will show the aggregated negative and positive effect on the cashflow. Any increase in arbitrage revenue will increase the cashflow while the associated increase in replacement frequency will increase the OpEx thus decreasing the cashflow. The IRR will therefore show the optimal parameter values where the increase in revenue and OpEx are optimal.

Figure 3.17 shows alternating window sizes and the corresponding effect on the IRR and energy cycled through the battery. As can be seen, windows containing more hours will increase the energy cycled through the battery. The scenario depicted shows an AWE-Battery system where the battery is used both for smoothing and arbitrage. At a window size of 0 hours, the IRR represents the case where the battery is used solely for smoothing. At window sizes from 1 upwards the battery is also used for arbitrage. The figure clearly shows that there is an optimal point at a window size of 4 hours where the IRR is the highest. Any increase in window size will result in more frequent arbitrage operations but the

IRR values show that at these sizes the increase in battery replacement is more costly than the increase in revenue.

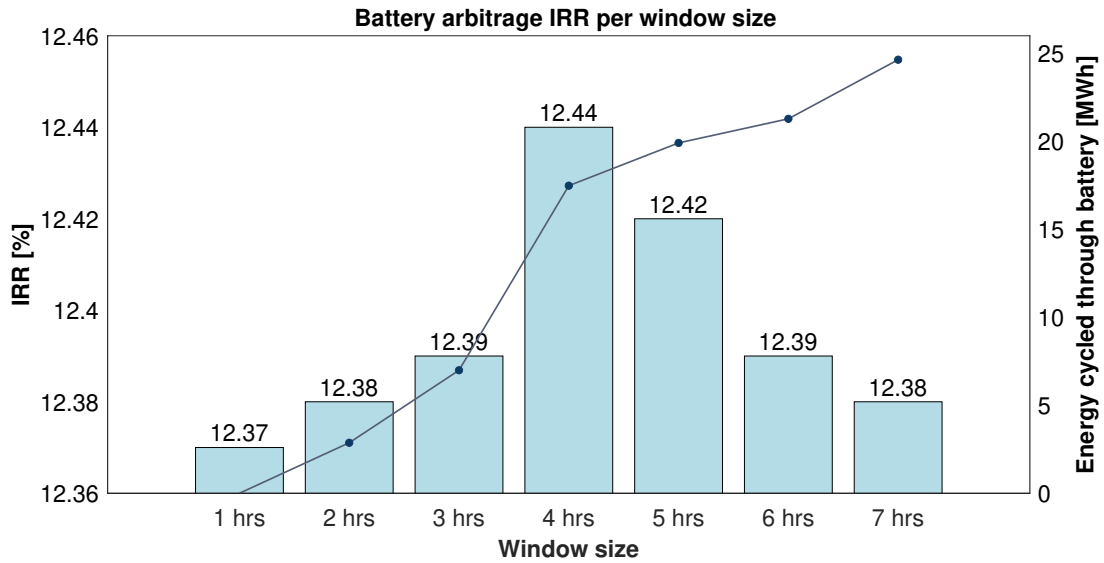


Figure 3.17: Arbitrage operation window size effect on energy cycled through storage and IRR

The volatility bounds work similarly to the window size in terms of an optimal value resulting in an optimal frequency of operation. This value is found to be the volatility or standard deviation of the yearly DAM market data. The optimal operation within the arbitrage model developed in this research results in a relatively low load factor compared to storage arbitrage research. This is because the model only takes into account operation at full battery power capacity. The discussion of optimal arbitrage operation compared to the strategy proposed in this research will be described in Chapter 4.

Having defined the performance of the AWE component, the performance of the storage component, and the operational strategies of the battery for multiple use cases, the assessment of performance is possible. The metrics through which the system performance can be assessed are described in the next section.

### 3.6. Hybrid Power System value assessment

In a grid-connected context, the energy provided to the grid by a renewable power plant is exposed to fluctuating prices of electricity. As such, the revenue of the plant depends on the price of electricity on the DAM at the moment of production of RES energy. To assess the economic performance of the plant, the value of the energy at the moment it is sold to the grid is a key factor for investigation. The simulation of this research registers the energy offered to the grid by the HPP and the price at that same time point. Using this information, the revenue of capturing that value of energy combined with the costs of the system used to generate the energy offered can be used to calculate certain economic indicators. The LCoE and LCoS, representing the costs of the components of the HPP have been described in section 3.3 and 3.4.1 respectively. The value of the energy sold by the HPP is represented by the revenue of the plant over a year. Since the AWE production does not use any type of fuel there is no direct cost associated with the revenue. For battery arbitrage, the revenue is defined by the price at the moment of offered to the grid subtracted by the price at the moment where the battery was charged. The revenue of a power plant is given by the following formula:

$$\text{Revenue} = \text{Energy offered to Grid} \cdot \text{Energy price} \quad (3.21)$$

in the case of the AWE energy,

$$R = \sum_{t=1}^{t=8760} (p_{\text{DAM},t} + p_{\text{sub}}) \cdot E_{\text{AWE},t} \quad (3.22)$$

in the case of battery arbitrage,

$$R = \sum_{t=1}^{t=8760} p_{\text{DAM},t} \cdot (\eta \cdot E_{\text{dis},t} - E_{\text{cha},t}) \quad (3.23)$$

where:

- $R$  = yearly revenue
- $t$  = Time instant
- $p_{\text{DAM},t}$  = Energy price at current timepoint
- $p_{\text{sub}}$  = Subsidy scheme price
- $E_{\text{AWE},t}$  = AWE produced power to grid
- $E_{\text{dis},t}$  = Battery energy discharged to grid
- $E_{\text{cha},t}$  = Battery energy charged from grid
- $\eta$  = Battery round-trip efficiency

The revenue provides information on the value of the energy sold over the year but to show the performance of the plant the profit over the year is needed. The levelized profit of energy (LPoE) can be calculated by first calculating the levelized revenue of energy (LRoE) and the subtracting the LCoE. The LRoE and LPoE are calculated using equations 3.24 and 3.25 respectively. In the case of storage arbitrage, the revenue relative to the installed

storage capacity over a year is also an important indicator. This metric is called the value of storage arbitrage (VoSA) and is used to compare the value of arbitrage of a storage system to other systems and other market zones. This metric is calculated using equation 2.1, described in chapter 2.

$$\text{LRoE} = \frac{\sum_{t=1}^T \frac{R_t}{(1+r)^t}}{\sum_{t=1}^T \frac{E_t}{(1+r)^t}} \quad (3.24)$$

$$\text{LPoE} = \text{LRoE} - \text{LCoE} \quad (3.25)$$

where:

LRoE = levelised revenue of Energy

LPoE = levelised profit of Energy

LCoE = levelised cost of Energy

$R_t$  = yearly revenue

$E_t$  = yearly energy sold to grid

$r$  = discount rate

The LPoE is a revenue and cost-based metric and is levelized over the discounted energy offered to the grid. This metric provides valuable information on the relation between the revenue, cost, and energy exchanged to the grid. In the context of this research, however, the economic performance of different configurations of HPP need to be compared. The revenue of the AWE component is levelized over the AWE energy sold and the revenue of arbitrage is levelized over energy discharged to the grid. To compare configurations that combine these different HPP aspects, the LPoE while providing valuable insight into the revenue is not directly applicable. The profit of the configurations could all be levelized over their total energy discharged to the grid but this would show warped metrics that are not directly comparable. A more appropriate metric is the value-based metric of net present value (NPV) and the related metric internal rate of return (IRR). These metrics are not comprised of factors using discounted energy to the grid but are instead based on the net flow of cash of the project. The NPV is the discounted value of the operation of the plant over its lifetime relative to the initial investment. The IRR is the discount rate for which the NPV is 0, giving a metric for investment return independent of a discount rate assumption. These metrics are given by the following equations:

$$\text{NPV} = -\text{CapEx} + \sum_{t=1}^T \frac{R_t - \text{OpEx}}{(1+r)^t} \quad (3.26)$$

$$0 = \text{NPV} = -\text{CapEx} + \sum_{t=1}^T \frac{R_t - \text{OpEx}}{(1+\text{IRR})^t} \quad (3.27)$$

where:

NPV = Net present value  
IRR = Internal rate of return  
CapEx = initial investment of project  
OpEx = operational expenditures per year  
 $R_t$  = yearly revenue  
T = Project lifetime  
r = dicount rate

The resulting economic indicators calculated for the different configurations of HPP analyzed in this research are described in chapter 4. The results consist of combinations of model components simulated using the methods described in this chapter. The economic performance is then reported, discussed, and compared.

# 4 | Results and Evaluation

In this chapter the results of the simulations as described in Section 3 will be analyzed. Section 4.1 states the context of the four scenarios, Section 4.2 discusses the results of the simulation of AWE + ultracapacitor scenario, Section 4.3 discusses the results of the simulation of AWE + Battery scenario, Section 4.4 discusses the results of the simulation of the Battery arbitrage scenario and Section 4.5 discusses the results of the simulation of AWE + Battery arbitrage scenario. Finally, a general discussion of the results and analysis of the sensitivity of the simulations will be made in Section 4.6.

## 4.1. Scenario configurations

As identified in chapter 3, the chosen location of the scenarios is Haringvliet. This location is based on the existence of a Wind - PV - Batteries HPP at this location. This HPP, built and operated by Vattenfall was installed to research HPP grid net congestion. For the past two years, it has been collecting data, potentially adding AWE units to this plant could be interesting to research the spread of RES production at this location. The location wind environment and DAM market dynamics have been previously analyzed in section 3.2. As stated in the research approach in chapter 3, the goal of the developed model is to be used for the assessment of the economic value of different AWE-Storage HPP systems. These scenarios are; an AWE + ultracapacitor for smoothing, an AWE + batteries for smoothing, a battery system used in DAM arbitrage, an AWE system + battery system for smoothing and using the excess capacity in DAM arbitrage. A suitable set of input parameters was created for the different components within each scenario as described in their respective sections in chapter 3. By varying one component in each scenario the relative addition in economic value can be ascertained. The variance in components can be seen in Table ??.

	Scenario 1: AWE + UC	Scenario 2: AWE + Battery	Scenario 3: Battery arbitrage	Scenario 4: AWE + Battery arbitrage
AWE system	100 kW	100 kW	-	100 kW
Storage system	UC	Battery	Battery	Battery
Storage application	Smoothing	Smoothing	Arbitrage	Smoothing Arbitrage

Table 4.1: Overview component configuration per scenario

## 4.2. Scenario 1: AWE + UC

The first configuration scenario is the AWE component with an ultracapacitor for power smoothing purposes. The AWE energy is directly sold to the DAM and revenue is based on a subsidy scheme. This scenario provides a reference for the other scenarios as any change in components will result in a change in performance. Given the many assumptions of the model concerning costs and performance that are not easily verified, using scenario 1 as a base case to which to compare other scenarios provides a relative performance assessment within the same set of assumptions. An overview of the components of this first configuration can be seen in figure 4.1.

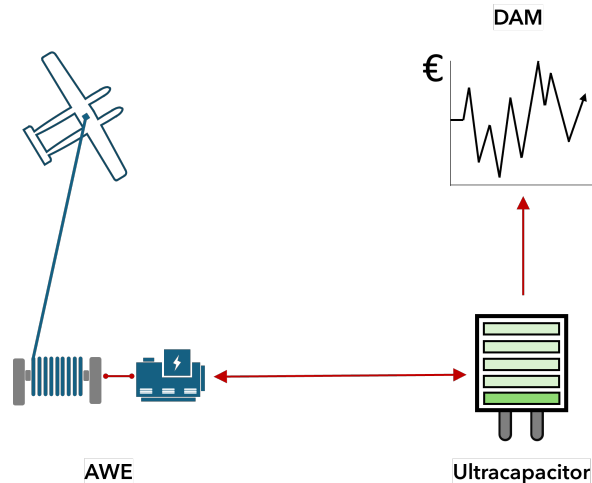


Figure 4.1: Scenario 1 AWE ultra-capacitor overview

Table 4.2 states the inputs and assumptions for this scenario. The subsidy scheme is a feed-in-tariff (FIT) that offers eligible renewable plants a fixed price independent of the DAM price for all RE of the plant offered to the grid. This FIT is represented by the subsidy value shown and is based on the potential AWE subsidy scheme in Germany. This subsidy scheme proposes a subsidy level where AWE-produced energy gets 1.55 the value of the onshore wind auctions which may lead to values of 10-11 ct/kWh [59]. For this research, a subsidy of the maximum value of 11 ct/kWh or 110 €/MWh has been chosen. The assumptions and specifications of the ultracapacitor are what define the performance of the smoothing component.

Parameter	Description	Value	
AWE $P_{\text{rated}}$	Rated power of AWE component	100	kW
Subsidy	AWE subsidy	110	€/MWh
Type	Storage technology type	UC	
Storage capacity	Installed storage capacity	0.93	kWh
Storage cost	Storage technology cost	60	k€/kWh
$N_{\text{cycles}}$	Lifetime of unit	$10^6$	cycles
$N_{\text{years}}$	Lifetime of unit	15	years
SoC <sub>min</sub>	State of charge lower limit	0	%
SoC <sub>max</sub>	State of charge upper limit	100	%
$\eta$	round-trip efficiency	100	%

Table 4.2: Parameter inputs scenario 1: AWE + UC

This configuration, consisting of the AWE system with the ultracapacitor component for intermediate smoothing, shows a certain economic prospect in the scenario context. Given the economic performance seen in Table 4.3, it is immediately clear from the LPoE and NPV that the system is profitable, the costs of the system are overcome by the sale of its produced energy given the market context, though not by a large margin. The IRR shows a rate slightly higher than the discount rate assumed in this research of 10%, which results in the comparatively low return on investment represented by the NPV value of 7500 €.

The overall cost of the UC component in this scenario can also be seen in Table 4.3. It can be observed that the initial investment of the ultracapacitor system is relatively high at 56 k€ for the component, which represents roughly 12% of the entire AWE system. In the wind environment of the scenario, the power smoothing operation results in a required replacement of 0.11 times per year, meaning it will have to be replaced at least two times throughout the lifetime of the AWE system.

Metric	Description	Result	
AEP	Annual energy produced	492	MWh
LCoE	Levelized cost of energy	148	€/MWh
LPoE	Levelized profit of energy	1.7	€/MWh
NPV	Net present value	7.55	k€
IRR	Internal rate of return	10.2	%
$f_{\text{repl}}$	Storage replacement frequency	0.11	/year
CapEx	Storage capital expenditures	55.9	k€
OpEx	Storage operational expenditures	6.73	k€

Table 4.3: Results scenario 1: AWE + UC

The interaction with the DAM price fluctuation of the AWE energy results in a sub-optimal value gained from bids. As can be seen clearly in figure 4.2, peaks in AWE energy production do not necessarily coincide with high DAM prices. In the zones indicated by the dashed lines, the high value of energy in the operation over two weeks shown it is observed that the hours with production nearing 70 kW, the DAM prices are actually below the yearly average. This results in a potential for using the hours at which low or no AWE power is produced to capture the higher value DAM hours.

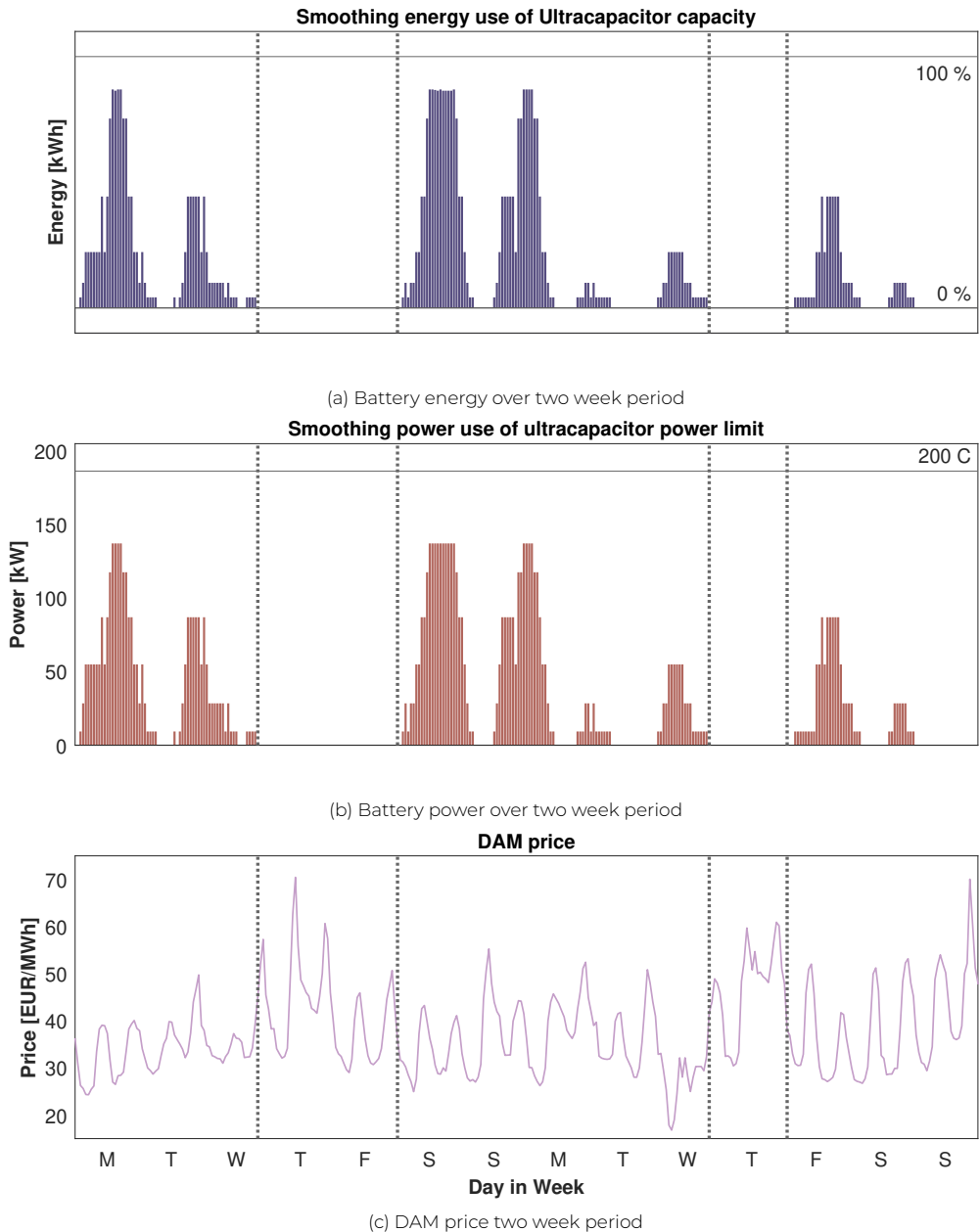


Figure 4.2: Smoothing Energy and Power performance through battery

The economic performance of the AWE + UC configuration indicates that the cost of the AWE system is high compared to the revenue from DAM participation. Comparing the performance of the configuration in this simulation with the performance of the same system inputs in the cost model developed by Joshi and Trevisi [22], shows the effect of DAM participation. That cost model determines economic performance based on a stable electricity price, Weibull distribution of wind speeds, and a subsidy scheme. The LCoE of that sim-

ulation is 154 €/MWh while the IRR is 12.6 %. The higher LCoE at the same system cost means the AWE-produced energy yield is higher in the simulation of this research. The higher IRR however, means that the profit of the system is lower in the simulation of this research. This means that even though more energy is bid on the DAM, the value of the energy at the moment of production is lower overall.

### 4.3. Scenario 2: AWE + battery

The second configuration scenario is the AWE system with a battery for power smoothing applications. The AWE energy is directly sold to the DAM and revenue is based on a subsidy scheme. This scenario provides insight on the performance of an AWE-HPS with a battery system for power smoothing sized according to the power and energy requirements determined in Chapter 3. The storage performance of this scenario will show the difference in storage energy and power use due to power smoothing. The results from this scenario also show the capacity of the battery component after power smoothing has been performed, this is the excess capacity. An overview of the components of the scenario 2 configuration can be seen in figure 4.3.

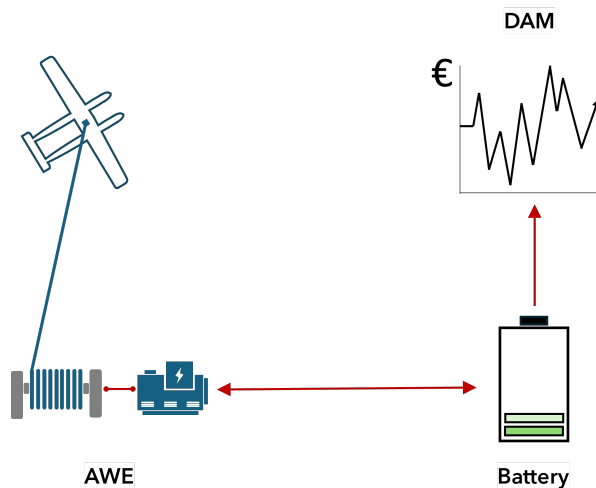


Figure 4.3: Scenario 2 AWE Battery overview

Table 4.4 states the inputs and assumptions for this scenario. The subsidy scheme is identical to that of scenario 1. The assumptions and specifications of the battery are what define the performance of the smoothing component. Due to the AWE input parameters being identical to those of scenario 1, any changing results will be directly related to the difference in operation of the smoothing storage component. The results presented here are simulated using the optimistic battery costs, the results for higher battery prices will be presented in Section 4.6.2.

Parameter	Description	Value
AWE $P_{\text{rated}}$	Rated power of AWE component	100 kW
Subsidy	AWE subsidy	110 €/MWh
Type	Storage technology type	Battery
Storage capacity	Installed storage capacity	140 kWh
Storage cost	Storage technology cost	130 €/kWh
$N_{\text{cycles}}$	Lifetime of unit	$10^5$ cycles
$N_{\text{years}}$	Lifetime of unit	10 years
SoC <sub>min</sub>	State of charge lower limit	10 %
SoC <sub>max</sub>	State of charge upper limit	90 %
$\eta$	round-trip efficiency	90 %

Table 4.4: Parameter inputs scenario 2: AWE + Battery

The second scenario, consisting of the AWE system with a battery component for intermediate smoothing, shows a positive economic prospect. Given the economic performance seen in Table 4.5, it is immediately clear from the LCoE that in this scenario, the costs of the system are lower due to the lower costs of the battery system. The LPoE, NPV, and IRR show that this system is an investment with positive returns. When comparing the storage component capital and operational investments in table 4.3 and table 4.5 respectively, it is clear to see that the increase in profit stems from the significant decrease in investment due to the alternative storage component. This combined with the simulation showing that there is an excess of battery capacity after consideration of smoothing shows potential for use in alternative activities.

The storage metrics of the second scenario can also be seen in Table 4.5. The battery as a replacement for smoothing power has a much higher installed capacity that is required to allow for the power capacity to be high enough for smoothing at rated wind speeds. The replacement of the battery component is limited not by the lifetime cycles, but by the lifetime years of the storage unit. This is because, at the oversizing needed to obtain the power required, the capacity is largely unused throughout the project's lifetime. While the replacement frequency is near the same value as that of scenario 1, the actual OpEx stemming from this frequency is lower due to the lower cost of the storage system.

Metric	Description	Result
AEP	Annual energy produced	492 MWh
LCoE	Levelized cost of energy	131 €/MWh
LPoE	Levelized profit of energy	19.2 €/MWh
NPV	Net present value	85.7 k€
IRR	Internal rate of return	12.37 %
$f_{\text{repl}}$	Storage replacement frequency	0.10 /year
CapEx	Storage capital expenditures	18.2 k€
OpEx	Storage operational expenditures	1.82 k€

Table 4.5: Results scenario 2: AWE + Battery

The interaction with the DAM price fluctuation of the AWE energy results in the same sub-optimal value gained from bids as in the first configuration. The hours of high production, coincide at some points with low DAM price points. This results in a potential for using the hours at which low or no AWE power is produced to capture the higher value DAM hours. In this configuration, a battery component is used, which has an excess capacity throughout its operation. The availability of this capacity can be seen in figure 4.4, where the excess capacity is compared to the AWE production and DAM price fluctuation. The periods where the AWE system is not producing power, indicated by the dotted lines, convey the market value that is not captured due to the dependency on the wind speeds of the system.

Beyond these unused hours there are also hours where the AWE is producing power, but below rated power. At these hours the battery power smoothing is using energy and power but has an excess in both of these. Figure 4.4a shows that the oversizing of the storage system results in almost no energy capacity being used for power smoothing. At all hours throughout the year the excess energy capacity is near full battery capacity. Figure 4.4b shows that at these hours where there is excess energy capacity, there is not always an excess of power capacity. The horizontal line indicated by '1C' shows the battery power limit. At the hours when the power nears that 1C limit, no excess power capacity exists. At hours when the smoothing power is below the 1C point, there is an excess power capacity.

Figure 4.4c shows the DAM price fluctuation throughout the two weeks illustrated in this figure. During the windows indicated by the dotted lines, high DAM prices with relatively high volatility occur. This suggests a high potential for market interaction using the excess capacity of the battery at these hours.

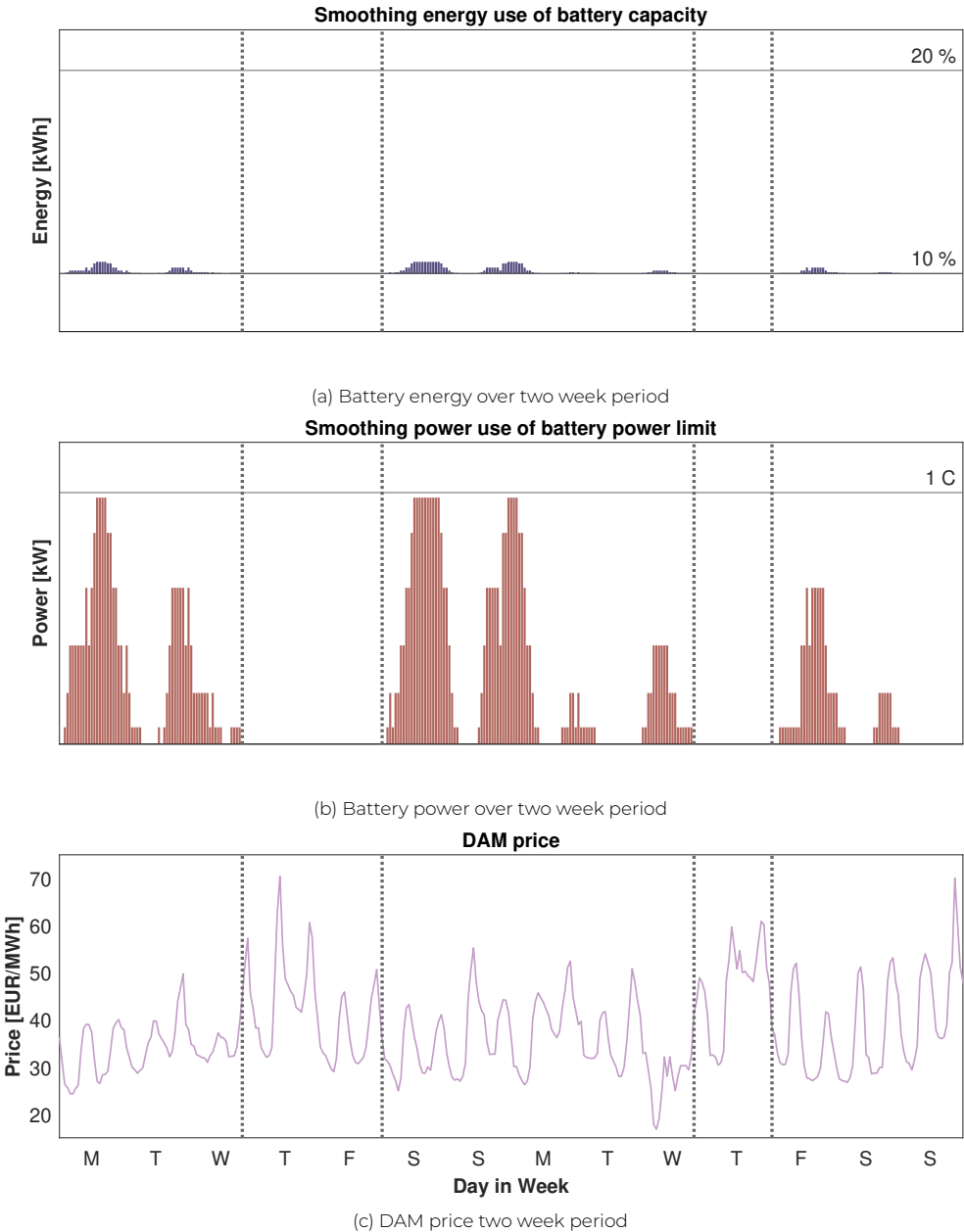


Figure 4.4: Smoothing Energy and Power performance through battery

## 4.4. Scenario 3: Battery Arbitrage

The third configuration scenario is the battery system used for DAM arbitrage. The battery is operated using the operation strategy defined in chapter 3. An overview of the components of this first configuration can be seen in figure 4.5. This overview shows the context of isolated battery DAM interaction. First, the scenario input and assumptions will be described, after that the operational strategy will be evaluated for its performance in this scenario and after that, the economic performance of the system is described.

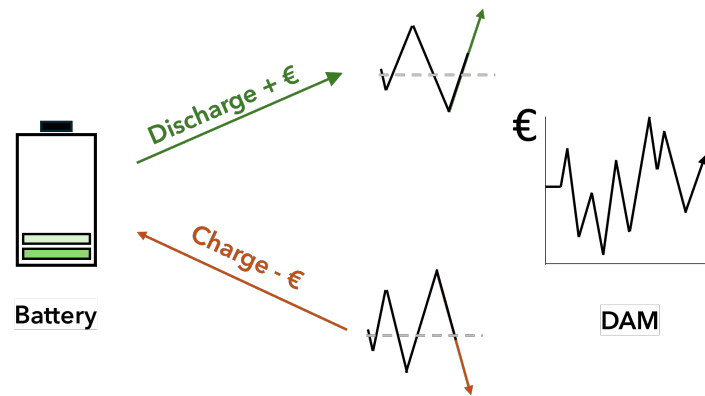


Figure 4.5: Scenario 3 Battery arbitrage overview

The battery price for the system is the optimistic price defined in chapter 3. The inputs of storage lifetime, round-trip efficiency, and usable capacity are what define the performance when participating in DAM arbitrage. These input values can be seen in table 4.6. The trading of energy is based on the operational strategy proposed in chapter 3. The implementation of that operational strategy will be evaluated first.

Parameter	Description	Value
Type	Storage technology type	Battery
Storage capacity	Installed storage capacity	140 kWh
Storage cost	Storage technology cost	130 €/kWh
$N_{\text{cycles}}$	Lifetime of unit	$10^5$ cycles
$N_{\text{years}}$	Lifetime of unit	10 years
$\text{SoC}_{\text{min}}$	State of charge lower limit	10 %
$\text{SoC}_{\text{max}}$	State of charge upper limit	90 %
$\eta$	round-trip efficiency	90 %

Table 4.6: Parameter inputs scenario 3: Battery arbitrage

In the third scenario, consisting of the Battery system used independently in arbitrage, the performance is harder to compare to the other three scenarios. Considering that several performance metrics of the costs and profits are levelized over discounted energy, where

the energy is usually energy produced. In the case of storage technologies, the cost is usually levelized over discounted energy discharged to the grid. This means the results are not directly relatable to the AWE HPS scenario. It becomes preferable in this case to focus on the metrics that do not include total energy but rather total profit and costs. The NPV, for instance, shows there is a net negative cash flow in this context.

The market value capture of the configuration does not directly matter, since the aim of this scenario is to provide a reference of the arbitrage modeling and the difference in operation when combining smoothing and arbitrage. As such it is the operational revenue we are interested in and not as much the degree to which this operational profit relates to initial investment. This is because, in the case of storage used for combined smoothing and arbitrage, the initial investment is a required cost of the AWE system.

The economic performance can be seen in table 4.7. These metrics clearly show the operation of the battery in arbitrage is not profitable enough to recoup the installation cost. It does show how much value can be gained from a battery system of the installed size comparable to the size required for smoothing a 100 kW AWE system. This value captured is expressed in the value of storage arbitrage (VoSA) which is explained in chapter 2. This shows the market value captured by a storage system in this DAM environment using the operational strategy proposed in this research. The VoSA is 7730 euros per year per MW of installed capacity, which is on the lower side compared to other studies on storage arbitrage in the NL bidding zone in 2019. This arbitrage performance is further discussed in section 4.6.

The battery system in scenario 3 is sized according to a battery system similar in size to the power smoothing component for a 100 kW AWE system. As such the storage component CapEx is the same as those in scenario 2 and 4. The replacement frequency in cycle lifetime is 0.067/year, however, due to the calendar year lifetime the replacement frequency is 0.1 /year. This replacement frequency and the OpEx of the storage system show that using the arbitrage operation the use of the battery is low, leading to a situation where the initial investment is not recouped over the project lifetime.

Metric	Description	Result	
AED	Annual energy discharged	48.7	MWh
LCoS	Levelized cost of storage	60.4	€/MWh
LPoS	Levelized profit of storage	-38.2	€/MWh
VoSA	Value of storage arbitrage	7.7	k€/MW/year
NPV	Net present value	-20.2	k€
$f_{\text{repl}}$	Storage replacement frequency	0.10	/year
CapEx	Storage capital expenditures	18.2	k€
OpEx	Storage operational expenditures	1.82	k€

Table 4.7: Results scenario 3: Battery arbitrage

In terms of the operational strategy of the battery in arbitrage, Figure 4.6b and 4.6c show the charging and discharging at certain DAM prices. The behavior is similar to the example operation shown in Section 3.5.1. It also clearly shows it is not an optimal dispatch of bids since the battery does not charge at all hours and at all peaks. The charging and discharging power levels remain well below the 1 C limit, due to the SoC limits imposed on the system. While the battery can theoretically sustain 140 kW over a full hour, due to the SoC limits the battery can only store 80 % of 140 kWh. This results in a power level of 112

kW, due to the usable battery capacity of 112 kWh.

Figure 4.6b and 4.6c show that the arbitrage modeling does result in more trading when the price is volatile. At the start of the week the battery charges and discharges more often due to the high and volatile prices, in the middle the battery is used less due to the low and less volatile prices. However, the limitations can also clearly be seen since the battery still charges and discharges the full capacity later in the week, when the prices are lower and less volatile than at the start.

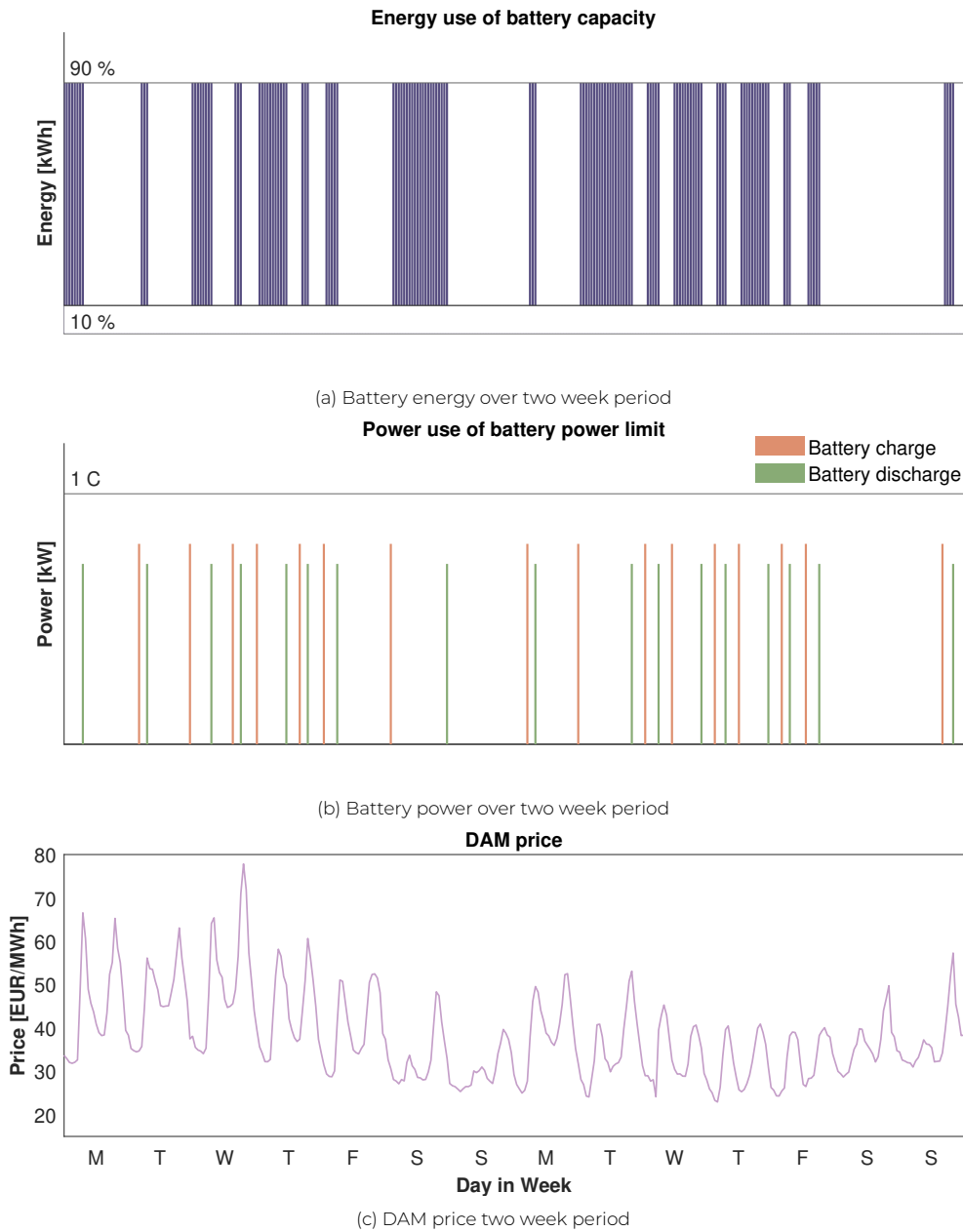


Figure 4.6: Arbitrage Energy and Power performance through battery

## 4.5. Scenario 4: AWE + Battery arbitrage

The fourth and final configuration scenario is the AWE component with a battery system for combined power smoothing and arbitrage purposes. The AWE energy is directly sold to the DAM and revenue is based on a subsidy scheme. The Battery energy is sold to the DAM at moments directed by the arbitrage operational strategy. An overview of the components of this fourth configuration can be seen in figure 4.3.

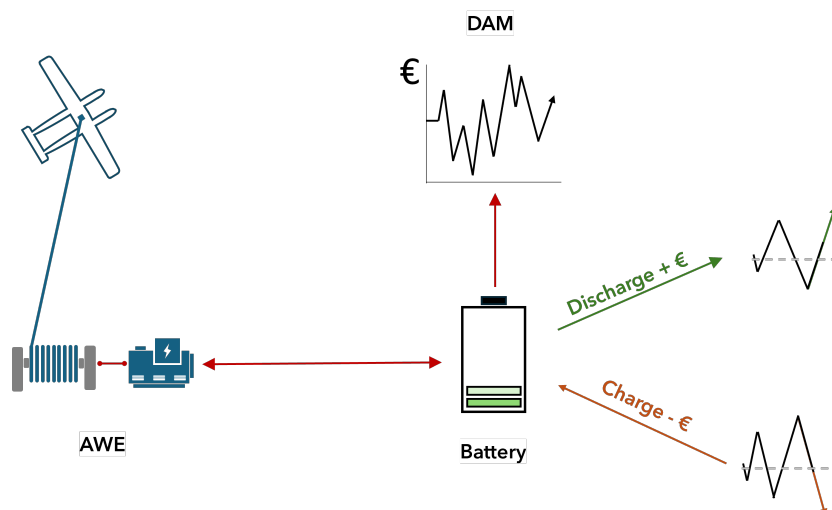


Figure 4.7: Scenario 4 AWE Battery arbitrage overview

Table 4.8 states the inputs and assumptions for this scenario. The subsidy scheme is identical to that of scenario 1. The assumptions and specifications of the battery are what define the performance of the smoothing component. Since the battery input parameters are identical to those in scenario 2, the added application of arbitrage will show the relation between the added revenue and the added use of the battery. The IRR compared to that of scenario 2 will therefore show whether the added value of arbitrage is more than the added replacement of the battery due to its higher use.

Parameter	Description	Value	
AWE $P_{\text{rated}}$	Rated power of AWE component	100	kW
Subsidy	AWE subsidy	110	€/MWh
Type	Storage technology type	Battery	
Storage capacity	Installed storage capacity	140	kWh
Storage cost	Storage technology cost	130	€/kWh
$N_{\text{cycles}}$	Lifetime of unit	$10^5$	cycles
$N_{\text{years}}$	Lifetime of unit	10	years
SoC <sub>min</sub>	State of charge lower limit	10	%
SoC <sub>max</sub>	State of charge upper limit	90	%
$\eta$	round-trip efficiency	90	%

Table 4.8: Parameter inputs scenario 4: AWE + Battery arbitrage

The fourth scenario combines all operation types in the battery component. That combined operation results in a higher OpEx of the storage component as can be seen in table 4.9. The CapEx remains the same as in scenario 2 since the installed capacity remains the same. The OpEx increased by 540 euros per year due to the arbitrage operation. This is however not the full representation of the additional stress on the battery system due to the arbitrage operation. Since the battery replacement is defined as either the lifetime in calendar years or the lifetime in cycles, one is leading in the replacement. In the case of only power smoothing operation, the battery is replaced according to the calendar lifetime, whereas in the case of combined smoothing and arbitrage operation, the lifetime is defined by the cycle lifetime. The difference in replacement frequency in scenario 2 and scenario 4 is therefore smaller than the difference in stress on the battery system.

The storage result metrics of the fourth scenario can also be seen in table 4.9. The battery as a replacement for smoothing power has a much higher installed capacity that is required to allow for the power capacity to be high enough for smoothing at rated wind speeds. The replacement of the battery depends on the combined cycles of soothing and arbitrage. As such the battery system will have to be replaced more often due to the added use of its capacity. The replacement frequency of scenario 4 is slightly higher (0.101) than that of scenario 2 (0.10), however, the value of the system is increased overall, at an IRR of 12.43% compared to the 12.37% of scenario 2. The slight difference in replacement frequency is due to the lifetime years being the dominant factor, this will be analyzed further in Section 4.6.

Metric	Description	Result	
AEP	Annual energy produced	492	MWh
AEP	Annual energy stored	17.5	MWh
LCoE	Levelized cost of energy	127	€/MWh
LPoE	Levelized profit of energy	19	€/MWh
NPV	Net present value	87.9	k€
IRR	Internal rate of return	12.43	%
VoSA	Value of storage arbitrage	1.86	k€/MW/year
$f_{\text{repl}}$	Storage replacement frequency	0.10	/year
CapEx	Storage capital expenditures	18.2	k€
OpEx	Storage operational expenditures	2.36	k€

Table 4.9: Results scenario 4: AWE + Battery arbitrage

The combined operation of the battery system can be seen in figure 4.8. This figure shows the operation of the battery over two weeks. In figure 4.8a the capacity use can be seen. As can be expected from the analysis of the battery capacity used for smoothing in section 4.3, the capacity used for smoothing is insignificant compared to the total battery capacity. As such it is barely noticeable when graphing the battery capacity use. In figure 4.8b, the power use of the battery is depicted. In this graph, the smoothing power can be seen to take up most of the power capacity of the battery when it is operating near rated kite power. This figure also shows that in the time windows indicated by the dotted lines, when the kite is not operational the battery can be fully utilized for arbitrage operation. At moments where the kite power is between cut-in and rated power, the battery is occasionally also used for arbitrage, making use of the remaining power capacity.

As can be observed from the horizontal line indicating the 1 C power limit of the battery, when the battery is not used for smoothing and only for arbitrage, the power output of the battery is not fully used for arbitrage. This is because the capacity limit of using the battery is between 10 and 90% resulting in the power of charging the battery being lower than the maximum to charge the battery to full capacity within the hour.

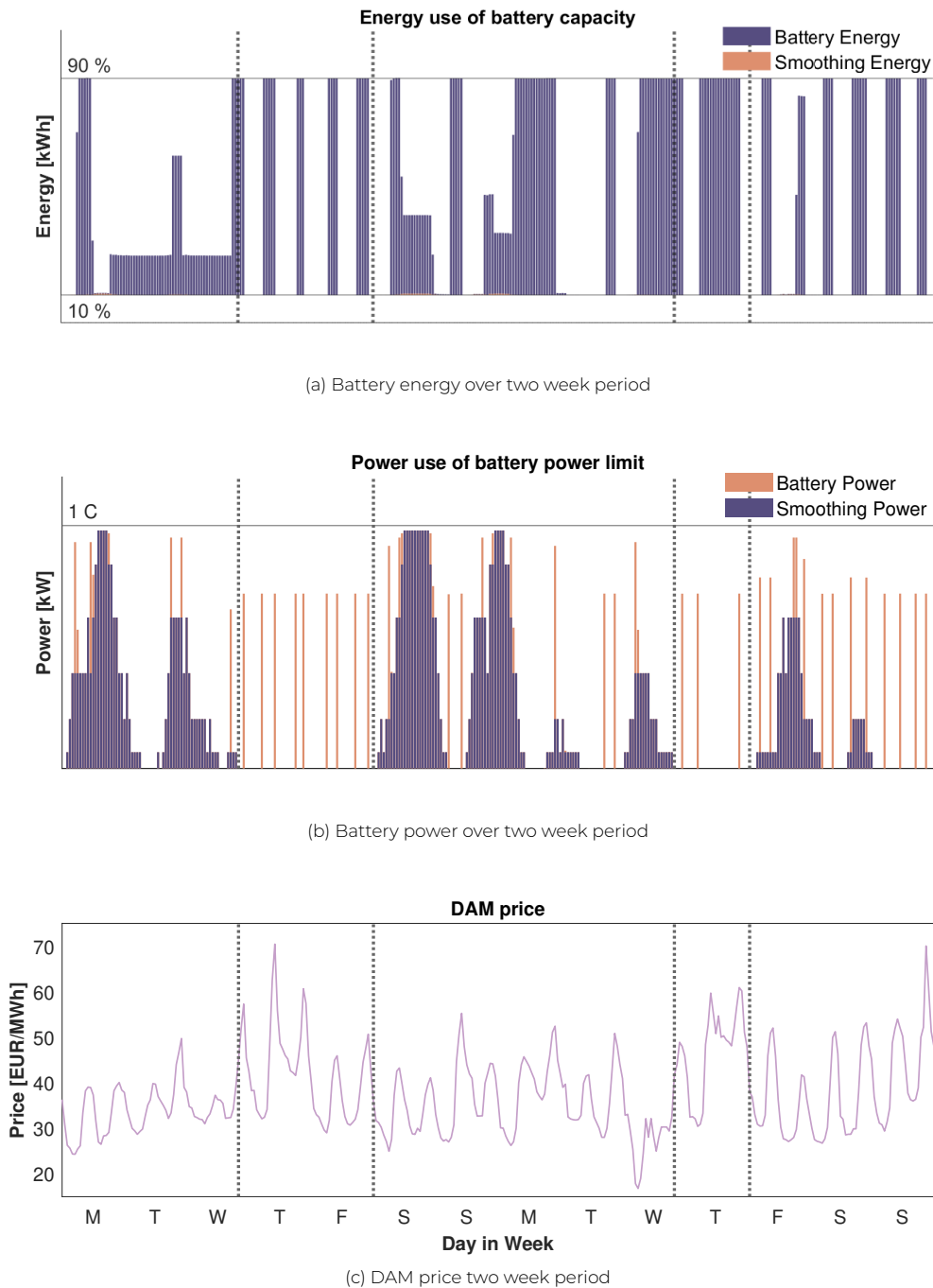


Figure 4.8: Smoothing Energy and Power performance through battery

In terms of the relative use of the battery system, it is interesting to evaluate the replacement of the battery and the effect of combined interaction. Figure 4.9 shows the relation between battery replacement and operation use. The power smoothing cycles are identical to those in scenario 2 but the overall higher frequency due to combined operation results in a ratio between the two. Arbitrage takes up 26% of the overall replacement in this scenario, representing a use where power smoothing still dominates the rate at which the battery has to be replaced. This share of battery replacement could end up higher if the arbitrage would use more cycles when it is bid more often. This could happen in a scenario of an alternative arbitrage operational strategy.

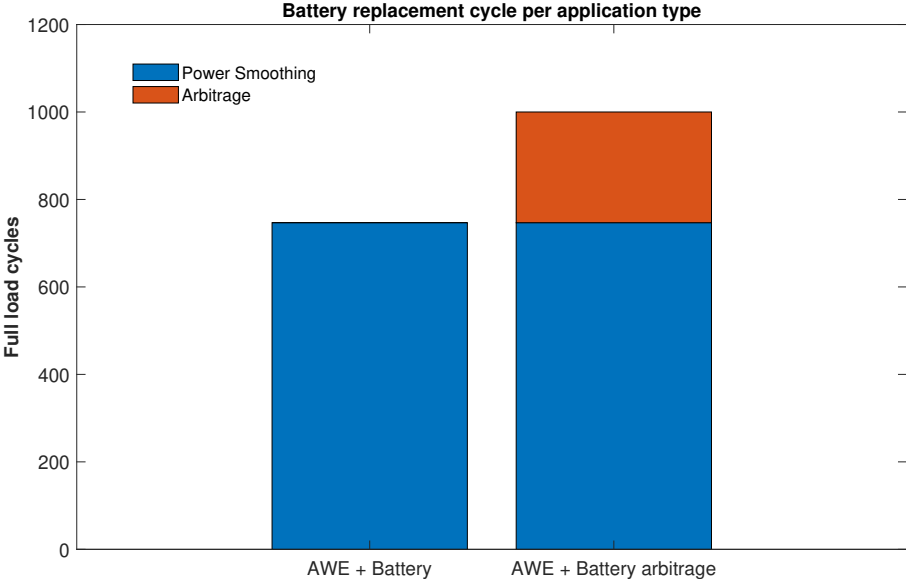


Figure 4.9: Share of replacement frequency by operation type

## 4.6. Discussion of results

A study of three different configurations of AWE HPP and one Battery system has been analyzed using the developed simulations. The study was comprised of four different types of power system configurations; AWE + Ultracapacitor, AWE + Battery, Battery arbitrage, and AWE + Battery arbitrage. The scenarios have been analyzed for DAM-based revenue generation. The main aim of this study was to use the simulations to understand the difference in the market value capture. The model is used to compare the configurations based on their LCoE, LRoE, NPV, and IRR. Special focus is given to the CapEx, OpEx, and storage replacement frequency due to the unique situation of shared CapEx for multiple operation types influencing replacement frequency. The LCoE is calculated by leveling over all energy discharged to the grid, to include battery arbitrage energy levels. The subsidy scheme for AWE-produced energy is taken into account for the directly sold AWE energy, but not for the battery arbitrage energy.

### 4.6.1. Comparison value assessment

This research aimed to find the added market value of sizing a battery system that could be implemented to serve the purpose of power smoothing for an AWE system and to identify the possibility and potential of using the excess capacity of this battery system in arbitrage. Table 4.10 shows the qualitative comparison of the scenarios evaluated in order to find the market value capture of each scenario. This overview shows the relative advantage of the battery smoothing of the AWE Battery configuration due to its drastically lower storage costs. Furthermore, it shows the added market value capture when using this same system in arbitrage, even though this use case decreases the replacement performance of the system.

Criteria	AWE ultracapacitor	AWE Battery	Battery Arbitrage	AWE Battery Arbitrage
LCoE	≅	↑	↓↓	↑
LPoE	↓	≅	↓↓	≅
NPV	↓↓	≅	↓	↑
IRR	↓↓	≅	↓	↑
Replacement frequency	≅	≅	↑	↓
Storage CapEx	↓↓	≅	≅	≅
Storage OpEx	↓↓	↑↑	↑↑	↑

≅ = comparable    ↑ = advantageous    ↓ = disadvantageous

Table 4.10: Qualitative comparison of scenario configuration performance

Table 4.10 provides a qualitative comparison of the scenarios, which relates the relative performance to the other scenarios. This is a good method to indicate the performance as the metrics are rather difficult to compare. This is perhaps best illustrated by Figure 4.10, where the LCoE values are given for each scenario. The bars and axis on the left represent the LCoE values, with the cost levelized over the discounted energy discharged to the grid. The line and right axis represent the discharged total energy. This clearly shows that the LCoE metric is hard to use to compare the scenarios since the values don't directly relate due to the different energy values over which they are levelized.

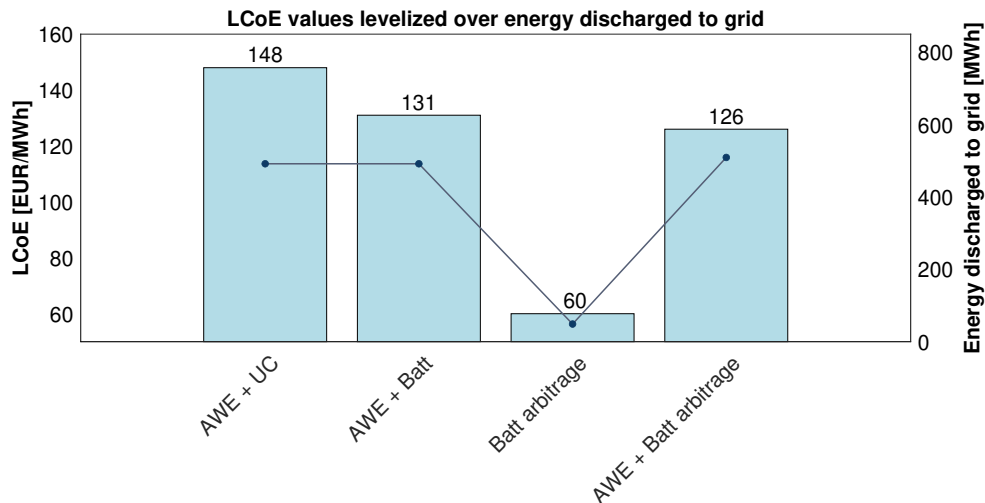


Figure 4.10: LCoE values and energy discharged to grid of the four scenarios

The net present value represents the value of the project over the lifetime compared to the initial investment. The NPV values can be seen in Figure 4.11, the bar graph and left axis represent the NPV. The blue line and right axis represent the CapEx of the scenario. This clearly shows the negative economic prospects of scenarios 1 and 3. The investment in scenario 3 is especially negative, given the low CapEx value combined with the low NPV. The NPV values rely on the assumed discount rate of 10%. The CapEx values of scenarios 3 and 4 are identical but the NPV of scenario 4 is slightly higher, concluding that the return on investment is higher for the scenario combining AWE and arbitrage.

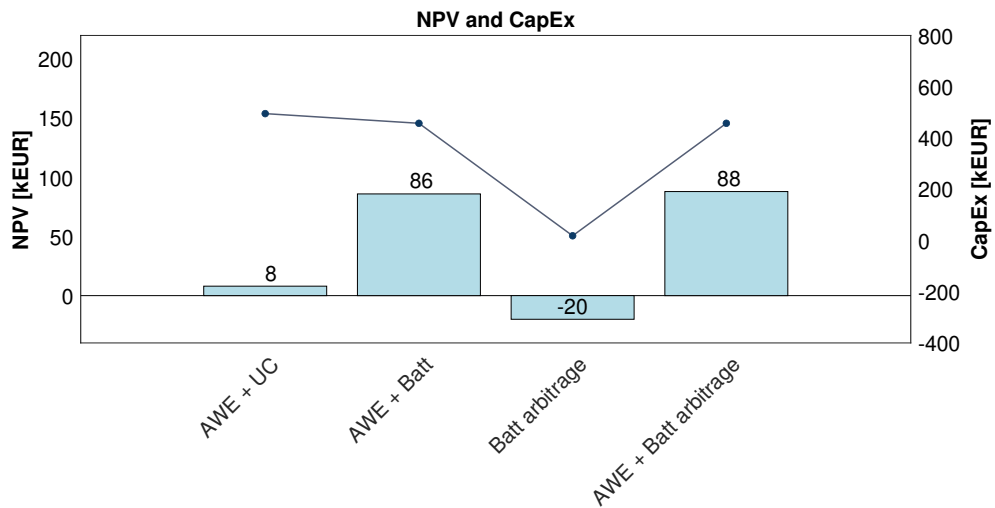


Figure 4.11: NPV values and CapEx of the four scenarios

The IRR shows the rate at which the initial investment is recovered at the end of the lifetime, the higher the rate the better the return on investment. Compared to the NPV this metric shows more clearly the return on investment since no discount rate assumption is made. Figure 4.12 shows the IRR values of scenarios 1, 2, and 4. Scenario 3 was excluded since the IRR is incredibly low, as indicated by the NPV relative to the CapEx seen in Figure 4.11. Figure 4.12 also shows the assumed discount rate of this thesis, showing once again that scenario 1 results in the lowest return on investment, since the IRR is only slightly above the discount rate of 10%. The IRR values for scenarios 3 and 4 show a slightly higher IRR with the addition of storage arbitrage.

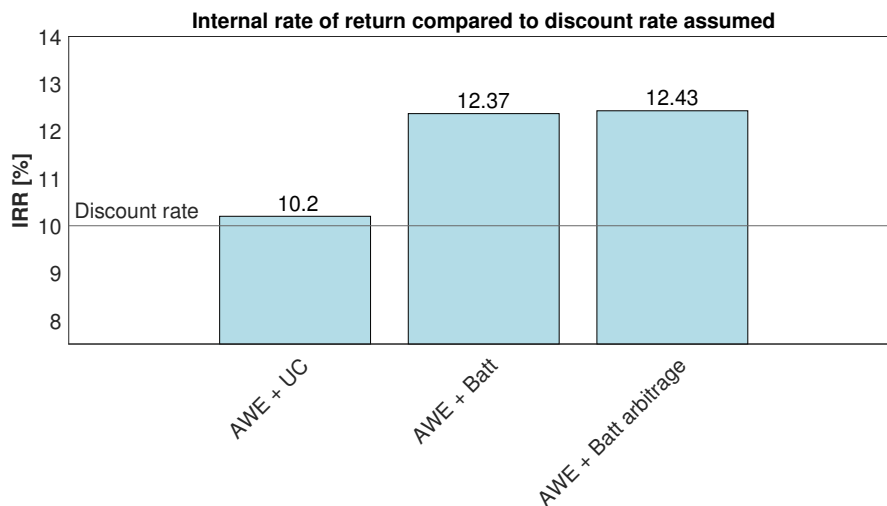


Figure 4.12: IRR values of scenario 1, 2, and 4 and the discount rate assumed in this thesis

The payback year shows the year at which the project breaks even based on the cashflow and the initial investment. The lower the payback year, the higher the return on investment will be. Figure 4.13 shows the payback year values of scenarios 1, 2, 3, and 4. Scenario 3 has no payback year since the cashflow of this scenario is too low to break even

with the initial investment. The payback year shows clearly that the difference in cashflow between scenarios 2 and 4 is not enough to make a difference in the payback year. The payback year of scenario 1 is a year later than those of scenarios 2 and 4 due to the lower cost due to the cheaper battery storage component.

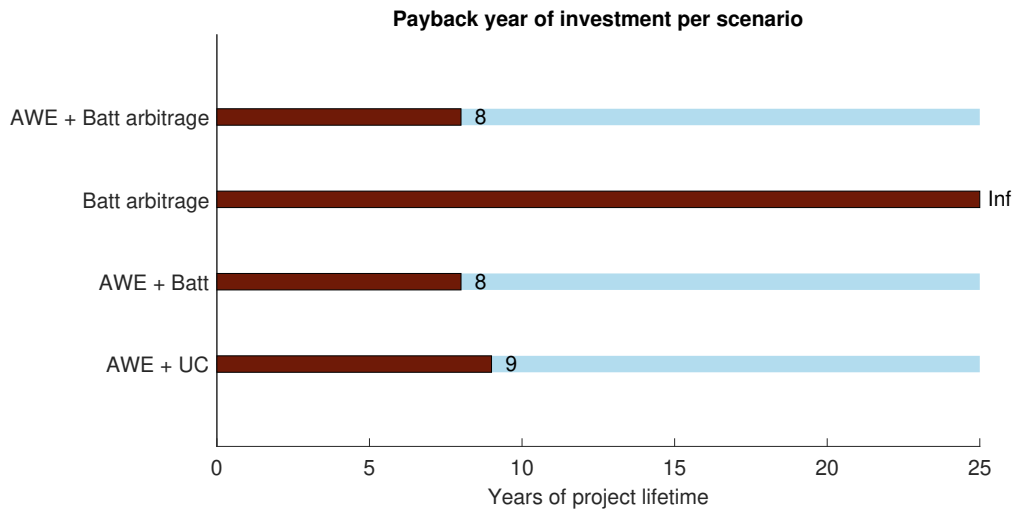


Figure 4.13: Payback year of each project, from top to bottom: scenario 4, 3, 2 and 1

The replacement frequency of the storage component shows when the storage component has to be replaced due to battery degradation. A higher replacement frequency results in a higher OpEx since the component needs to be replaced more often. The replacement frequency depends on either the lifetime in terms of years or the lifetime in terms of cycles. The higher frequency is dominant since that determines the actual moment of replacement. Figure 4.14 shows the replacement frequencies both in terms of lifetime years, and lifetime cycles. This indicates a more significant difference in battery use between scenarios than appears from just the dominant frequencies. The storage component in scenario 1, being the UC, is replaced based on lifetime cycles, since this results in a higher frequency. The same is true for scenario 4, though this difference is significantly lower. The replacement frequencies of scenarios 2 and 4 show that the arbitrage operation increases the replacement frequency by 0.03 per year. The actual difference is low, however, since the lifetime in years dominates the replacement of scenario 2.

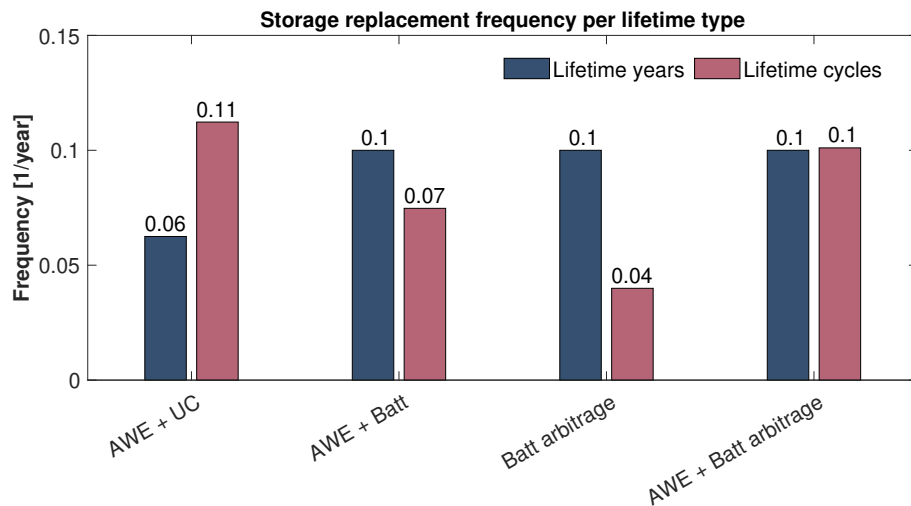


Figure 4.14: Storage component replacement frequency breakdown by factors of lifetime years and lifetime cycles per scenario

Comparing the economic performance of the different scenarios requires attention to the limits of the simulation. As can be seen in Table 4.7, the value of storage arbitrage is near 7.7 k€/MW/year. As can be expected the value of storage arbitration of scenario four is lower, around 1.87 k€/MW/year. This can be explained due to the smoothing application of the same battery system limiting how much the battery can be used. While the IRR results show that at these values of the exploitation of the battery results in a net gain for using the excess capacity for arbitrage in scenario four, the potential value increase is likely higher.

Research into battery arbitration has shown that even though profit depends on many variables in most cases they are expected to be closer to 50 k€/MW/year [55]. This value of arbitrage depends in large part on the volatility of the market prices since this determines the price difference amplitude to be exploited. In the price data of the simulation, the volatility of the price was 11.3, which compared to other periods and zones is on the lower end of the average. This shows that the simulated arbitrage underperforms by some degree, but does show the connection between DAM profit and additional battery replacement costs.

#### 4.6.2. Sensitivity analysis

Many factors influence the economic performance of the different systems within the scenarios. A sensitivity analysis is made to investigate how the IRR of the scenarios is affected by changing certain variables. First, the sensitivity of the simulated performance to the price of batteries is analyzed. Then the round-trip efficiency of the batteries is varied to investigate how this affects the profitability.

The simulated scenarios are compared based on the IRR, the difference in IRR shows which configuration is more profitable. Since the profitability of the configurations using batteries depend on the revenue being comparatively larger than the costs of the battery system, the costs factor into this to a large degree.

Table 4.11 shows the sensitivity of the economic performance to the battery price. Scenario three was not taken into consideration as the configuration of battery use in arbitrage was mainly used to compare arbitrage revenue possibilities but due to its significantly lower profitability in any use case does not provide additional insight in comparing

the scenarios. It can be seen that the AWE ultracapacitor scenario has no sensitivity to the battery price, as can be expected due to it not using any battery capacity. The Profitability of scenario two and four do show a relation to the battery price. Both the profitability values, represented by the IRR decrease at higher battery prices. This is due to the initial investment being higher as well as the subsequent battery replacements costing more. Scenarios two and four present a linear regression based on the battery price, further defining the extra battery replacement due to arbitrage being compensated by the additional revenue.

Battery price €/kWh	Scenario 1: AWE + Ultracapacitor	Scenario 2: AWE + Battery	Scenario 4: AWE + Battery arbitrage
130	10.2	12.37	12.43
145	10.2	12.26	12.31
160	10.2	12.14	12.20
175	10.2	12.02	12.08
190	10.2	11.90	11.96
205	10.2	11.79	11.85
220	10.2	11.68	11.73

Table 4.11: Sensitivity IRR to battery price

Figure 4.15 further illustrates the relative decline in profitability as battery price increases. The IRR values for both scenarios experience the same inclination. This shows that an increase in battery price does not change the relative added value of arbitrage. This may differ for alternative arbitrage operation strategies where the relation between battery use and arbitrage revenue is different. In the operational strategy used in this study, the arbitrage is based on maximum capacity charge/discharge at local price extrema. In a more optimal dispatch, the traded capacity could differ from none or all of the capacity, which could change the overall battery use and effect on battery replacement.

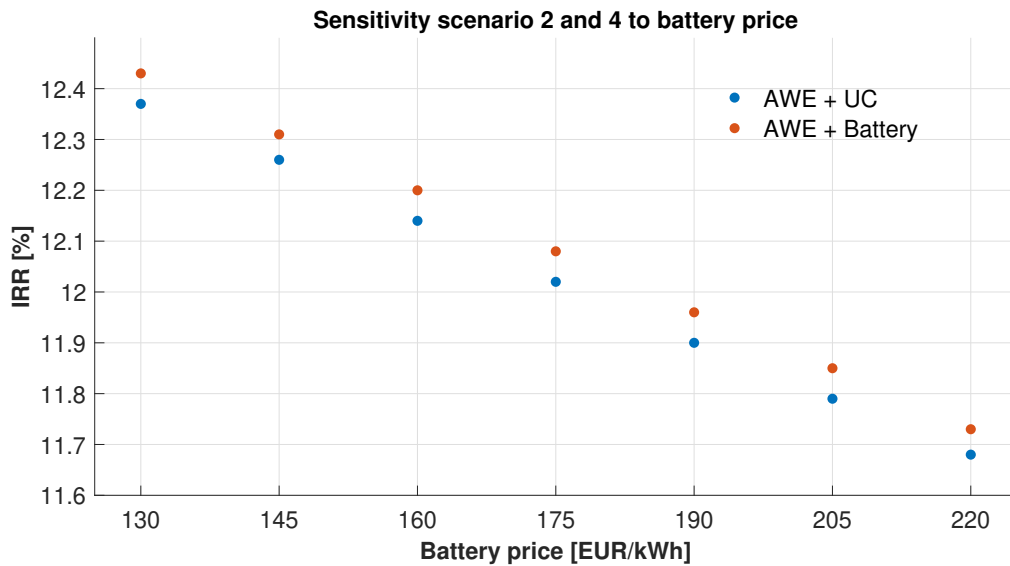


Figure 4.15: Sensitivity IRR to battery price scenario 2 and 4

Figure 4.16 shows the sensitivity of scenario 4 IRR values to the round-trip efficiency of the battery. Studies related to battery arbitrage have concluded a significant relationship between arbitrage revenue and battery efficiency. As the figure shows, higher efficiencies result in higher IRR values and also more energy cycled through the battery.

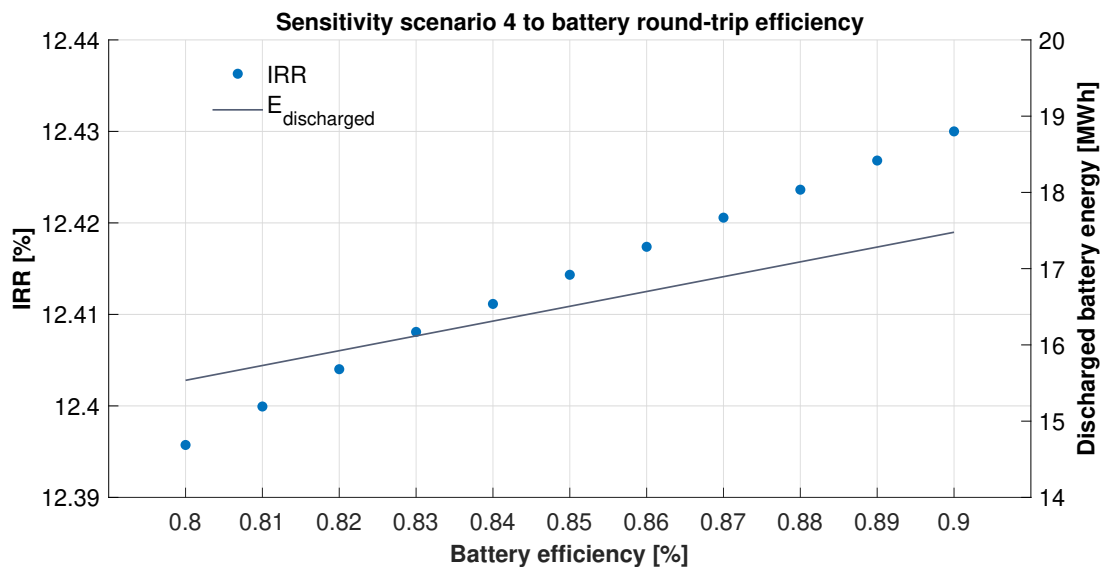


Figure 4.16: Sensitivity IRR to battery round-trip efficiency scenario 4

Figure 4.17 shows the sensitivity of scenario 4 IRR values to the battery installed capacity or size. As can immediately be seen an increase in battery size results in a decrease in IRR. This is because at the size of 140 kWh required for power smoothing in this context, the initial investment is shared over multiple applications. At any size over this value the initial investment increases which is not recouped by the increased arbitrage use. This in-

crease in arbitrage use can be seen by the energy discharged by the battery increasing as the size increases. The resulting sensitivity shows that at the battery price point of this analysis, the arbitrage is not economically viable for any additional capacity but does result in an increase in value of the system when the excess capacity is used.

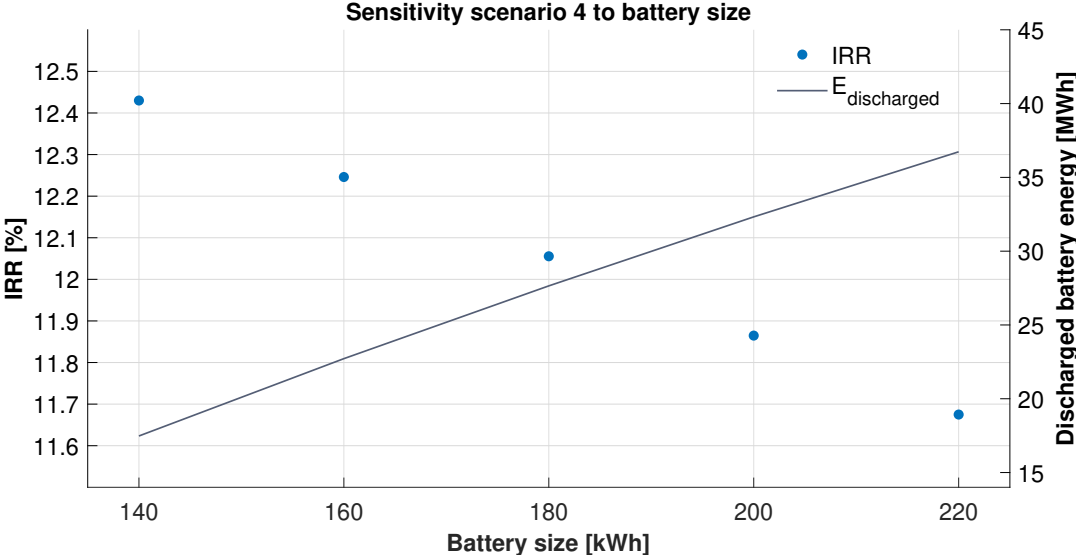


Figure 4.17: Sensitivity IRR to battery size efficiency scenario 4

# 5 | Conclusion

The literature review led to the following research questions: In a scenario of grid connection, In a scenario of grid connection, how can the value of hybrid power systems (HPS) using airborne wind energy (AWE) be maximized? The answer to that question will be provided in this section.

## 5.1. Key findings

The literature review was conducted to find the essential information needed to conduct this study. In a grid-connected scenario, revenue generation on the day ahead market (DAM) depends on the value of the energy bid to the grid. It was identified that combining an airborne wind energy (AWE) system with batteries to provide power smoothing application was beneficial to the system profitability. Studying the power smoothing capabilities of ultracapacitors (UCs) and batteries as well as the ramping limitations of the DAM indicated the possibility of incorporating battery power smoothing in the AWE system. It was then identified how to determine the system sizing of the replacement power smoothing component. The level of increased DAM-generated profit was then identified using simulations.

- The value of grid-connected fixed-wing AWE systems in DAM participation is increased when batteries are used for power smoothing.

The simulated profitability of the UC and battery configurations identified the answer to the first research subquestion; to what extent can grid-connected profitability be increased when replacing the UC intermediate storage with a battery system in the configuration of an Airborne Wind Energy system? To answer this a model was developed that could simulate the market value captured by an AWE system and determine the performance and replacement of the power smoothing component. The results confirmed the battery smoothing component performed similarly to the UC in terms of power output but at significantly lower system lifetime costs. The internal rate of return of the AWE + battery system was 2.17% higher than the AWE + UC system, showing a higher return on investment over the project lifetime. Simulations also showed a significant excess storage capacity being present in the battery system due to over-sizing.

- The value is further increased when batteries are used for combined power smoothing and arbitrage operation.

The excess power and energy capacity of the storage component were analyzed to determine the increase in system value. This leads to an answer to the second research subquestion; to what level can the excess capacity present in the battery power smoothing storage be used to increase profitability? A model was developed to simulate the excess capacity and a strategy was created to operate the arbitrage. The additional operation of the excess power smoothing capacity in DAM arbitrage resulted in an increase in IRR of 0.06% compared to the AWE + battery system without using arbitrage. This shows the added battery degradation due to increased battery use is offset by the additional revenue due to storage arbitrage.

- The use of batteries in DAM storage arbitrage is not profitable at the projected cost but when combined with AWE systems will result in profit.

Simulations of a battery system operating in storage arbitrage on the DAM environment defined in this research resulted in a negative economic prospect. The revenue generated

using the arbitrage operation proposed in this thesis was insufficient to recover the initial investment and battery replacement cost. The combination of DAM arbitrage and AWE power smoothing results in combined revenue that is sufficient to recover the initial investment and battery replacement cost as well as generate profit. Sensitivity analysis of the battery size showed no increased profit beyond the minimum required battery size for AWE power smoothing. This further determines the optimal profit of battery arbitrage at current cost projections to be at the capacity sized for smoothing, only using the excess capacity for arbitrage.

## 5.2. Reflections and recommendations

This research was conducted to provide insight into the possibilities of increasing the value of AWE systems combined with battery storage. It shows that when the batteries are used for arbitrage on the DAM, the initial investment of the system is used more efficiently for multiple purposes. The current developed model shows a good foundation for identifying areas where additional value can be gained. The arbitrage operational strategy does rely on assumptions of perfect forecast and was shown to not result in revenues comparable to those found in similar market price environments. Instead of heuristics, the use of optimization algorithms could be used to compute more theoretically ideal arbitrage bids.

Additional inputs, such as wind and market data forecast error, could be used to research alternative use cases for the excess capacity. The imbalance between generated power and bid power resulting from wind forecasting errors could be compensated by the battery capacity. It has been shown in the past that such application of batteries is possible at comparable rated power/installed battery capacity ratios. Beyond this internal imbalance, the imbalance market could also prove profitable for the system analyzed in this study. By including these alternative applications the optimal use of the excess capacity can be identified.

This research identifies the beneficial effect of arbitrage using a battery system also used for power smoothing. The simulated scenarios could be expanded to include other renewable energy sources such as solar PV. Within that context, the complementary intermittency could perhaps be used efficiently by a battery system of the size required for AWE power smoothing.

The battery system size identified as the required capacity for smoothing proved the optimal sizing for profitability, since at that capacity the initial investment was recouped by multiple applications of the battery. Combining this inherent battery capacity with a long-term storage component could provide insight into the benefits of long-term storage in addition to the present short-term storage.

# Bibliography

- [1] E. spot, "Vattenfall combines wind, solar and batteries in hybrid energy park." <https://www.epexspot.com/en/market-data?marketarea=NLauction=MRCtradingdate=2024-09-10deliverydate=2024-09-11> (Accessed 08-09-2024).
- [2] R. Joshi, D. Von Terzi, M. Kruijff, and R. Schmehl, "Techno-economic analysis of power smoothing solutions for pumping airborne wind energy systems," in *Journal of Physics: Conference Series*, vol. 2265, p. 042069, IOP Publishing, 2022. DOI: 10.1088/1742-6596/2265/4/042069.
- [3] M. Blanch, A. Makris, and B. Valpy, "Getting airborne—the need to realise the benefits of airborne wind energy for net zero," *White Paper for Airborne Wind Europe*, pp. 1–44, 2022. <https://airbornewindeurope.org/studies-papers/white-paper-for-the-airborne-wind-energy-sector-by-bvg-associates-commissioned-by-airborne-wind-europe/> (Accessed 25-05-2024).
- [4] F. Mulder, "Implications of diurnal and seasonal variations in renewable energy generation for large scale energy storage," *Journal of Renewable and Sustainable Energy*, vol. 6, no. 3, 2014. DOI: 10.1063/1.4874845.
- [5] Vattenfall, "Ervaringen energiepark haringvliet zuid," February 2024. <https://haringvlietzuid.vattenfall.nl/2024/02/28/nieuwsbrief-12-ervaringen-energiepark-haringvliet-zuid/> (Accessed 28-03-2024).
- [6] C. Augustine and N. Blair, "Storage futures study: Storage technology modeling input data report," tech. rep., National Renewable Energy Lab.(NREL), Golden, CO (United States), 2021. DOI: 10.2172/1785959.
- [7] D. Bogdanov, M. Ram, A. Aghahosseini, A. Gulagi, A. S. Oyewo, M. Child, U. Caldera, K. Sadovskaia, J. Farfan, L. D. S. N. S. Barbosa, *et al.*, "Low-cost renewable electricity as the key driver of the global energy transition towards sustainability," *Energy*, vol. 227, p. 120467, 2021. DOI: 10.1016/j.energy.2021.120467.
- [8] I. R. E. A. IRENA, *Renewable power generation costs in 2020*. eBook Partnership, 2022.
- [9] I. Westphal, "The effects of reducing renewable power intermittency through portfolio diversification," *Renewable and Sustainable Energy Reviews*, vol. 197, p. 114415, 2024. DOI: 10.1016/j.rser.2024.114415.
- [10] P. Bechtle, M. Schelbergen, R. Schmehl, U. Zillmann, and S. Watson, "Airborne wind energy resource analysis," *Renewable energy*, vol. 141, pp. 1103–1116, 2019. DOI: 10.1016/j.renene.2019.03.118.
- [11] K. Van Hussen, E. Dietrich, J. Smeltink, K. Berentsen, M. van der Sleen, R. Haffner, and L. Fagiano, "Study on challenges in the commercialisation of airborne wind energy systems," *European Commission*, 2018. DOI: 10.2777/87591.
- [12] E. Tapoglou, J. Tattini, A. Schmitz, A. Georgakaki, M. Dugosz, S. Letout, A. Kuokkanen, A. Mountraki, E. Ince, D. Shtjefni, G. Joanny Ordonez, O. Eulaerts, and M. Grabowska, "Clean energy technology observatory: Wind energy in the european union - 2023 status report on technology development, trends, value chains and markets, publications office of the european union," *European Commission*, 2023. DOI: 10.2760/618644.
- [13] H. Schmidt, G. de Vries, R. J. Renes, and R. Schmehl, "The social acceptance of airborne wind energy: A literature review," *Energies*, vol. 15, no. 4, p. 1384, 2022. DOI: 10.3390/en15041384.

- [14] M. L. Loyd, "Crosswind kite power (for large-scale wind power production)," *Journal of energy*, vol. 4, no. 3, pp. 106–111, 1980. DOI: 10.2514/3.48021.
- [15] R. H. Luchsinger, "Pumping cycle kite power," in *Airborne wind energy*, pp. 47–64, Springer, 2013.
- [16] K. Dykes, J. King, N. DiOrio, R. King, V. Gevorgian, D. Corbus, N. Blair, K. Anderson, G. Stark, C. Turchi, *et al.*, "Opportunities for research and development of hybrid power plants," tech. rep., National Renewable Energy Lab.(NREL), Golden, CO (United States), 2020. DOI: 10.2172/1659803.
- [17] A. H. Schleifer, D. Harrison-Atlas, W. J. Cole, and C. A. Murphy, "Hybrid renewable energy systems: The value of storage as a function of pv-wind variability," *Frontiers in Energy Research*, vol. 11, no. NREL/JA-6A20-81902, 2023. DOI: 10.3389/fenrg.2023.1036183.
- [18] K. Das, A. D. Hansen, D. H. Vangari, M. J. Koivisto, P. E. Sørensen, and M. Altin, "Enhanced features of wind based hybrid power plants," in *4th International Hybrid Power Systems Workshop*, 2019. <https://orbit.dtu.dk/en/publications/component-sizing-of-an-utility-scale-hybrid-power-plant> (Accessed 22-02-2024).
- [19] P. Gipe and E. Möllerström, "An overview of the history of wind turbine development: Part ii—the 1970s onward," *Wind Engineering*, vol. 47, no. 1, pp. 220–248, 2023. DOI: 10.1177/0309524X221122594.
- [20] U. Zillmann and P. Bechtle, "Emergence and economic dimension of airborne wind energy," *Airborne wind energy: Advances in technology development and research*, pp. 1–25, 2018.
- [21] R. Joshi, R. Schmehl, and M. Kruijff, "Performance modelling and scaling of fixed-wing ground-generation airborne wind energy systems," *Wind Energy Science*, vol. 2024, pp. 1–37, 2024. DOI: 10.5194/wes-2024-86.
- [22] R. Joshi and F. Trevisi, "Reference economic model for airborne wind energy systems," tech. rep., IEA Wind TCP Task 48, 2024. <https://re.public.polimi.it/bitstream/11311/1218933/1/JOSHR01-22.pdf> (Accessed 21-04-2024).
- [23] Z. Zhang, T. Ding, Q. Zhou, Y. Sun, M. Qu, Z. Zeng, Y. Ju, L. Li, K. Wang, and F. Chi, "A review of technologies and applications on versatile energy storage systems," *Renewable and Sustainable Energy Reviews*, vol. 148, p. 111263, 2021. DOI: 10.1016/j.rser.2021.111263.
- [24] K. Mongird, V. V. Viswanathan, P. J. Balducci, M. J. E. Alam, V. Fotedar, V. Koritarov, and B. Hadjerioua, "Energy storage technology and cost characterization report," tech. rep., Pacific Northwest National Laboratory (PNNL), Richland, WA (United States), 2019. DOI: 10.2172/1573487.
- [25] P. Denholm, W. Cole, and N. Blair, "Moving beyond 4-hour li-ion batteries: challenges and opportunities for long (er)-duration energy storage," 2023. DOI: 10.2172/2000002.
- [26] M. R. D. Quitoras, M. L. S. Abundo, and L. A. M. Danao, "A techno-economic assessment of wave energy resources in the philippines," *Renewable and Sustainable Energy Reviews*, vol. 88, pp. 68–81, 2018. DOI: 10.1016/j.rser.2018.02.016.
- [27] E. C. Malz, V. Walter, L. Göransson, and S. Gros, "The value of airborne wind energy to the electricity system," *Wind Energy*, vol. 25, no. 2, pp. 281–299, 2022. DOI: 10.1002/we.2671.
- [28] S. Reuchlin, R. Joshi, and R. Schmehl, "Sizing of hybrid power systems for off-grid applications using airborne wind energy," *Energies*, vol. 16, no. 10, p. 4036, 2023. DOI: 10.3390/en16104036.
- [29] R. Schmehl, M. Rodriguez, L. Ouroumova, and M. Gaunaa, "Airborne wind energy for martian habitats," in *Adaptive On-and Off-Earth Environments*, pp. 145–197, Springer, 2024. DOI: 10.1088/2753-3751/ad3fbc.

- [30] L. Ouroumova, D. Witte, B. Klootwijk, E. Terwindt, F. van Marion, D. Mordasov, F. C. Vargas, S. Heidweiller, M. Géczi, M. Kempers, *et al.*, "Combined airborne wind and photovoltaic energy system for martian habitats," *arXiv preprint arXiv:2104.09506*, 2021. DOI: 10.7480/spool.2021.2.6058.
- [31] M. Rodriguez, "Airborne wind energy systems for mars habitats," 2022. <http://resolver.tudelft.nl/uuid:52a156ae-c758-4d3a-a403-54ce5fce2e5e> (Accessed 08-09-2024).
- [32] H. Vos, F. Lombardi, R. Joshi, R. Schmehl, and S. Pfenninger, "The potential role of airborne and floating wind in the north sea region," *Environmental Research: Energy*, vol. 1, no. 2, p. 025002, 2024. DOI: 10.1088/2753-3751/ad3fbc.
- [33] R. Joshi, "Influence of the european electricity market on the system design of airborne wind energy: A method to quantify the merit order effect of wind power on the revenue generation of the systems," 2020. <https://resolver.tudelft.nl/uuid:a19bf3fb-9f86-4fc2-985d-d9af6481e273> (Accessed 15-09-2024).
- [34] S. Reuchlin, "Modelling and sizing of a hybrid power plant using airborne wind energy," 2022. <https://resolver.tudelft.nl/uuid:041b3cf7-4b10-44c2-9b49-8f58b6f8419c> (Accessed 08-04-2024).
- [35] R. E. Megazine, "Vattenfall combines wind, solar and batteries in hybrid energy park," August 2019. <https://www.renewableenergymagazine.com/panorama/vattenfall-combines-wind-solar-and-batteries-in-20190814> (Accessed 23-05-2024).
- [36] R. Zhu, O. Lindberg, K. Das, P. E. Sørensen, and A. D. Hansen, "Impact of renewable power and market price forecasts on the operational profitability of hybrid power plants," 2023. DOI: 10.1049/icp.2023.2736.
- [37] G. van Holthoon, "Electricity market bidding strategies for wind-storage hybrid systems," 2021. <https://resolver.tudelft.nl/uuid:d1f3b628-cd9b-47ca-863f-970e6b44d62f> (Accessed 11-03-2024).
- [38] M. Mehta, G. van Holthoon, D. von Terzi, and M. Zaaier, "Technical and economic value of utility-scale wind-storage hybrid power plants," in *Proceedings of Hybrid Power Systems Workshop, 2021*, 2021. <https://research.tudelft.nl/en/publications/technical-and-economic-value-of-utility-scale-wind-storage-hybrid> (Accessed 01-04-2024).
- [39] W. Cole, A. W. Frazier, and C. Augustine, "Cost projections for utility-scale battery storage: 2021 update," tech. rep., National Renewable Energy Lab.(NREL), Golden, CO (United States), 2021. <https://www.nrel.gov/docs/fy21osti/79236.pdf> (Accessed 13-03-2024).
- [40] J. Iori, M. Zaaier, D. von Terzi, and S. Watson, "Design drivers for the storage system of baseload hybrid power plants," 2024. DOI: 10.1049/icp.2024.1844.
- [41] C. Zhao, P. B. Andersen, C. Træholt, and S. Hashemi, "Grid-connected battery energy storage system: a review on application and integration," *Renewable and Sustainable Energy Reviews*, vol. 182, p. 113400, 2023. DOI: 10.1016/j.rser.2023.113400.
- [42] M. Jabir, H. Azil Illias, S. Raza, and H. Mokhlis, "Intermittent smoothing approaches for wind power output: A review," *Energies*, vol. 10, no. 10, p. 1572, 2017. DOI: 10.3390/en10101572.
- [43] K.-N. D. Malamaki, A. Fu, J. M. Mauricio, M. Cvetković, and C. S. Demoulias, "Evaluation of ramp-rate limitation at distribution transformer level via central and distributed storage systems," in *2023 IEEE Belgrade PowerTech*, pp. 1–6, IEEE, 2023. DOI: 10.1109/PowerTech55446.2023.10202995.
- [44] N. Nederland, "Niet-limitatieve eisen (nle's) van verordening (eu) 2016/631 (nc rfg)," 2016. <https://eepublicdownloads.entsoe.eu/clean-documents/cnc-active-library/Netherlands/voorstel-br-2018-1386-rfgsobegrippen-bijlage-3-nles-rfg.PDF> (Accessed 15-08-2024).

- [45] S. M. Alhejaj and F. M. Gonzalez-Longatt, "Impact of inertia emulation control of grid-scale bess on power system frequency response," in *2016 International Conference for Students on Applied Engineering (ICSAE)*, pp. 254–258, IEEE, 2016. DOI: 10.1109/ICSAE.2016.7810198.
- [46] X. Li, D. Hui, and X. Lai, "Battery energy storage station (bess)-based smoothing control of photovoltaic (pv) and wind power generation fluctuations," *IEEE transactions on sustainable energy*, vol. 4, no. 2, pp. 464–473, 2013. DOI: 10.1109/TSTE.2013.2247428.
- [47] A. Soto, A. Berrueta, M. Mateos, P. Sanchis, and A. Ursúa, "Impact of micro-cycles on the lifetime of lithium-ion batteries: An experimental study," *Journal of Energy Storage*, vol. 55, p. 105343, 2022. DOI: 10.1016/j.est.2022.105343.
- [48] TenneT, "Types and operation of market types," September 2024. <https://netztransparenz.tennet.eu/electricity-market/about-the-electricity-market/what-kind-of-markets-are-there-and-how-do-they-work/> (Accessed 14-08-2024).
- [49] S. E. Analytics, "Energy procurement made simple," September 2024. <https://synertics.io/blog/39/understanding-day-ahead-intraday-markets> (Accessed 28-08-2024).
- [50] N. Nederland, "Basisdocument over energie-infrastructuur (oktober 2019)," 2019. <https://www.netbeheernederland.nl/publication/basisdocument-over-energie-infrastructuur-oktober-2019> (Accessed 14-08-2024).
- [51] T. Brijs, F. Geth, C. De Jonghe, and R. Belmans, "Quantifying electricity storage arbitrage opportunities in short-term electricity markets in the cwe region," *Journal of Energy Storage*, vol. 25, p. 100899, 2019. DOI: 10.1016/j.est.2019.100899.
- [52] J. Liu, C. Hu, A. Kimber, and Z. Wang, "Uses, cost-benefit analysis, and markets of energy storage systems for electric grid applications," *Journal of Energy Storage*, vol. 32, p. 101731, 2020. DOI: 10.1016/j.est.2020.101731.
- [53] K. Bassett, R. Carriveau, and D. S.-K. Ting, "Energy arbitrage and market opportunities for energy storage facilities in ontario," *Journal of Energy Storage*, vol. 20, pp. 478–484, 2018. DOI: 10.1016/j.est.2018.10.015.
- [54] P. Mercier, R. Cherkaoui, and A. Oudalov, "Optimizing a battery energy storage system for frequency control application in an isolated power system," *IEEE transactions on Power Systems*, vol. 24, no. 3, pp. 1469–1477, 2009. DOI: 10.1109/TPWRS.2009.2022997.
- [55] T. Mercier, M. Olivier, and E. De Jaeger, "The value of electricity storage arbitrage on day-ahead markets across europe," *Energy Economics*, vol. 123, p. 106721, 2023. DOI: 10.1016/j.eneco.2023.106721.
- [56] WindEurope, "Database for wind + storage co-located projects," Jul 2019. <https://windeurope.org/about-wind/database-for-wind-and-storage-colocated-projects/> (Accessed 10-02-2024).
- [57] ENTSO-E, "Entso-e," May 2024. <https://transparency.entsoe.eu> (Accessed 17-04-2024).
- [58] ECMWF, "Era5," april 2023. <https://cds.climate.copernicus.eu> (Accessed 15-04-2024).
- [59] A. für Klimaschutz und Energie, "Zweite beschlussempfehlung und zweiter bericht des ausschusses für klimaschutz und energie (25. ausschuss)," 2024. <https://www.bundestag.de/ausschuesse/a25klimaschutzundenergie/berichte> (Accessed 10-09-2024).